The influence of root traits on soil reinforcement and erosion mitigation.

Emma Burak

BSc (Hons) Outdoor Education with Environmental Education
Liverpool John Moores University, UK

MSc Water and Environmental Management
University of Bristol, UK

Declaration

I hereby declare that the content of this thesis is my own work, except where reference are made to other sources, and that it was not previously presented for a higher degree elsewhere.

Emma Burak

Lancaster University, May 2019

Statement of authorship

Chapters 2, 3 and 4 are intended for submission to peer reviewed journals. The papers are presented in the thesis as intended for submission, with the exception of a consolidated bibliography, shortened introductions, and where references are made to other chapters. Both papers have multiple authors and their contributions are detailed below.

Chapter 2 has been submitted as:

Burak, E., Quinton, J.N., and Dodd, I.C., 2019. Root hairs are the most important root trait for rhizosheath formation. Annals of Botany. (Submitted 31st May 2019).

EB designed, set up, organised, and carried out, all growing, sampling, laboratory work, data analysis, and prepared the revised manuscript. ICD and JNQ gave advice on experimental design and contributed to the revision of the manuscript, and provided laboratory space.

Chapter 3 is intended for submission as:

Burak, E., Dodd, I.C., and Quinton, J.N., 2019. Do root hairs of barley and maize roots reinforce soil under shear stress?

EB designed, set up, organised, and carried out, all growing, sampling, laboratory work, data analysis, and prepared the revised manuscript. ICD and JNQ gave advice on experimental design and contributed to the revision of the manuscript, and provided laboratory space.

Chapter 4 is intended for submitted as:

Burak, E., Dodd, I.C., and Quinton, J.N., 2019. A mesocosm-based assessment of whether root hairs influence soil erosion under simulated rainfall.

EB designed, set up, organised, and carried out, all growing, sampling, laboratory work, data analysis, and prepared the revised manuscript. ICD and JNQ gave advice on experimental design and contributed to the revision of the manuscript, and provided laboratory space.

Acknowledgements

I cannot send enough thanks to my supervisors Professor Ian Dodd and Professor John Quinton. This thesis would not have been possible without their help, support, advice, reassurance, constructive criticism, and occasionally much needed bluntness and over the past few years.

I would like to thank Maureen Harrison, Vassil Karloukovski, John Crosse, Geoff Holroyd, and Dave Lewis for their help in the lab, growth spaces or with equipment. As well as Rhys Ashton at Rothamsted for use of their Universal Testing Machine. Thanks also go to Paul Knox, Andrew Galloway, and Jumana Akhtar for help with their soil adhesion assay and Lawrie Brown for advice on measuring root hairs.

The wider support and training provided by the STARS CDT were invaluable with extra thanks to Olivia Lawrenson for all her organisation and support. I would also like to thank my STARS cohort: Hannah Cooper, Paul George, Beckie Draper, Jasmine Burr-Hersey, Malika Mezeli, and Dan Evans for their companionship and moral support, with specific mention to and Fiona Seaton for her patient and invaluable help with stats.

Thank you also to the Plant Physiology lab group, Fish Bowl members and wider LEC community for all their helpful discussions, practical advice and friendship: Emma Biles, Rob Kempster, Noorliana Mohd Zahn, Antonio Capponi, Xiaoqing Li, Esti Leibar, Rachel Baxter, Dennis Touliatos, Paul McLachlan, Nathan Magnall, Shane Rothwell, and Jaime Puertolas. With special mention to both Sarah Donaldson and Aimee Brett for their extra contributions to maintaining my sanity throughout my PhD.

My field work would not have been possible without the willingness of my volunteers to spend a day or three playing with mud and water in the middle of a field on a beautiful sunny summer day… and for their hard labour: Rob Kempster, Chris Blacklock, Ash Routh, Kittington Jones, Emma Biles, Myron Burak and Caz Russell.

Extra special thanks to Caz, for keeping me sane, fed and functioning as a human being as well as providing the appropriate enthusiastic or thoughtful noises when I'm bombarding you with the intricacies of my thesis. And I'm forever grateful to my family, Mum, Dad, Katey, and Isla for your love, support, understanding and general awesomeness. I would not be where I am now without your support.

Abstract

Soil erosion is a global concern as it reduces the quality of the soil and restricts its ability to provide essential ecosystem services such as supplying the nutrients and substrate for the majority of the world's food. Without the fertile top soil, more fertilisers are needed to achieve the same yield. Additionally, the displaced soil clogs waterways, increasing both the risk and magnitudes of flooding and landslides. Plant roots have beneficial traits that can reinforce the soil and mitigate erosion. However, there is a large gap in the knowledge regarding the relative contribution of individual root traits. Root hairs can bind soil particles at the root-soil interface and anchor roots during growth, but their influence on wider reinforcement of soil and erosion mitigation has not yet been evaluated. This thesis subjected root systems with varying traits to erosion events and evaluated which traits are more beneficial to preventing erosion.

Initially, pot experiments evaluated the ability of root hairless mutants of barley (*brb*), maize (*rth3*), and *L. japonicus* (*Ljrhl1*) to bind soil at the root-soil interface and form a rhizosheath. Root exudate adhesiveness and root hair traits were compared with wild type (WT) genotypes. Root hair development proved to be the most influential trait for rhizosheath formation.

Pots containing one each of the barley and maize genotypes were subjected to shear stress in a laboratory shearing rig to establish which root traits most influenced the root system's ability to reinforce the soil. The presence of roots significantly increased soil reinforcement, but unlike with rhizosheath development, root hairs showed no propensity to influence this. Root diameter was the trait most dominant in determining a root system's effectiveness as soil reinforcement.

A mesocosm experiment evaluated the impact of root hairs on erosion mitigation under a controlled laboratory environment. Multiple barley plants were grown in mesocosms modified to collect eroded sediment and subjected to a gravity fed laboratory rainfall simulator. The presence of roots significantly decreased the yield of sediment in the runoff in comparison to the unplanted mesocosms and the presence of root hairs enhanced this reduction.

Lastly, barley genotypes were grown in field plots and subjected to simulated rainfall from a portable field rainfall simulator. The presence of roots significantly reduced the yield of sediment in the runoff. However, under the less controlled field conditions, there was no correlation with soil yield and increasing root presence. Consequently the influence of root hairs was swamped by other uncontrolled variables.

Thus, it was concluded that in a small scale homogenous environments root hairs can enhance a root system's ability to mitigate soil erosion, however their contribution is small and can easily become overshadowed by more dominant forces such as larger roots or intense rainfall so that in some scenarios their contribution is negligible.

Table of Contents

List of Figures

List of Tables

Chapter 1. General introduction.

1.1. Introduction

Soil is one of the planet's major natural resources and is integral to sustaining life on Earth by providing a plethora of goods and services. Arguably, to the human population, one of the most immediately relevant ecosystem services provided by soil is the nutrient rich substrate in which the majority of the world's food is grown. Additionally, the presence of clay minerals, organic matter and soil biota acts as a filter and buffer for the world's drinking water by retaining and degrading nutrients and pollutants, such as agriculturally applied pesticides (Keesstra *et al.* 2012). Other services provided by soil include, but are not limited to: construction materials (McNally 2017), antibiotics (Ehrlich *et al.* 1947; Wright 2015), mineral resources (Kesler *et al.* 2015), and dampening of flood peaks (Moore 2007). Soil's complex structure allows small-scale heterogeneity and thus, sustains an extensively diverse population of organisms (Nielsen *et al.* 2010). Soil is one of the most bio-diverse habitats on the planet, with over 10^6 distinct genomes of bacteria occurring in a single gram of soil (Giller *et al.* 1997; Gans *et al.* 2005). Soil also accommodates the > 80 000 fungal species (so far catalogued) at some stage in their life cycle (Bridge and Spooner 2001) and uncountable numbers of nematodes, protozoa, earthworms and other meso- and macro-fauna (Giller *et al.* 1997). With the aid of these organisms, soil maintains a large portion of the planet's nutrient cycle, which accounts for the second largest carbon sink on the planet (Schlesinger and Andrews 2000). However, the planet's soils are being put under increasing stress due to the demands of an increasing human population.

The human population has already increased by over 1 billion in the past 12 years, reaching over 7.3 billion today, and is predicted to reach 9.7 billion by 2050 and 11.2 billion by 2100. This population increase has a direct impact on the global food demand and predictions suggest that agricultural production will need to increase by over 100% between 2005 and 2050 in order to compensate (United Nations 2015). We have, thus far, been able to keep up with the exponentially increasing demand for food by breeding 'improved' crop species and developing agricultural technologies such as irrigation, pesticides and synthetic fertilisers to boost crop yields, technologies which are collectively known as the "Green Revolution" (Pingali 2012).

At the time, the Green Revolution's success was to stall the starvation of a growing population, decrease rural poverty and prevent expanses of natural land being converted for agricultural use (Evenson and Gollin 2003; World Bank 2007; Hazell 2009). However, crop yield increases have begun to plateau (Janaiah *et al.* 2005; van Wart *et al.* 2013) and the dependency of these high yielding monocultures on fertilizer, irrigation, and pesticides is causing widespread degradation of both land and water (Singh 2000; World Bank 2007; Gupta and Seth 2007; Rockström *et al.* 2007; Lal 2009; Rodell *et al.* 2009). The reaction to the current crop yield stagnation has been to proliferate and intensify agricultural land. Thus an extra 13 % of wild land will need to be converted to agriculture by 2050, exposing more of the earth's surface to degradation processes (Lambin *et al.* 2003; Tilman *et al.* 2011). Being able to increase yield without further degrading the soil or converting land for agricultural purposes is essential for sustainable agriculture. It is becoming widely accepted that we should learn from the inadequacies of the Green Revolution and base any further progression in the context of sustainability, where yield is increased without exacerbating and preferably decreasing any negative environmental impact (FAO,

2011; Lynch, 2007; Matson et al., 1997; Tilman et al., 2011, 2002; World Bank, 2007).

1.2. Soil physical properties and degradation

The natural progression of healthy soil formation starts as the bedrock is broken down and dissolved, primarily due to (slight) acidity of rain water but also aided by soil organisms. This is cyclically combined with decaying organic matter (usually plant matter) to form aggregates predominantly 0.25-10 mm in size. In "natural" soils, nutrients initially originate from the dissolved bedrock, but are also added through the deposition of organic matter and microbial N fixation from the atmosphere by bacteria and plants (Jenny 1941; Lehmann and Kleber 2015). In agricultural soils, nutrients are also added in the form of chemical and biological fertilisers. The structure of the soil is determined by the shape, size, and arrangement of soil particles which in turn determines the characteristic of the soil pores and their ability to facilitate water retention and flow within the soil (Bronick and Lal 2005). The stability of soil structure is quantified by aggregation.

1.2.1. Aggregation

Aggregates are secondary particles formed by combining organic and mineral particles. Soil aggregates are categorised by size, the main groups being microaggregates (< 250 μm) and macroaggregates (> 250 μm) (Tisdall and Oades 1982). Microaggregates are primarily formed through the bonding of organic molecules to clay with polyvalent cations such as Si^{4+}, Fe^{3+}, Ca^{2+}, and Al^{3+} acting as bonding agents. Macroaggregates can form through the accumulation of microaggregates (Edwards and Bremner 1967; Totsche *et al.* 2018). Alternatively macroaggregates can form as microbial activity breaks down particulate organic

matter to produce adhesive exudates that bind surrounding particles. Plant roots and fungal hyphae can also produce adhesive exudates that can bind soil as well as physically enmeshing particles (Six *et al.* 2004). These processes lead to a complex, heterogeneous substance that determines the functionality, productivity, and overall quality of the soil. The breakdown of soil structure limits the quality of the soil and can have detrimental environmental impacts.

Aggregate stability is integral for maintaining soil porosity. Soil pores can range from < 100 µm to > 1000 µm including micropores and macropores (Stirzaker *et al.* 1996; Pagliai *et al.* 2004). The former can be classed as textural porosity and is usually located within aggregates and is more affected by soil texture than by soil management. The latter can be classed as structural porosity and comprise voids such as cracks, bio-pores, and anthropogenically induced macrostructures (a result of tillage for example). Structural porosity represents interconnected pathways that facilitate the movement of water into and through the soil (a mechanism called hydraulic conductivity) and is more sensitive to soil management practices and compaction than textural porosity (Guérif *et al.* 2001; Dexter 2004). Soil porosity is also required for gaseous exchange in the soil resulting from the respiration of micro-organisms and the decomposition of organic matter. Soil infiltration rates are dependent on soil hydraulic conductivity which determines how efficiently it can drain surface water.

1.2.2. Soil degradation

Studies show that the quality of our soils is rapidly declining and estimate that between 24 % (Bai *et al.* 2008) and 40% (Caspari *et al.* 2015) of the Earth's land mass is already degraded to a moderate or high degree. Some soil degradation is a product of the soil characteristics and climate, however most has anthropogenic origins.

Current agricultural practices are widely understood to be a significant contributing factor to the poor state of our soil and intensification will only exacerbate this (Bai *et al.* 2008; Tscharntke *et al.* 2012; Gibbs and Salmon 2015; Lal 2015). When soil becomes initially degraded, practices are intensified to keep up with demand which, in turn, degrades the soil further in a self-perpetuating loop (Braun et al., 2013).Yet, soil degradation is not a contemporary or inconsequential issue. Indeed, entire previous civilisations failed to adequately manage otherwise fertile soil, contributing to their demise (Olson 1981; Lal 2009). As the Maya population grew, they were unable to maintain their sustainable crop rotations and kept up with demand by intensifying their agricultural practices that lead to catastrophic degradation and erosion of their soil (Beach *et al.* 2006). The Maya population so severely degraded the soil that even after 100 years of abandonment to the rain forest, the depleted soil has not yet recovered and still show signs of nutrient depletion (Olson 1981). More modern examples of catastrophic mismanagement of soil include the erosion of the American dust bowl and Russian steppes (Baveye *et al.* 2011). Many of the scenarios leading up to the failure of Mayan agriculture are being witnessed today, so it would be prudent to learn from our history and not follow in their footsteps.

Soil degradation is the result of a complex, interlinked and multifaceted group of processes that result in the general decline of soil quality and productivity. Conceptually, soil degradation can be split into three categories: chemical, biological, and physical. Degrading processes are linked and can have cascading effects. If the causes are not alleviated, or if the symptoms are too severe that they cannot be mitigated, the process of degradation is a negative feedback loop that both increases soil degradation and its susceptibility to further degradation (Figure 1.1).

Chemical degradation is related to impacts on soil chemical properties that limit the availability of nutrients through the loss of soil nutrients or organic matter. Loss of nutrients can be caused by excessive mono-cropping (Horst and Härdter 1994) and nutrient leaching (of water soluble nutrients such as nitrogen and phosphorus) (Gärdenäs *et al.* 2005). Other processes such as salination and acidification are usually the result of poor irrigation practises (Rengasamy 2006; Guo *et al.* 2010) and can reduce the availability of nutrients such as phosphorus, calcium, magnesium, and potassium (von Uexküll and Mutert 1995). Soil with depleted organic matter are prone to other forms of degradation such as compaction and crusting which destroys structural pores that enable infiltration and increases runoff. Surface flow is one of the main mechanisms that facilitate soil erosion and leads to a further reduction of aggregate stability (Lal, 2015).

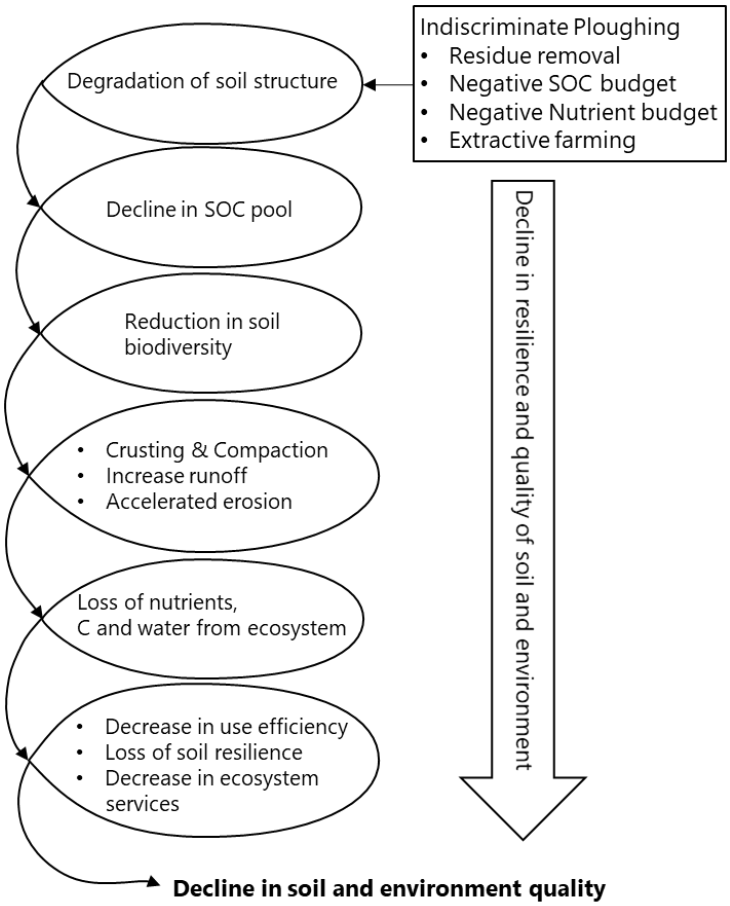

Figure 1.1. The downward spiral of soil quality as a result of some anthropogenic factors (redrawn from Lal, 2015).

Biological degradation is often a consequence of chemical degradation as it relates to the reduction in the bio-diversity of the soil micro- and macro-organisms, which are essential for the breakdown and availability of nutrients as well as many other

beneficial qualities (Tilman *et al.* 1996; Maeder *et al.* 2002). Other causes can include drought, ploughing, and surface sealing (due to construction). Biological degradation also refers to the depletion of soil organic carbon pool which causes the emission of greenhouse gasses into the atmosphere and can make soil a net source as opposed to a net sink for CO_2 (Lal 2003). All aspects of chemical and biological degradation limits the productivity of the soil, however, this thesis will focus on physical degradation.

Physical degradation refers to the breakdown in soil structure and displacement of soil from its site of origin. The ecosystem services that soil provides rely on the maintenance of its structure. Good soil structure requires a complex network of interconnected pores. These pores are essential for nutrient transport, efficient soil gas regimes (to below-ground soil biota and from emissions from soil respiration), unimpeded passage of soil biota (such as plant roots, micro- and macro- organisms) and infiltration. The soil structure can be degraded by anthropogenic processes such as ploughing and the passage of machinery and livestock as well as processes that reduce the organic matter content in the soil.

1.3. Soil erosion

Soil erosion encompasses a three part process in which soil particles are detached and then transported away from their original location by erosive agents such as water and wind and deposited elsewhere (Morgan 2005), but water is the most prominent erosive force in Europe (Verheijen et al., 2009). With an estimated 56 % of arable land at risk, soil erosion is one of the main concerns resulting from soil degradation (Jankauskas *et al.* 2008). The implications of soil erosion are far reaching and estimated to cost the UK more than £460 million per year (Posthumus *et al.* 2015). The largest and most costly economic impact of soil erosion is the damage to property and other

inconveniences that come with increased flood risk and magnitude (Posthumus *et al.* 2015). On-site effects result in farmers needing to apply increasing amounts of fertiliser to compensate for the loss of fertile topsoil, increased difficulty of working the land, and reduced rooting depth for crops (Evans and Nortcliff 1978; Lal 2009). The average rate of soil production is estimated to 114 ± 11 mm kyr^{-1} (Stockmann *et al.* 2014), however, this is highly variable and dependent on a plethora of environmental and physiological factors, including climate, topography, vegetation cover, land use, parent material, and hydrological cycles (Heimsath *et al.* 2001; Montgomery 2007). Nevertheless, in the short term soil is regarded as a non-renewable or finite resource (Doran 2002; McBratney *et al.* 2014; Lal 2015). However, in some places in the world, soil erosion is reaching rates 100 times greater than that of its production (Banwart 2011).

The severity of soil erosion depends on the detachment force of runoff/raindrops, and the cohesive bonds in the soil (Laflen *et al.* 1991). For a particle to be displaced, the erosive force of water (its quantity and velocity) has to exceed that of forces keeping it stationary (its mass and bonds to the rest of the soil). Once soil particles have been detached, they are then transported down slope. Finer soil particles are preferentially transported over larger particles as they require less force to move, however, with greater erosive force comes the ability to move greater sizes of soil particles. The kinetic energy of water can be dissipated by increased surface roughness so that only a fraction remains for erosion (Pearce 1976). Thus, protruding stones/rocks and plant matter as well as topographical features in the soil (such as peaks and cracks) can reduce the velocity of surface flow and consequent erosive forces. With inter-rill or sheet erosion, the erosive force is spread across a large surface area of soil, so only small amounts of soil is lost from a wide area, but on slopes of increasing gradient,

runoff can develop into concentrated flow and score channels in the soil called either rills or gullies, depending on their size (Shi *et al.* 2012). Rills are commonly on a smaller but more numerous scale, whereas gullies are often much larger depressions (Gyssels and Poesen 2003). The erosion rate in rills and gullies far exceed that of sheet erosion because the kinetic energy of the flowing water is more focused into a smaller hydraulic radius thus producing a greater velocity (Morgan 2005).

During rainstorms, soil pores get saturated and infiltration rates decrease. Once infiltration rates decrease below rainfall intensity, surface water will form (Horton 1945). The infiltration capacity of soil is heavily dependent on soil texture and porosity. Soils consisting of large particles (such as sand) or stable macroaggregates generally have a more extensive network of pores and therefore a bigger infiltration capacity. The kinetics of the erosive force, in this case water, influences the severity of erosion, with increasing force comes a greater capacity to transport soil particles. The breakdown of aggregates also exacerbates soil erosion as it has already disrupted the bonds between soil particles making them easier to transport (Morgan 2005).

1.3.1. Breakdown of aggregates by water

The breakdown of soil aggregates is detrimental to soil quality and limits soil hydraulic conductivity thereby reducing its infiltration capacity and increasing its susceptibility to erosion (Figure 1.2). The breakdown of aggregate stability leads to the reduction of pore space, either due to the reduction in the internal strength of soil aggregates or by the infill of displaced particles. The reduction in soil porosity decreasing the rate at which water can be drawn down from the surface and consequently increase the amount of surface water and the risk of erosion. This

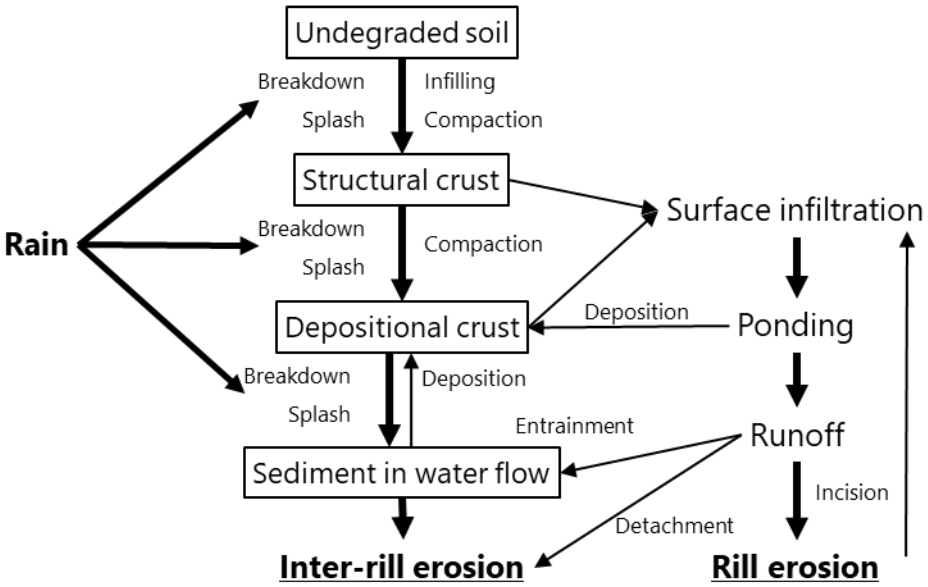

Figure 1.2. Diagram showing the relationship between aggregate breakdown, crusting and erosion (redrawn from Le Bissonnais, 1996).

phenomenon directly reduces a soils effectiveness to supply ecosystem services such as food production and increases the risk of soil erosion (Oldeman 1994; Lal and Stewart 2012).

The causes of aggregate breakdown by water are numerous and complex, but four distinct categories can be found: slaking, breakdown by differential swelling, physico-chemical dispersion due to osmotic stress, and breakdown by raindrops (Le Bissonnais 1996). The processes involved in the disaggregation of soil can range in scale from the dispersion of clay particles to the breakup of larger macroaggregates (Tisdall and Oades 1982; Oades 1984). Disaggregation processes are influenced by the quality of the soil inter-particle bonds, the kinetics of the breakdown process, soil physical properties (such as texture and cation exchange capacity), and the size, nature, and distribution of the causal mechanisms (Bresson and Boiffin 1990; Le Bissonnais 1996). The size of the resulting fragments and the intensity of the disaggregation process will determine how severe the implications are.

Slaking is caused by the internal pressure resulting from the compression of air trapped inside dry aggregates when rapidly wetted (Figure 1.3). The pressure exerted on the trapped air forces it out of the aggregate, destroying and dispersing soil particles in the process (Hillel 2008). The severity of slaking increases with the quantity of trapped air inside the aggregates and the speed at which wetting occurs, whereas aggregate stability reduces the risk of slaking (Loch 1994). Slaking usually acts on the pores of macroaggregates so the resulting fragments are usually microaggregates, with sizes increasing with the clay content of the soil (Chan and Mullins 1994; Le Bissonnais 1996; Ruiz-Vera and Wu 2006). Greater clay content means that the primary particles are larger and more resistant to slaking. However, as this process can break aggregates down into their component parts, its impact on infiltration can be severe as small particles can easily block pores.

Differential swelling is the result of soils swelling when wet and shrinking again when dry and such cycles cause cracks to form in aggregates (Piccolo *et al.* 1997). The soil properties regulating disaggregation by this process are similar to those involved with slaking, such as speed of wetting/drying and aggregate stability. However, whereas the risk of slaking decreases with increasing clay content, the risk and severity of breakdown by differential swelling increases with increasing clay content. The greater

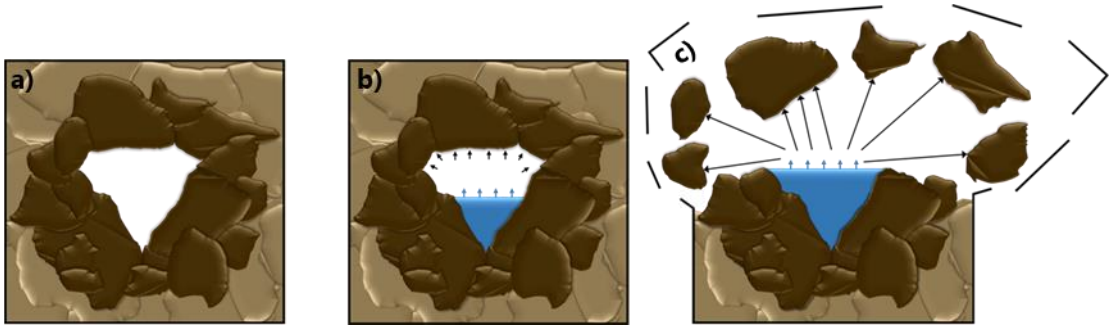

Figure 1.3. The mechanisms involved with slaking. When the aggregate is dry (a), the pores are filled with air. As the aggregate is wetted, water starts to fill the pores and the trapped air is compressed and put under increasing pressure (b). The pressure of the trapped air continues to build until it exceeds the bonds of the aggregate, resulting in an explosive force that both destroys the aggregate and disperses the particles (c).

the clay content, the more susceptible to swelling the soil becomes (Ruiz-Vera and Wu 2006). The particle fragments resulting from breakdown due to differential swelling are usually bigger than the size of slaking and are restricted to soils with a large clay content so therefore have a lesser impact on infiltration (Le Bissonnais 1996). Additionally, the swelling and shrinking of clay soils can increase the volume of pores in the soil facilitating infiltration (Chertkov and Ravina 1999).

Aggregation of clay particles in soil is largely controlled by the chemical bonds resulting from the polarisation of clay particles (faces are negatively charged, whereas the edges are positively charged). The polyvalent cations in the soil facilitate the aggregation of clay particles, however, the hydrated cations in water often have smaller charges and are more effective at dispersion than flocculation (Chibowski 2011). Physico-chemical dispersion is essentially the reduction of chemical attractiveness between the elementary particles making up the soil aggregates (Lagaly and Ziesmer 2003). The size and valance of the cations in the soil and water will determine the severity of dispersion. Physico-chemical dispersion of soil particles disaggregates soil at a molecular level, resulting in very small fragments that can easily block pores (Bresson and Boiffin 1990).

The speed at which raindrops hit the soil is determined by their size and consequent terminal velocity. The size of a raindrop can range from 0.1 mm to 5 mm (Marshall and Palmer 1948). Thus, the terminal velocity of a raindrop 5 mm in diameter will be 9 m s^{-1} at impact with the soil (Udoimuk, *et al.* 2013). Repeated exposure of this can have an incredible impact on soil. When droplets hit the soil, the compressive force of the falling water is redirected laterally at flow velocities eight times greater than the velocity of impact (Engel 1955), referred to as the splash effect. Thus, the initial

impact of raindrops break up soil aggregates, then dislodge and disperse the resulting fragments (Nearing and Bradford 1985). Dispersed fragments can travel up to 1.5 m away from their original location (Al-Kaisi and Licht 2005). However, increasing surface water will dissipate the erosive force of raindrops (Torri *et al.* 1987). Due to the forces achieved by raindrops, they can disrupt large and stable aggregates and the resulting fragments can be reduced to small microaggregates or elementary particles (Le Bissonnais 1996). Thus, disaggregation by raindrops can have severe impacts on infiltration and other ecosystem system services that rely on the stable network of soil pores.

1.3.2. Soil crusts

As mentioned above, the breakdown of aggregates can block pores, negatively impacting infiltration rates and other ecosystem services that rely on the existence of a structured pore network. However, another consequence of disaggregation is the formation of surface crusts (Valentin 1991). Soil crusts form in two ways. Structural soil crusts result from the gradual coalescing and packing of small microaggregates and particles derived from passive disaggregation processes such as slaking (as mentioned above). Depositional or sedimentary crusts are formed as fine soil particles and microaggregates are preferentially sorted through dispersion (from raindrops) or sedimentation (under waterlogged conditions). Structural crusts are normally rapidly formed during initial wetting whereas depositional crusts coincide with water levels required for erosion (Le Bissonnais 1996). Disaggregation accelerates the formation of crusts under both scenarios as it reduces the mean size of soil aggregates and consequently crusting is influenced by the same properties as disaggregation, such as the quality of soil inter-particle bonds, kinetics of dispersion processes, and soil

physical properties (Le Bissonnais 1996). Soils with greater clay contents are more susceptible to the development of crusts.

1.3.3. Mass movement of soil

Mass soil wasting events occur when soil fails on a shear plane and can range in scale from riverbanks to entire mountainsides. Small scale events can increase sedimentation of rivers, whereas large scale events can destroy properties and cause loss of life. Landslides, like most erosive processes, are a result of hydraulic pressure causing soil to succumb to gravity. Put simplistically, landslides occur if the shear strength of the soil is surpassed by the shear stress exerted on the soil. The weight of the soil and the pull of gravity are the main stressors acting on a sloped soil and the added weight of rainwater from a storm event is often the catalyst for a mass wasting event. In this case, the added weight of precipitation exploits a layer of weakness (a failure plane) in the soil and detaches sheets of soil (Iverson 2000). However, mass wasting events can also be caused by overloading of other kinds (such as development) and through shakes and tremors (a result of tectonic movement or anthropogenic causes such as explosions or large machinery). Ground water incursion can also form a layer of weakness that can be exploited by shear stresses (Záruba and Mencl 2014). As well as spatial scales, mass soil wasting events can occur in a range of temporal scales, from the dramatically fast flowing landslips to the slower paced soil creep. The susceptibility of a soil to erosion can be reduced by either internally promoting aggregate stability or introducing soil reinforcement.

1.4. Plant mitigation of soil erosion

1.4.1. Plant canopies and stems

Much research has investigated the effects of above-ground plant biomass on soil erosion. Vegetation has widely been credited with dampening the impact of water on soil, thus limiting soil erosion (Mohammad and Adam 2010). Vegetation cover can intercept raindrops reducing the dispersion of soil particles by up to 80% compared with bare soil (Mills and Fey 2004). Plants can reduce the amount of surface water, thus reducing its erosive force, by storing rainwater in the canopy delaying or preventing it from reaching the soil surface (Hall and Calder 1993). Furthermore, they can reduce the amount of water in the soil by evapotranspiration, allowing greater infiltration during rainfall events (Jobbágy and Jackson 2004). When rainfall events occur at such intensity that surface water is produced, plant stems can act as physical barriers, increasing surface roughness and dampening concentration flow and limiting erosive forces (Fasching and Bauder 2001; Melville and Morgan 2001; Xiao *et al.* 2011; Lambrechts *et al.* 2014; Mekonnen *et al.* 2016; Li and Pan 2018). Additionally, plant derived organic matter facilitates aggregate stability, which in turn benefits soil structure and infiltration (Martens and Frankenberger 1992). However, recent research emphasises that plant roots can prove more influential in mitigating soil erosion than the above-ground matter (Prosser *et al.* 1995; Ghidey and Alberts 1997; Mamo and Bubenzer 2001a; De Baets *et al.* 2006; Zhou and Shangguan 2007, 2008; Burylo *et al.* 2012).

1.5. Root mitigation of soil erosion

Although dense grass stems significantly reduced surface erosion by increasing flow resistance, following their removal the remaining dense root matting prevented erosion from scouring further than 0.7 mm deep, even after a prolonged period of

concentrated surface flow (Prosser *et al.* 1995). Generally, the ability of roots to impact aggregate stability and soil erosion can be summarised into two key concepts. Firstly, mechanical reinforcement provided by the roots bind the soil, providing physical support for structural pores and anchor the aggregates together. There is a strong negative relationship between increasing biomass and sediment yield (Gyssels *et al.* 2005; Vannoppen *et al.* 2015). Living and decaying root matter can contribute up to 2.3 times more organic matter than above-ground biomass (Kätterer *et al.* 2011) having a greater effect on aggregate stability (Li and Li 2011). Thus roots facilitate structured water pathways that reduce overland flow and the risk of displacing soil particles. Secondly, the chemical reinforcement resulting from root exudates act as soil binding agents, forming hydrophobic barriers between soil particles that maintain aggregate stability. Roots and their exudates also attract micro-organisms that contribute further to the chemical soil binding agents (Swaby 1949; Gyssels and Poesen 2003). It is a testament to the ability of roots to reinforce the soil that they are frequently used in models to assess slope stability (Dietrich *et al.* 1995; Gyssels *et al.* 2005; Stokes *et al.* 2009).

Anchorage is one of the main mechanisms by which plants reinforce the soil. Ennos (1989) explains that the anchorage ability of a root is a result of a complex balance between forces. The strength of the soil and roots as well as their level of adhesion are the key factors determining the resistance to shear stress. If the strength of the root-soil bond and the tensile strength of the root is greater than that of the soil's structural strength, the fracture zone will travel the length of the root until it is pulled out. If the root-soil bond and soil strength is greater than that of the root, the failure front will travel down the root in equilibrium until the shear strength outweighs the tensile strength of the root, in which case the root will break (Pollen 2007). The

characteristics of different roots, such as diameter, branching and orientation lend themselves to different aspects of reinforcement. The perpendicular protrusions of lateral roots form a dense matting in shallow soils. Though small in diameter, the branching lateral roots enmesh the soil dispersing the fracture zone and increasing the pull out resistance of the root and, by association, the in-plane tensile strength of the soil (Anderson *et al.* 1989; Stokes *et al.* 1995; Zhou *et al.* 1998). Axile roots are larger in diameter and can withstand greater forces than lateral root. Vertical axile roots cross failure planes anchoring the dense lateral root mats into the deeper and more stable soil. The anchorage capability of roots increase with length up to a critical breaking point which is largely determined by root diameter and structure (Ennos 1989, 1990).

1.5.1. Fine roots

There are large gaps in the understanding of fine root function, due largely to the arbitrary diameter classification homogenising all roots < 1-2 mm and sometimes < 3 mm in a non-uniform terminology (Gyssels *et al.* 2005). In cereal crops, two easily distinguishable subcategories of fine roots have been identified. The first category includes the larger seed-derived seminal roots and stem-derived nodal roots and brace roots (hitherto referred to as axile roots). The second category consist of thinner roots derived from lateral branches (hitherto referred to as lateral roots). Lateral and axile roots have distinctive functionality. Axile roots have a low mortality rate and are relatively slow growing, whereas lateral roots tend to make up the majority of the root mass, developing quickly in response to available nutrients. However, these are more ephemeral, dying off when no longer needed (Drew 1975; Cahn *et al.* 1989). Their divergent functions are also evident from their differing morphologies. Lateral roots have a greater capacity for water absorption; whereas

axiles are more equipped to transport water and nutrients absorbed by the laterals (Varney *et al.* 1991; Doussan *et al.* 1998; Carminati 2013; Ahmed *et al.* 2015). Although lateral and axile roots vary in their traits, their relative impact on soil erosion has not yet been evaluated.

1.5.2. Root hairs

Though studies have identified a relationship between roots and their ability to affect soil degradation and erosion, little is known about how root traits, such as root hairs and mucilage, contribute to this phenomena. Root hairs play a significant part in binding soil particles to the root. Root systems with longer, denser root hairs bind more soil particles, thus increasing rhizosheath diameter, more so than root systems with lesser root hairs (Watt *et al.* 1994; Haling *et al.* 2014; George *et al.* 2014). The soil that remains adhered to the root after extraction is called the rhizosheath and root hairs are integral to its formation (McCully 2005; Ma *et al.* 2011; Brown *et al.* 2017; Pang *et al.* 2017). Several studies comparing the rhizosheath forming capacity of root

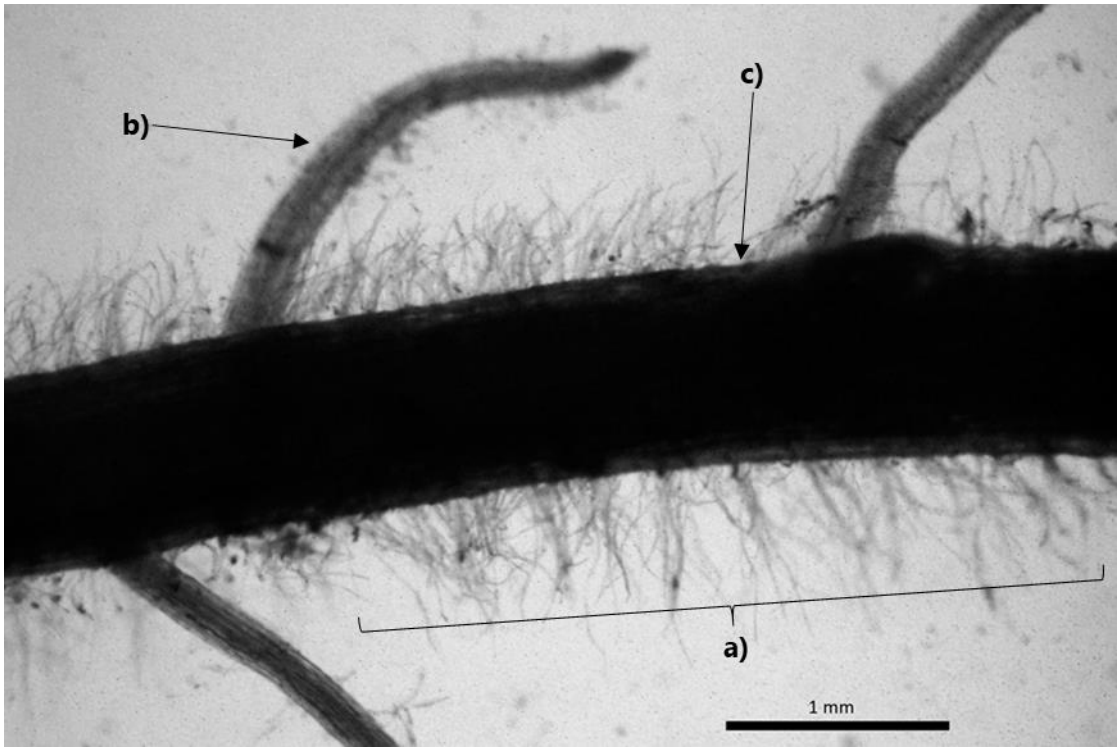

Figure 1.4. Image of root hairs (a) and lateral roots (b) on a maize axile root (c) of a maize root.

systems with and without root hairs have shown that root hairs can account for more than 80 % of the soil bound to the roots (Haling, Richardson, *et al.* 2010; George *et al.* 2014; Brown *et al.* 2017). Species that are naturally void of root hairs, such as several species from the *Allium* genus, do not form a rhizosheath (Brown *et al.* 2017).

A root hair is a tubular protrusion from a root's epidermal cell (Figure 1.4). They are present on all major groups of vascular plants which signifies a long evolutionary history and indicates a link between root hairs and a plant's ability to cope with a changing environment (Peterson and Farquhar 1996). Their development is initiated by the unequal division of cells in the meristematic zone called trichoblasts and atrichoblasts. All atrichoblasts have the potential to elongate perpendicular to the root and form root hairs. Depending on the species, the diameter of root hairs can be between 5 µm and 17 µm, the length can be as long as 1500 µm or as short as 80 µm, with no correlation between the length and width (Dittmer 1949). Root hairs cover most fine roots and can account for as much as 77 % of the total surface area of a root system (Parker *et al.* 2000) and their total length is 20 times that of the larger root system (Wulfsohn and Nyengaard 1999). The physiological significance of root hairs has only recently been investigated.

Root hair characteristics are determined by the species, as previously mentioned, but also by environmental factors (Datta *et al.* 2011), such as nutrient (Nestler *et al.* 2016) and water availability (Haling *et al.* 2014), as well as soil structure. Root hair growth, as with other roots, is restricted by increased soil strength resulting in shorter length (Haling *et al.* 2014). However, root hairs compensate for increased mechanical impedance by increasing in number (Misra and Gibbons 1996). This reaction may be because root phytohormonal responses to mechanical impedance also regulate root

hair growth (Kays *et al.* 1974; Dolan 1997; Pitts *et al.* 1998). Indeed, greater soil mechanical impedance stimulated root hair growth in a barley mutant (*NRH*) that otherwise would not have produced root hairs (Haling *et al.* 2014). When comparing root hair traits between soil and solution cultures, root hairs are more abundant when the roots were in contact with the soil (Mackay and Barber 1984) and root hairs lengthen as soil aggregate size increases (Misra *et al.* 1988). Therefore, many environmental factors affect root hair proliferation, and soil penetration resistance is a prominent factor.

One of the main functions of root hairs is believed to be providing roots with anchorage. Root hairs are initiated immediately behind the root elongation zone (Bertin *et al.* 2003). The theory behind this is that root hairs anchor the growth tip allowing it to penetrate the soil without deforming the rest of the root or pushing the plant from the soil (Bengough *et al.* 2011; Haling *et al.* 2013). Root hairs are much smaller in diameter than their parent roots, allowing them to penetrate pore spaces that other roots cannot access (Rasse *et al.* 2005). Further to this, Bengough *et al*. (2016) found that seedlings with root hairs are more efficient at establishing themselves in the soil and required five times the force to pull out than seedlings without root hairs. Other research has also noted cohesive forces of root hairs (Stolzy and Barley 1968; Ennos 1989; Czarnes *et al.* 1999). Since root hairs are so strongly associated with root anchorage, it is logical to assume that they also reinforce the soil they are anchored to.

Adhesive bonds within rhizosheath soil can be so strong that they can resist sonication (Brown *et al.* 2017) and rhizosheaths can remain intact in a field setting long after the root has died (Williams and Weil 2004). Though not explicitly connected with soil stability the presence of root hairs significantly increases the amount of soil that a root

can bind. However, studies involving root hairless mutants report that roots void of root hairs still can bind soil, albeit at a far reduced amount, showing that there are other factors involved in rhizosheath formation (Haling, Richardson, *et al.* 2010; George *et al.* 2014; Brown *et al.* 2017).

1.5.3. Mucilage

Root exudate is a term that encompasses the total range of compounds released by the root system. The exact composition differs between species, but exudates include a range of compounds, including those that have no apparent function except as waste products of internal metabolic processes and others that aid external processes, such as root lubrication and facilitation of nutrient uptake (Bertin *et al.* 2003). Polysaccharides are the molecules in root exudates that are most associated with soil aggregation and rhizosheath formation, and are collectively referred to as root mucilage. Their gelatinous glue-like consistency is well known to bind soil particles together (Morel *et al.* 1991; Piccolo and Mbagwu 1999; Czarnes, Hallett, *et al.* 2000; Galloway *et al.* 2018). As root mucilage binds soil it can form hydrophobic barriers that aid water retention at the soil-root interface (Young 1995; Carminati *et al.* 2010). However, not all substances in root exudates are adhesive (Read *et al.* 2003; Akhtar *et al.* 2018). Organic acids have been linked to the dispersion of soil particles, and limit soil aggregation (Oades 1984; Goldberg *et al.* 1990; Read *et al.* 2003; Naveed *et al.* 2017), but are believed to increase the availability of root accessible phosphate and micronutrients in the soil solution (Hinsinger 2001). Thus, root exudate composition can readily alter the interactions at the root-soil interface depending on the plants water and nutrient uptake strategies.

1.6. Thesis structure, aims and objectives

This thesis aims to understand whether various root traits contribute to soil reinforcement and erosion mitigation. There is currently limited knowledge relating to the impact of root hairs and root exudates on soil reinforcement. Both can potentially bind and anchor soil in close proximity to the root, e.g. the rhizosheath soil, but neither have been assessed in their ability to aid the root in mitigating soil erosion on larger scales. To evaluate this, mutants lacking root hairs were compared to their respective wild-types (root hairs present) and subjected to various erosion environments across different spatial scales:

Chapter 2 will aim to understand which root traits, including root hairs and exudates, most influence a plant's ability to bind soil and form a rhizosheath, using individual plants grown in pots.

Chapter 3 will assess whether the traits identified above as having a significant impact on rhizosheath formation also reinforce soil under shear stress, again using individual plants grown in pots.

Chapter 4 will utilise a laboratory rainfall simulator and multiple plants grown in a mesocosm to assess whether the ability to bind soil on a small scale translates to mitigating soil erosion under rainfall conditions.

Chapter 5 will assess whether any of the observations made under laboratory settings in the previous chapter translate to a more stochastic "natural" environment with field-grown crops.

Chapter 2. Root hairs are the most important root trait for rhizosheath formation.

2.1. Introduction

2.1.1. Rhizosheath history

Reportedly first described as a "peculiar sheath" by Volkens (1887), the rhizosheath has since been defined as the soil that remains adhered to the root after the root has been extracted from the bulk soil (McCully 2005; Ma *et al.* 2011; Brown *et al.* 2017; Pang *et al.* 2017). This differs from the rhizosphere, which is a spatially and temporally varying area of influence around the root (Hinsinger *et al.* 2005). Rhizosheaths were first thought to only be a trait of grasses in sandy, arid environments (Price 1911; Bristow *et al.* 1985), a misconception that has persisted and constrained much of the rhizosheath research carried out to date (Moreno-Espíndola *et al.* 2007; Bergmann *et al.* 2009; Shane *et al.* 2010; Hartnett *et al.* 2013; Benard *et al.* 2016). However, rhizosheaths have since been reported in a multitude of climates (Smith *et al.* 2011), soil types (Haling, Simpson, *et al.* 2010; Pang *et al.* 2017) and on the roots of many species, including cacti (Huang *et al.* 1993; North and Nobel 1997), legumes (Sprent 1975; Unno *et al.* 2005), cereal crops (Watt *et al.* 1994; Ma *et al.* 2011), and many others (Brown *et al.* 2017). The almost ubiquitous nature of the rhizosheath implies it is of physiological significance to plants and a fundamentally important root trait.

2.1.2. Rhizosheath formation

Rhizosheath formation is predominantly dependant on root traits such as the presence of root hairs (Watt *et al.* 1994; Haling *et al.* 2014; George *et al.* 2014), and root mucilage (Watt *et al.* 1994; Albalasmeh and Ghezzehei 2013; Carminati *et al.* 2017).

However, soil features such as strength, porosity (Haling *et al.* 2014), and water content (Watt *et al.* 1994; Czarnes, Dexter, *et al.* 2000; Haling *et al.* 2014) can influence the process. Soil biota associated with the root system can also contribute to rhizosheath formation via microbial-derived mucilage (Watt *et al.* 1993; Czarnes, Hallett, *et al.* 2000) and the enmeshing of soil hyphae from mycorrhizal fungi (Degens 1997; Moreno-Espíndola *et al.* 2007). Thus biological, chemical and physical interactions in the rhizosphere contribute to rhizosheath formation (McCully 1999).

2.1.3. Function

The capacity of the rhizosheath to protect the root against drought stresses has been observed for over 100 years (Price 1911). Recent studies have shown that rhizosheaths alter the water dynamics in the soil proximal to the root. The rhizosheath soil is more protected against shrinkage than the bulk soil resulting in fewer large gaps thus protecting the root from the high hydraulic resistance that air pockets cause (North and Nobel 1997; Koebernick *et al.* 2017), facilitating unimpeded movement of water throughout the root zone, however the barriers themselves can offer some resistance (Benard *et al.* 2016). Other studies have shown that the rhizosheath can not only decrease hydraulic resistance during rewetting, but rhizosheath properties help to retain water close to the root when the bulk soil is drying (Carminati *et al.* 2010). These traits generally result in the rhizosheath soil having a greater water content than in the bulk soil (Young 1995). In addition to relieving drought stresses, rhizosheath soil has been associated with alleviating nutrient deficiencies. Rhizosheaths can perform these functions because they alter the surrounding soil and maintain close contact at the soil-root interface (McCully 1995).

By maintaining close soil bonds at the root surface, the rhizosheath also reinforces the soil. As well as the added benefits to the roots, this enables the rhizosheath to provide

structure and stability to the soil (Watt *et al.* 1993; Czarnes *et al.* 1999; Czarnes, Dexter, *et al.* 2000; Ola *et al.* 2015; Brown *et al.* 2017). The stability of a rhizosheath has been reported to outlive the original root, leaving pathways for future root or water infiltration (Williams and Weil 2004). Stabilisation of soil can prevent degradation and maintain the productiveness and fertility of agricultural soils.

2.1.4. Formation

Root hairs are single celled cylindrical protrusions from the root epidermis of most plant species (Dolan and Costa 2001) and are a key component in rhizosheath formation. Root hair length is often deemed to determine the radial extent of the rhizosheath (Wullstein and Pratt 1981; Delhaize *et al.* 2015). They enmesh the soil particles and penetrate aggregates, further securing them to the root (Hinsinger *et al.* 2009; Brown *et al.* 2012). However, root hair length becomes less correlated with rhizosheath with increasing length (Brown *et al.* 2017) and roots void of root hairs can still form a deficient version of a rhizosheath (Wen and Schnable 1994; Haling, Simpson, *et al.* 2010; Haling *et al.* 2014; George *et al.* 2014), showing that other root traits are involved in rhizosheath formation.

Root mucilage is also deemed a necessary feature in rhizosheath formation. Root mucilage is a sticky polysaccharide-rich gel-like substance secreted from the root epidermis (Bertin *et al.* 2003; Akhtar *et al.* 2018). All parts of the root system produce mucilage, though the composition and quantity varies between species (Vančura and Hanzlíková 1972; Fan *et al.* 2001). Root hair mucilage is chemically dissimilar to that produced by the main root (Pena *et al.* 2012; Muszyński *et al.* 2015). Hydrated root mucilage permeates soil particles and, when dry, forms hydrophobic bonds between particles (Carminati *et al.* 2010; Albalasmeh and Ghezzehei 2013). At low concentrations, thin filaments are formed, but with increasing mucilage concentration,

these filaments can become a network of stable barriers (Carminati *et al.* 2017). At artificially high quantities, mucilage can form such a comprehensive network of hydrophobic barriers that they can impede the passage of water (Benard *et al.* 2016).

Due to the innate complications involved with harvesting root exudates from the soil (Oburger and Jones 2018) and the difficulties associated with observing root hairs *in situ* (Gyssels *et al.* 2005; Koebernick *et al.* 2017), direct comparisons are hard to find. Additionally, root hair traits differ greatly between species (Brown *et al.* 2017) and even show variation between different root types of the same root system (Dittmer 1949) as does the composition of root mucilage (Foster 1982; Pena *et al.* 2012; Muszyński *et al.* 2015). For these reasons, the effects of root mucilage and root hair traits on rhizosheath formation have not been compared in unison. This paper aims to combine methods previously used in isolation to quantify and compare the relative contribution of root hairs and root exudates to rhizosheath formation. This study will compare the rhizosheaths of root hairless mutants from three species [barley (*Hordeum vulgare* L.), maize (*Zea mays* L.), and *Lotus japonicus* (Gifu)], with their respective wild types (WT) with root hairs. Moreover, root hairs and exudates from different root orders will be investigated to determine intra-species variation in rhizosheath formation.

2.2. Materials and methods

2.2.1. Genotypes

The three mutants used in this experiment have different origins. The barley root hairless mutant is a spontaneous mutation with its genetic background in Pallas, a spring barley cultivar. It was discovered during a germination experiment by Gahoonia et al. (2001) and aptly named bald root barley (*brb*). Conversely, the maize

mutant, *rth3* (Wen and Schnable 1994) and the *L. japonicus* mutant, *Ljrhl1*(Karas *et al.* 2005) are the result of complex processes to isolate specific genes.

2.2.2. Germination and growth

Lotus japonicus seeds were first carefully scoured using sand paper and the maize seeds were initially sterilized using 10 % bleach for 5 minutes, then rinsed thoroughly with deionised (DI) water. Sterilization was unnecessary for the barley and *L. japonicus* seeds because of low levels of microbial contamination. Once sterilised, the maize seeds, as well as the barley seeds, were germinated in petri dishes containing two sheets of filter paper (Whatman no. 3) moistened with 5 ml of DI water, then left in the dark for approximately 3-5 days at room temperature (approximately 20 °C). The *L. japonicus* seeds were germinated in the soil of the filled pots, approximately five seeds per pot, and covered with foil until emergence at which point the seedlings were thinned out to one shoot per pot. The barley and maize seedlings were transplanted into pots when the radicles were of sufficient length to establish that the root hairs were visually apparent on WT plants and visually lacking in the hairless mutant. Due to the heterozygous[1] nature of the *rth3* seeds, the seedlings were assessed under a dissecting microscope to exclude any that had root hairs present. Since the *brb* and *Ljrhl1* mutants are homozygous[2] mutations, root hair presence did not need to be scrutinised.

After germination and the presence/absence of root hairs was established, the barley and maize seeds were planted 1 cm deep in 4 litre pots (22 cm tall, 17 cm top diameter, 13.5 cm bottom diameter), while *L. japonicus* seeds were germinated on 1.5 litre pots (10.8 cm tall, 15.5 cm top diameter, 11 cm bottom diameter). The soil used

[1] Seeds contain the mutated and the WT DNA sequence
[2] Seeds contain only the mutated sequence of DNA

was a sandy loam textured topsoil (Bailey's of Norfolk LTD; 12 % clay, 28 % silt, 60 % sand and 3 % gravel D50 6 mm, no particles greater than 8 mm, this soil is used throughout this thesis) packed at an approximate bulk density of 1.3 g cm^{-3}. The soil was watered and left to drain until dripping ceased (approximately 48 hrs). At this time, the weight of each pot was recorded as their drained capacity (DC). Each pot was rewetted to DC every second day, allowing for the wetting-drying cycles necessary for rhizosheath formation (Carminati *et al.* 2010; Albalasmeh and Ghezzehei 2013). *Lotus japonicus* plants transpired less water so were rewetted every 2-3 days. Water was withheld for up to three days before harvest to facilitate the effective excavation of the rhizosheath. The plants were cultivated in a walk-in controlled environment (CE) room, set at 24 °C during the day and 19 °C at night with a 12 hour photoperiod.

Each experiment comprised 20 replicates of each genotype, with five harvested on four occasions. For barley and maize these were 5, 10, 15 and 20 days after the seedlings were transplanted into pots. For the much slower growing *L. japonicus*, plants were harvested 32, 44, 58 and 71 days after seed germination.

2.2.3. Quantifying rhizosheath weight

At harvest, the whole plant was systematically extracted from the soil, whilst minimising soil disturbance to retain root-soil contact, as previously described (Young 1995; Veneklaas *et al.* 2003; Ma *et al.* 2011; Haling *et al.* 2014; Pang *et al.* 2017). The entire root system was then soaked in a metal dish filled with water and gently agitated until the rhizosheath separated from the root (Figure 2.1a). Larger aggregates were fragmented using a paint brush and a wash bottle. Immediately after extraction, all root material was sealed, moist, in a plastic bag and stored at 4°C for later analysis.

The dish was then placed in a drying oven at 105˚C to drive off excess water and the rhizosheath weight was recorded after a constant weight was established.

2.2.4. Root measurement

Root systems were scanned within five days of being extracted from the soil, to avoid any visual physical degradation. Roots were placed in a clear plastic tray with a thin film of water and splayed to avoid as much overlap as possible (Figure 2.1b). It was sometimes necessary to separate a single root system into multiple scans. Images were produced as .tiff files in 8-bit grayscale and at a resolution of 600 DPI for barley and *L. japonicus*, and 400 DPI for maize. For barley and maize, images were captured using an Epson Perfection V700, for *L. japonicus* an Epson Expression 11000XL Pro with transparency unit was used. Root length was analysed using WinRHIZO (2013e, Regent Instruments Inc.; Figure 2.1c). Debris with a width to length ratio less than 4 were excluded.

In this thesis, the terms axile and lateral roots are respectively defined as shoot/seed- and root-derived roots (McCully 1999). For *L. japonicus* axile roots include the tap

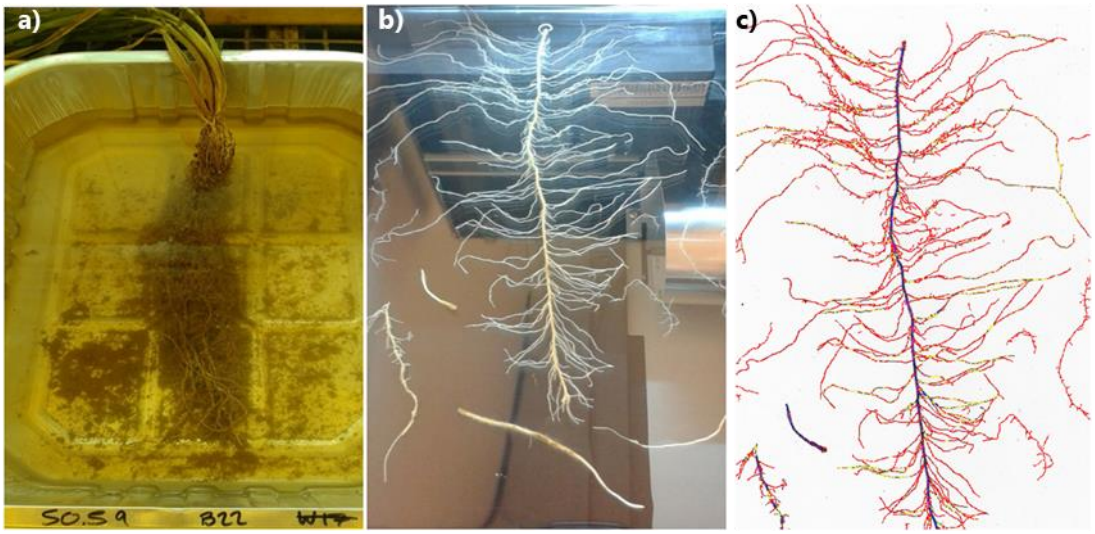

Figure 2.1. Determining rhizosheath weight and root length. First (a), the rhizosheath soil is washed from the whole root system which then gets oven dried to establish rhizosheath weight. Then (b), the roots are splayed out in a clear tray and scanned. The resulting images (c) are analysed in WinRHIZO. The colours on the scanned image represents how appropriate diameter classes can differentiate between root types, with red and yellow roots indicating lateral roots and blue roots indicating axile roots.

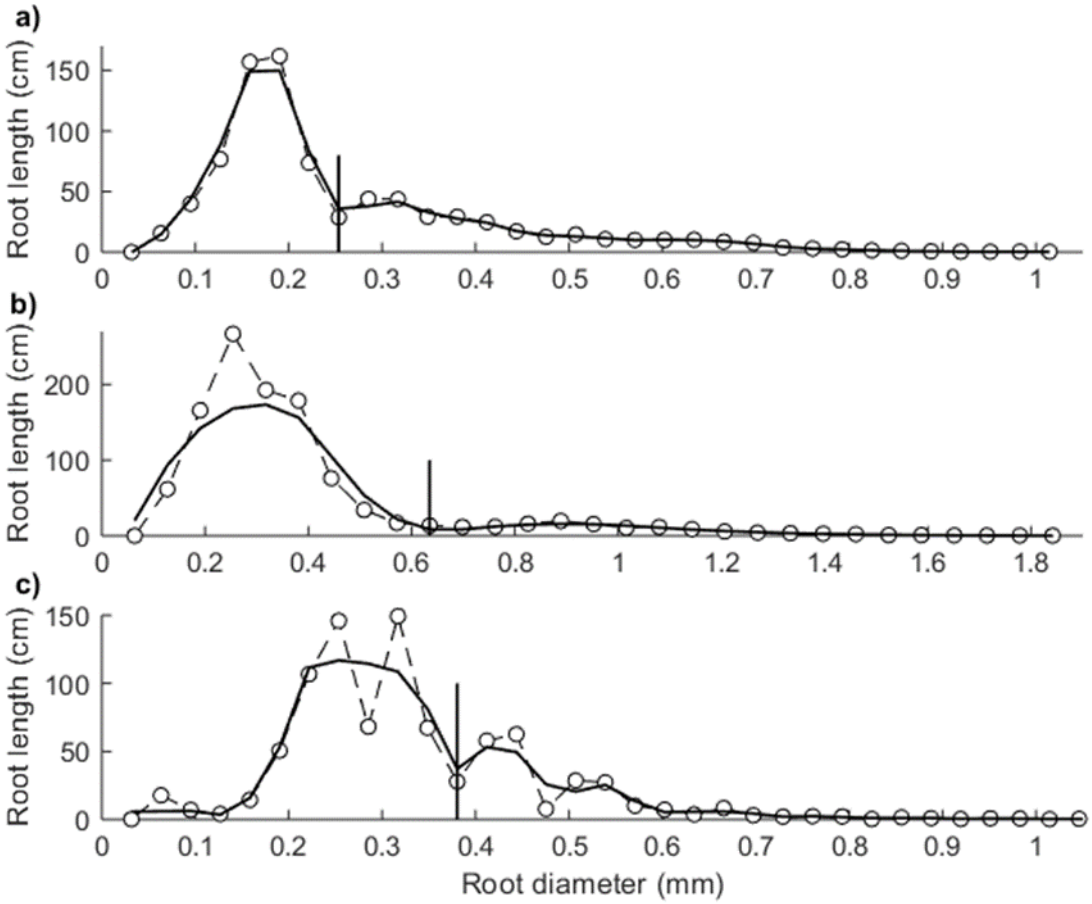

Figure 2.2. Root diameter thresholds distinguishing lateral from axile roots of, barley (a), maize (b), and *L. japonicus* (c) are depicted by the vertical line. Each marker represents the total root length in the diameter class. The dashed line depicts the actual data and the solid line represents a second degree polynomial model. Each species had a different diameter distribution so weightings were adjusted accordingly with a neighbourhood weighting of 20% for barley, 40% for maize, and 10% for *L. japonicus*. The diameter threshold were also assessed visually in WinRHIZO to ensure they accurately distinguished the root types.

root and any root derived from the tap root. Axile and lateral roots were distinguished by their diameter using the method developed by Hund *et al*. (2009). In WinRHIZO, root length was grouped in units of diameter, the unit increments were determined by the size of one pixel, 31.7 µm for 600 DPI and 63.5 µm for 400 DPI. The root data for all harvests were then combined and a second degree polynomial model, was fitted to the data using the `loess` smoothing function in MATLAB (R2017b) to reveal the two peaks of lateral roots and axile roots (Figure 2.2). The diameter that best distinguishes the two root types is represented as the lowest point in the trough between two peaks; 253.6 µm for barley (Figure 2.2a), 635.0 µm for maize (Figure 2.2b), and 380.4 µm for *L. japonicus* (Figure 2.2c). The maize threshold is consistent with previous findings (Hund *et al.* 2009), which puts the threshold for their maize cultivar at 650 µm. Absolute growth rates of both axile and lateral roots were calculated by dividing the average growth per harvest by the number of days after germination and expressed as an average across all four harvests.

2.2.5. Root hair measurements

Barley and maize WT genotypes were germinated and grown using the same methods and environments as previously mentioned. The slow growth rate of *L. japonicus* was not compatible with the experimental constraints. Wild type seeds were grown in 1.5 litre pots (dimensions as before) containing the sandy loam textured topsoil as previously mentioned. After three weeks of growing under well-watered conditions, the roots were removed from the soil and gently washed to remove soil particles whilst keeping the root hairs intact.

The roots were then photographed at 25x magnification using a camera (GX Optical GXCAM-H5) attached to a dissecting microscope. For barley 4 axiles and 6-7 lateral

roots were selected from each plant. The lateral roots were photographed every centimetre from the tip and the axile roots were photographed every 4 cm. For maize, 4-5 axile roots (representative of axile, primary and crown roots) were selected from each plant and 4-6 lateral roots. Both axile and lateral roots were photographed every 4 cm from the tip. Each species had four replicates. The subsequent images were then converted to 8 bit greyscale using Gimp 2.6.0. The brightness and contrast were also altered to counter the differing brightness of the images.

To establish average root hair length, ten root hairs were measured in each image using the line measuring function in ImageJ (Brown *et al.* 2017). WinRHIZO was used to measure the length of both the root hairs and the origin root. Due to the gradation of the illumination, the root-background threshold had to be manually adjusted for each image. Root hair length density (RHLD) was calculated by dividing the total length of root hairs by the length of the origin root segment.

2.2.6. Soil adhesion assay

This method was adapted from Akhtar et al. (2018). Seeds were germinated directly into Rockwool that were kept in a reservoir of 100 % Hoagland's solution. Four seeds for each of the barley and maize genotypes were used, again *L. japonicus* was excluded from this experiment due to its slow growth rate. When the roots were deemed long enough to reach the hydroponic solution (23 days) the plants were transferred to 5 litre aerated buckets filled with Hoagland solution, 50 % strength for barley and 100 % for maize.

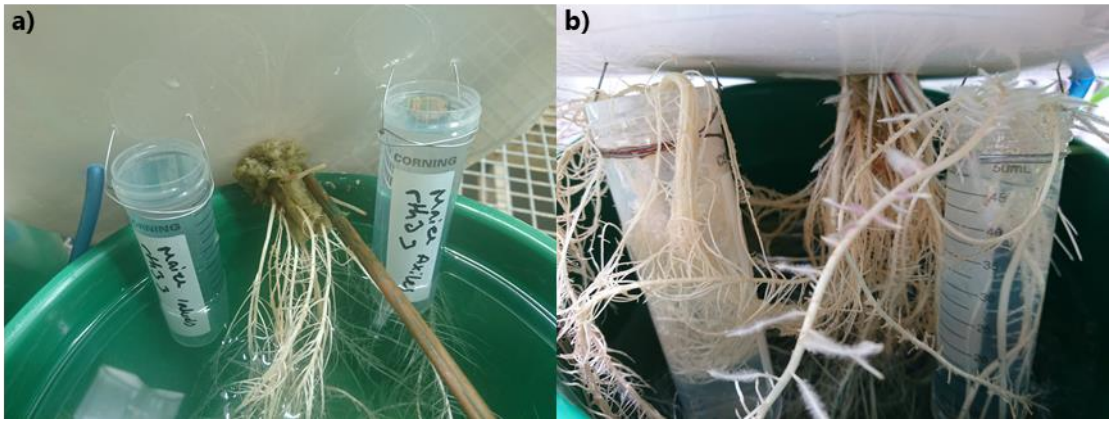

Figure 2.3. Shows the method of collecting root exudates. Two 50 ml falcon tubes were suspended from the bucket lid (a) and axile and lateral roots were isolated into each of the tubes (b).

After a further 25 days of growth, root exudates[3] were harvested in 50 ml Falcon tubes filled with DI water and suspended from the buckets' plastic covers, two per bucket. Some axile roots were isolated in one of the tubes and some laterals in the other leaving most of the root system with access to the nutrient solution (Figure 2.3). A control tube containing only DI water was also placed in half of the bucket to ensure no cross contamination occurred. The roots were left in the tubes for 4 days, topping up the DI water as needed.

After removing the tubes, the contents were filtered through filter paper (Whatman no. 3) to remove large root particles and then frozen. After lyophilising the samples to remove the water, the exudates from each replicate was consolidated into one. Exudates from each root were diluted into 4 aliquots (50 µg/5 µl, 25 µg/5 µl, 10 µg/5 µl and 1 µg/5 µl) and applied in triplicate onto a dry nitrocellulose membrane sheet (Amersham Protran 0.45 µm, Fisher Scientific, UK). Each 5 µl drop was placed within a 1 cm grid. The nitrocellulose sheets were then placed in aluminium dishes and left to air-dry for at least 1 hour before being re-wetted with DI water and covered

[3] Previously, this paper has referred to root mucilage as the compound that binds soil particles together in the rhizosheath. However, root mucilage includes only the polysaccharide rich secretions and the root produces more substances than just mucilage (Bertin *et al.* 2003). This methodology cannot separate these component parts so it is more accurate to refer to the substance collected as root exudate as this encompasses all the molecules and cells secreted by the root.

with approximately 1 cm of air-dried soil (as previously mentioned), sieved to ≤ 500 µm. The lid was then placed on the dishes and the nitrocellulose sheet left to dry over-night, with their soil covering. When dry, excess soil was shaken off and the nitrocellulose sheet submerged in DI water for two seconds, twice, to remove any extra soil not adhered. Each sheet was then recovered and left to air-dry.

Images of the soil adhered sheets were made using the A3 scanner previously mentioned at 1200 DPI and in 8-bit grey scale. The soil adhered to each spot was analysed using Image J. Mean grey scale value was used to determine how much soil adhered to the nitrocellulose sheet. Mean grey scale value was then converted into soil weight using a calibration curve developed using drops of Gum tragacanth (G1128, Sigma-Aldrich) at a dilution of 50 µg/5 µl to adhere varying amounts of soil onto small pieces of nitrocellulose sheets, and weighing the sheets before and after applying soil.

2.2.7. Statistical analysis

Analysis of co-variance (ANCOVA) assessed the differing abilities of the genotypes to bind soil, with rhizosheath as the main effect and root length as the covariate. ANCOVA was also used to determine if there were differences between the root length and root hair traits of the different root types, with root hair length as the main effect and root length as the covariate. Two-way analysis of variance tested whether the relative root lengths of the genotype were statistically different. Absolute root growth rate (AGR) was calculated as follows:

$$AGR = \frac{\delta L}{\delta t}$$

Where δL is the change in total length of the root and δt is the elapsed duration of growth. Data from multiple harvests were used to calculate AGR so root length was plotted against time and the slope of the trend line was regarded as AGR.

To assess the impact of each root type on rhizosheath formation, a linear model was fitted to the data of each species using the MATLAB function `fitlm`. To avoid the issue of auto-correlation, each predictor variable was modelled individually, so three models per species were created: with genotype, axile, and lateral root length as predictor variables, and rhizosheath weight as the response variable. The models calculated effect sizes, which were compared to establish their relative contributions of each root trait to rhizosheath formation.

2.3. Results

2.3.1. Rhizosheath formation

As expected, rhizosheath weight significantly increased with root length ($p < 0.001$), but in all three species the WT genotypes bound significantly ($p < 0.001$) more soil than their respective root hairless mutants (Figure 2.4). When comparing the slopes of the rhizosheath *versus* root length regression lines, barley showed the biggest genotypic difference, with WT binding 3.9-fold more soil than *brb* (Figure 2.4a). The *L. japonicus* WT bound 3.2-fold more soil than *Ljrhl1* (Figure 2.4c) and the maize WT bound 1.8-fold more soil than *rth3* (Figure 2.4b). Despite their lack of root hairs, all three root hairless mutants formed a rhizosheath, albeit to a lesser extent than their WT counterparts. These genetic differences in rhizosheath formation increased with increasing root length as indicated by a significant ($p < 0.05$) genotype x root length interaction for each species.

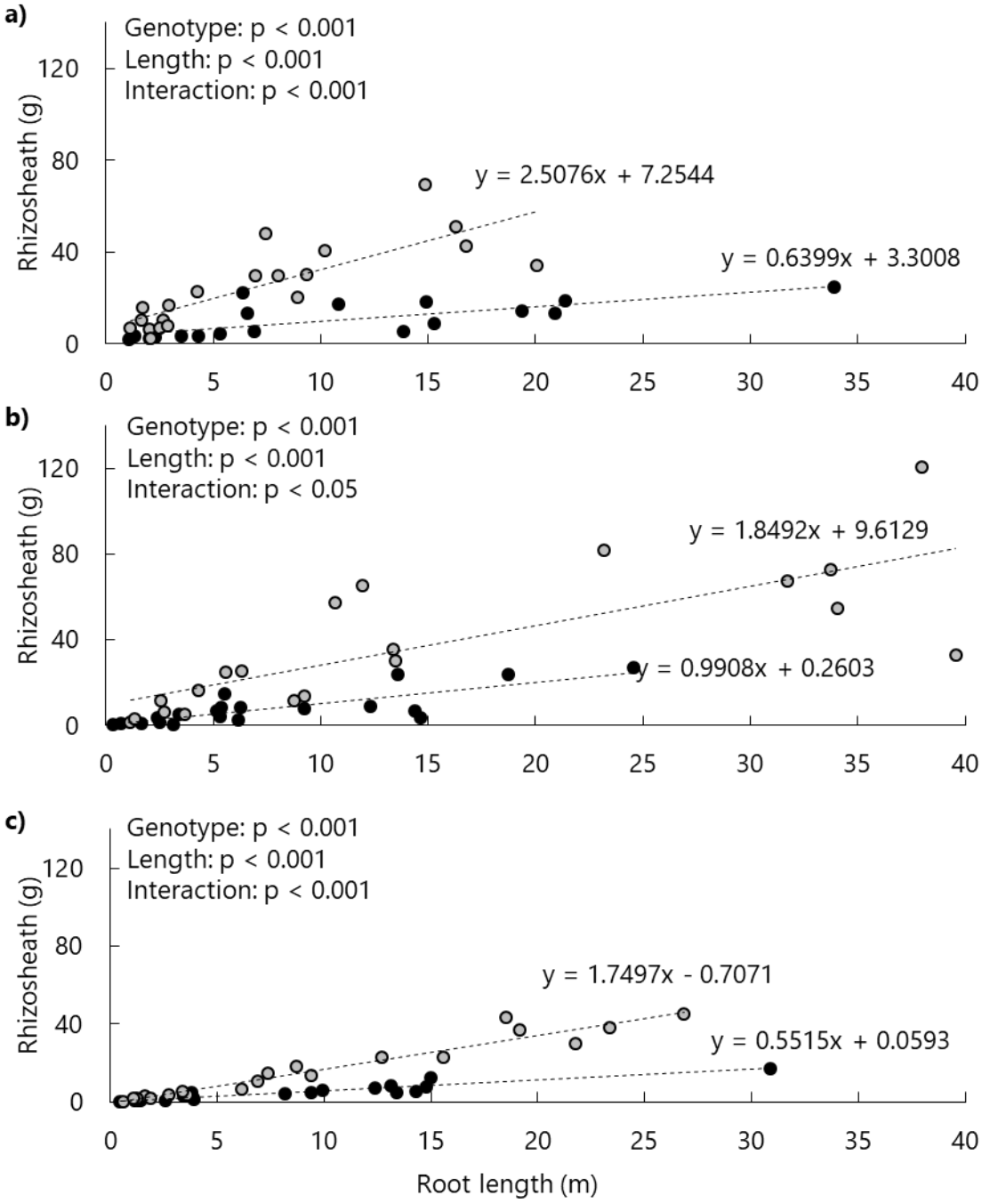

Figure 2.4. Rhizosheath weight plotted against the total root length. Filled symbols represents the hairless mutants *brb* (a), *rth3* (b) and *Ljrhl1* (c). Grey symbols represent their respective WT. Each marker represents an individual plant. Each panel shows all plants from all 4 harvests. A linear model was fitted to each genotype represented by the dashed lines and corresponding equation. All trend lines have a p value < 0.001 and an $R^2 > 0.57$. The displayed p values are the main effects and the interaction term from ANCOVA analysis.

2.3.2. Root length apportionment

Total root length varied between species and genotypes (Figure 2.5). The maize WT consistently produced a more abundant root system than *rth3* ($p < 0.001$). The *L. japonicus* WT tended to do the same, though the increase was not significant ($p = 0.23$). However, for barley, *brb* seemingly compensated for the lack of root hairs by proliferating their lateral roots to achieve a significantly greater root length than the barley WT ($p < 0.05$). Thus, when considering all the root hairless mutants, there was no consistent effect of lacking root hairs on root length.

Absolute root growth rates (AGR) statistically differed between the root types of all genotypes ($p < 0.05$) except for the barley WT ($p = 0.137$). Axile roots grew universally slower than the lateral roots, but their AGR did not vary much between the root hairless mutants and their WT. The total length of the axile roots of barley and maize increased by 28.45 ± 0.02 cm day^{-1} and 8.47 ± 0.11 cm day^{-1}, while *L. japonicus* increased at a slower rate of 0.13 ± 0.02 cm day^{-1}. Lateral root growth rates far exceeded those of the axile roots, and also showed more genotypic variation. Lateral root growth rates of *brb* and its WT were 97.0 cm day^{-1} and 57.1 cm day^{-1}, respectively. In maize, these rates were 111.8 cm day^{-1} and 205.74 cm day^{-1} for *rth3* and its WT, respectively. Again, *L. japonicus* was the slowest growing, with lateral root growth rates of *Ljrhl1* and its WT increasing 0.33 cm day^{-1} and 0.36 cm day^{-1}, respectively. Lateral roots comprised 65.8 %, 88.7% and 73.8% of the root system in barley, maize and *L. japonicus*, respectively. Their more prolific growth rate means that lateral roots comprise the bulk of the root system, and represented the cause of genotypic variation in root length. The differing growth rates of the *rth3* and *brb* lateral roots in comparison to their WT explain why they had statistically different root lengths, though the differences were much smaller for the *L. japonicus* genotypes.

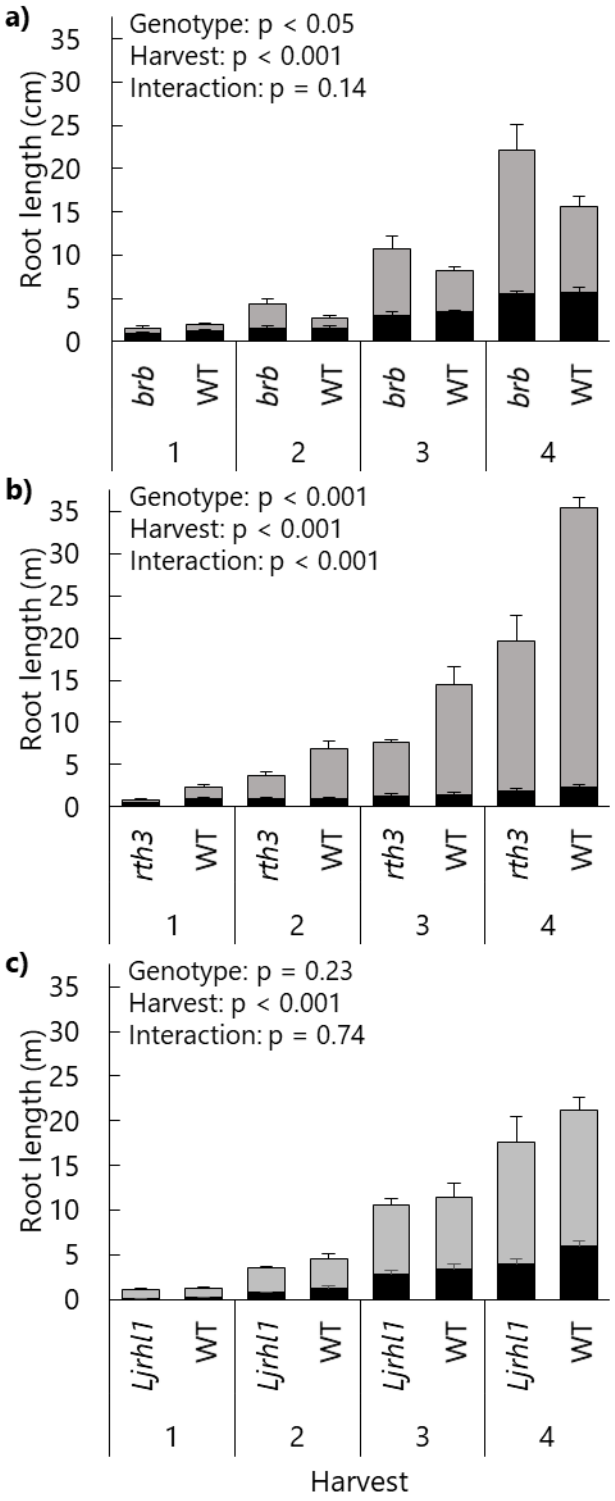

Figure 2.5. Total root length apportioned into axile (black) and lateral (grey) contributions per harvest for barley (a), maize (b) and *L. japonicus* (c). P values are from two-way ANOVA. Bars are equal to mean of 5 replicates + 1 SE of each root type.

Additionally the significant genotype*harvest interaction for maize ($p < 0.001$) suggests that the discrepancies in root length between *rth3* and its WT will continue to diverge with age but for barley and *L. japonicus*, the difference should remain relatively consistent.

2.3.3. Model effect size

As expected, all root types had a significant positive effect on rhizosheath formation (Figure 2.6). The presence of root hairs had the single biggest impact on rhizosheath formation across all species. For maize the presence of root hairs resulted in a mean of 29.2 ± 7.3 g increase in rhizosheath weight across the whole root system. For barley and *L. japonicus* the magnitude of the root hair effect was less, with a mean increase in rhizosheath weight of 15.7 ± 4.4 g and 11.5 ± 3.5 g, respectively. Increasing axile root length growth (by 1 m) had the next biggest influence on rhizosheath weight across all species. Again, barley and *L. japonicus* showed a similar response, with rhizosheath weight increasing by 5.6 ± 0.1 g m^{-1} and 5.1 ± 0.5 g $^{-1}$ per 1 m of axile root growth, respectively. In maize, axile root length increased rhizosheath weight by 26.2 ± 5.1 g. Although laterals were the fastest growing root type, they had the smallest impact on rhizosheath weight, resulting in a 1.0 ± 0.4 g m^{-1}, 1.9 ± 0.3 g m^{-1}, and 1.6 ± 0.2 g m^{-1} per 1 m increase of length for barley, maize and *L. japonicus*, respectively. Thus, rhizosheath weight increased with both axile and lateral root length, but the presence of root hairs had the greatest impact on rhizosheath formation.

2.3.4. Root hair analysis

Root hair length and RHLD were significantly correlated for both barley ($R^2 = 0.54$, $p < 0.001$) and maize ($R^2 = 0.36$, $p < 0.05$). Root hair length density did not differ between the axile and lateral roots of either barley or maize nor did RHLD change

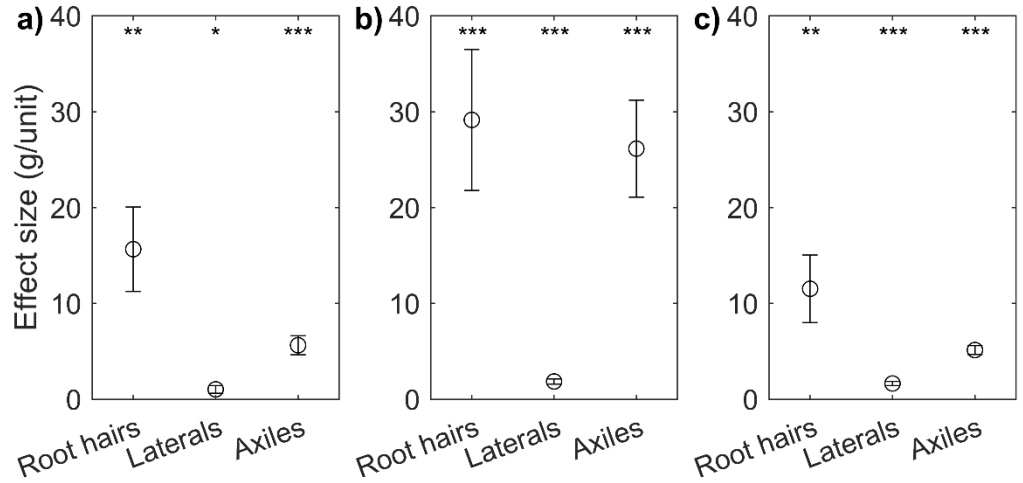

Figure 2.6. The estimated effect sizes of the three root types from a linear regression model for barley (a), maize (b), and *L. japonicus* (c). The units for root hairs is presence/absence and the units for axile and lateral roots are 1 m of root growth. Error bars are equal to 1 standard error. * = $p < 0.05$, ** = $p < 0.01$, *** = $p < 0.001$.

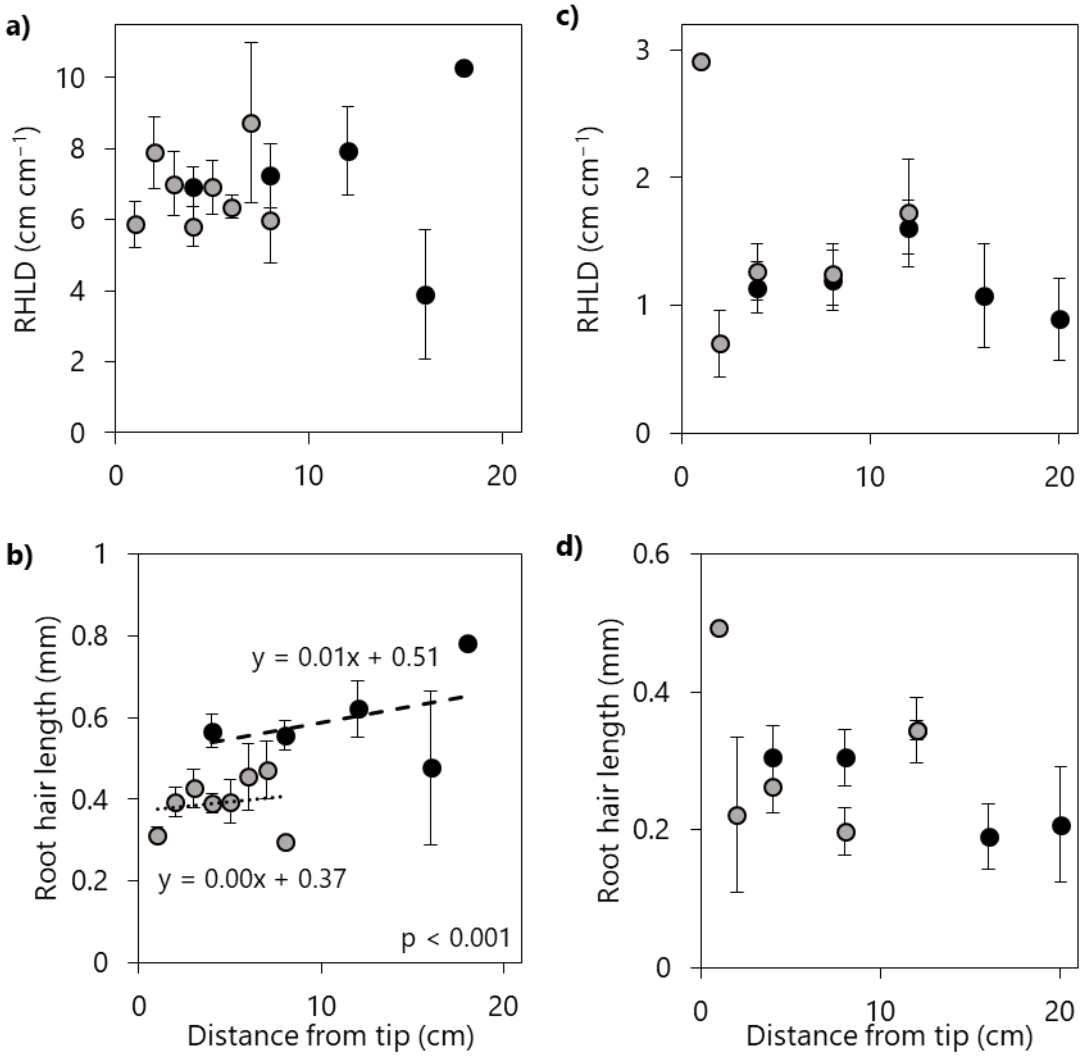

Figure 2.7. Root hair density (a, c) and length (b, d) versus distance from root tip in barley (a, b) and maize (c, d). Grey markers represent lateral roots and black markers represent axile roots. Data are means ± 1 standard error. Linear regressions fitted denote the significant difference between root types.

with increasing distance from the root tip (Figure 2.7). Similarly, the root hair length of both lateral and axile roots were comparable in maize and did not differ with distance from the tip. However, barley axile roots produced 26 % longer root hairs in comparison to their lateral roots (calculated by the intercept of the regression lines in Figure 2.7). In comparing species, barley produced significantly longer root hairs (2-fold, $p < 0.001$) at a greater RHLD (6-fold, $p < 0.001$) than maize. Since both root hair measurements did not change with increasing distance from the root tip for either species, it can be assumed that all ages of roots display a similar number and length of root hairs.

2.3.5. Exudate adhesiveness

Soil adhered to the root exudates placed on nitrocellulose sheets, with clear variation in the adhesive capacities of exudate from different roots (Figure 2.8). For barley, the exudates from *brb* showed a greater capacity to bind soil than its WT. Exudates from the barley WT axile and lateral roots were both relatively ineffective at binding soil, since soil adhesion was only just above background levels across the whole dilution scale, with no difference between the different root classes (Figure 2.9a).

Maize root exudates were generally more effective at binding soil than barley roots, with root exudates from WT maize axile roots adhering the

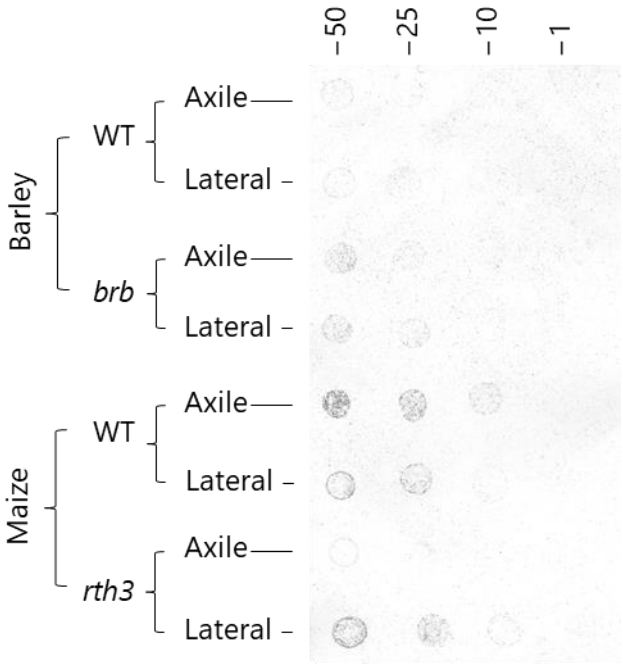

Figure 2.8. The scanned images of the soil adhesion assay. The drops are distributed in a 1 cm square grid. The dilution of exudates in DI water starts at 50 µg/5 µl and descends left to 1 µg/5 µl (5 µl is the size of a single droplet).

most soil of all the roots tested, in contrast to the *rth3* axile root exudates which were barely above background levels (Figure 2.9b). Root exudates from the maize lateral roots showed that *rth3* and its WT had a similar capacity to bind soil. Overall maize root exudates were more adhesive than barley roots, and the effect of root hairs varied with species.

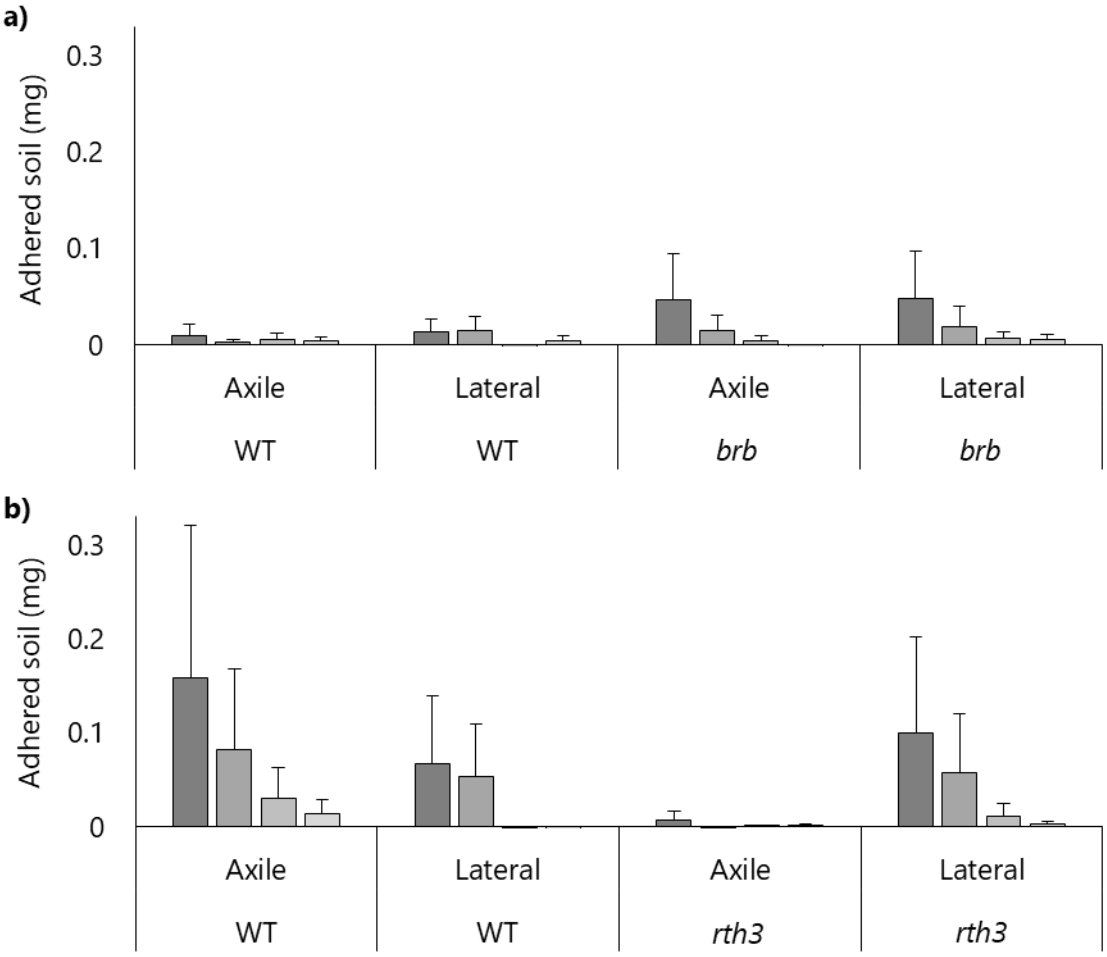

Figure 2.9. Amount of soil adhering to a nitrocellulose membrane spotted with root exudates collected from the axile and lateral roots of different species and genotypes. The bars are colour saturated to reflect the mucilage saturation of the droplet, darkest = 50 µg/5µl, 25 µg/5µl, 10 µg/5µl and the lightest = 1 µg/5µl. Bars are means of 3 replicated + 1 standard error.

2.4. Discussion

The significance of root hairs, and their length, in determining rhizosheath formation has been frequently observed (McCully 2005; Moreno-Espíndola *et al.* 2007; Haling, Simpson, *et al.* 2010; Haling, Richardson, *et al.* 2010; Brown *et al.* 2012, 2017; Delhaize *et al.* 2012, 2015; George *et al.* 2014; Adu *et al.* 2017; Pang *et al.* 2017). However, it is not yet understood to what extent other root properties, such as root hair density and variations in root exudates, contribute to rhizosheath formation. By observing the relative capacity of several root hairless mutants and their respective WTs to form rhizosheaths (Figure 2.6), and relating them to various root traits, including root hairs (Figure 2.7) and mucilage properties (Figure 2.9), root hair traits were found to be the most dominant factor determining the size of the rhizosheath (Figure 2.10).

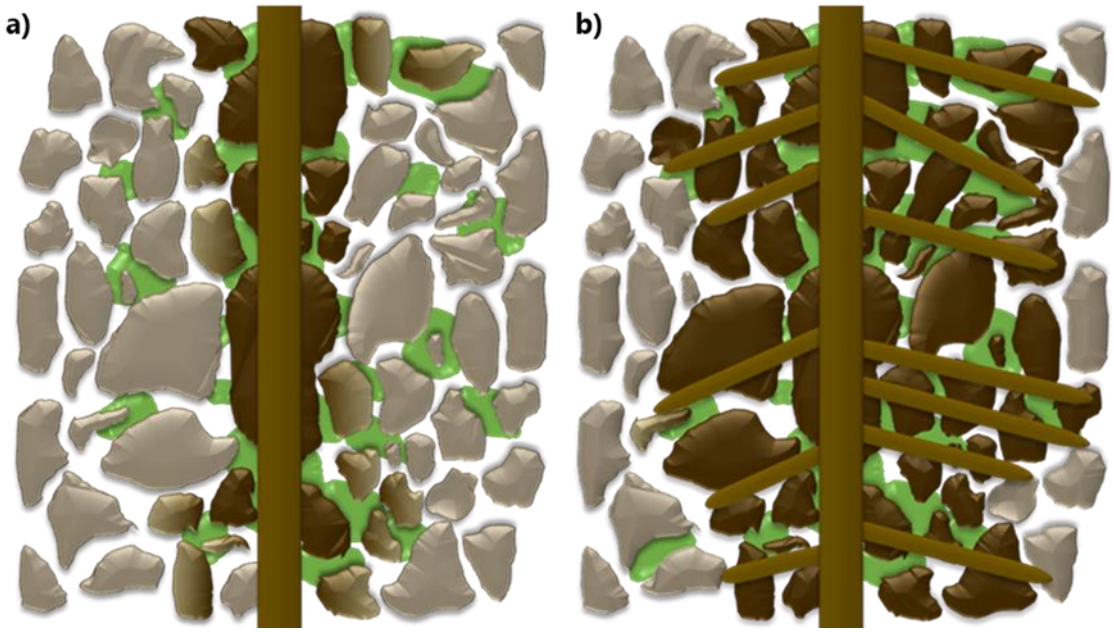

Figure 2.10. A conceptual representation of the contribution root hair and mucilage traits make to rhizosheath formation. For both images the soil particles that are not faded represent the rhizosheath soil, bound to the root. For roots without any root hairs (a) only soil particles that are in direct contact with the main root are bound as a rhizosheath. If the root produces a more adhesive mucilage then it will be able to bind more soil particles (as represented by the particles with a graduated fade). The presence of root hairs (b) increases the root surface area for the soil particles to bind to, resulting in a more prominent rhizosheath. Longer and denser root hairs (right side of b) increases the radial extent of the rhizosheath more than when root hairs are shorter and less dense (left side of b).

2.4.1. Contribution of root hairs to rhizosheath formation

The presence of root hairs significantly enhances rhizosheath formation, since root hairless mutants are much less effective at binding soil than their WT in three different species (Figure 2.4). Although the lack of root hairs can be compensated for by the increased total root length of older plants (Figure 2.4), genotypic differences increased with root length, meaning that the additional root length needed to compensate for lack of root hairs also increases. This is because root hair properties do not differ with increasing proximity to the tip (excluding the elongation zone; Figure 2.7), so, each new growth of root with root hairs would have a disproportionately greater impact on rhizosheath formation than the same length of new root without root hairs. However, as in previous studies (Wen and Schnable 1994; Haling, Simpson, *et al.* 2010; Haling *et al.* 2014; George *et al.* 2014) root hairless mutants still bound some soil, indicating that both physical (root hair enmeshment of soil particles) and chemical (root exudates adhering to soil particles) mechanisms contribute to rhizosheath formation.

2.4.2. Contribution of root hair length

Root hair length is widely recognised to influence the size of the rhizosheath (Wullstein and Pratt 1981; Haling, Richardson, *et al.* 2010; Brown *et al.* 2012; Delhaize *et al.* 2012, 2015; Haling *et al.* 2013; George *et al.* 2014; Adu *et al.* 2017) and can explain the species differences in rhizosheath development. The length of barley root hairs (0.6 mm and 0.4 mm for axiles and laterals, respectively) was much greater than those produced by maize (0.3 mm for both axiles and laterals). Which are just below what has been previously recorded for these species (Gahoonia *et al.* 2001; Zhu *et al.* 2005). These disparities in root hair length can explain why the genotypic difference in rhizosheath formation between the WT and hairless mutant were so much greater in barley than in maize (Figure 2.4). Additionally, the increased root hair

length meant barley WT was 1.5 times more effective at binding soil than the maize WT root system of the same accumulated length. However, increasing root hair length has increasingly limited effects on rhizosheath formation once length exceeded 0.28 mm (Brown *et al.* 2017). Although longer root hairs can enhance rhizosheath development, root hair distortion and density as well as variations in root exudates may also play a significant role in determining the size of the rhizosheath (Brown *et al.* 2017; Pang *et al.* 2017).

2.4.3. Contribution of root hair length density

Unlike root hair length, the impact of RHLD on rhizosheath development is, as yet, unknown. For barley, root hair length and RHLD were correlated but RHLD was more stochastic and did not show any differences between axile and lateral roots, as was evident with root hair length. Similarly for maize, there was no difference between the RHLD of axile and lateral roots. Further, the species variation in RHLD followed the trend of root hair length, with barley producing a significantly greater RHLD than maize. Assuming all roots were of average length, this would equate to 4-fold more roots per every mm or origin root. Although root hair length and density can respond similarly to environmental (Watt *et al.* 1994; Haling, Richardson, *et al.* 2010) and endogenous factors, such as auxin which promotes both root hair initiation and elongation (Ma *et al.* 2001), roots can compensate for short root hairs by increasing their density (Adu *et al.* 2017). So, even though root hair length and RHLD are correlated here, this is not always the case (Haling, Richardson, *et al.* 2010; Nestler *et al.* 2016; Adu *et al.* 2017). Additionally, root hair length and density can disproportionately contribute to other root functions such as nutrient uptake (Itoh and Barber 1983; Zygalakis *et al.* 2011). Thus, it cannot be assumed that root hair length

and RHLD contribute similarly to rhizosheath formation even though their relative contributions could not be distinguished in this experiment.

2.4.4. Lateral and axile roots

Although axile and lateral roots have different structures (Drew 1975; Cahn *et al.* 1989; McCully 1999) and consequently different functions (Varney *et al.* 1991; Doussan *et al.* 1998; Carminati 2013; Ahmed *et al.* 2015), their relative effects on rhizosheath formation are unknown. This study suggests that there is no difference between the relative contribution of axile and lateral roots to rhizosheath formation when their root hairs are the same length and at the same RHLD, in which case, any difference in effect are due to differing growth rates. Although axile root growth had more impact on rhizosheath formation than lateral root growth (Figure 2.6), lateral roots grew faster than axile roots, as previously observed (Drew and Saker 1975; Cahn *et al.* 1989; Pagès and Pellerin 1994). Indeed, the slower growth rate of maize and *L. japonicus*, axile roots (94.6 % and 62.9 % slower respectively than their lateral roots) was commensurate with their effect sizes on rhizosheath formation (axile root growth had 92.9 % and 68.0 % greater effect than the lateral roots of maize and *L. japonicus*, respectively). Root hair traits of maize axile and lateral roots did not differ (Figure 2.7). As the effect sizes of *L. japonicus* roots could also be largely explained by the difference in AGR, axile and lateral roots of *L. japonicus* are proposed not to differ in root hair development (as in maize). So, for roots with similar root hair development, their relative contribution to rhizosheath formation is dependent on their growth rate compared to the overall increase in root system size and not an increased affinity to rhizosheath formation.

However, when roots differ in root hair development (as in barley), root hair length influences the root's ability to form a rhizosheath. Barley axile roots affected rhizosheath formation disproportionately to their growth rates. Although barley lateral roots grew 63% faster than axile roots, the latter had 82% more effect on rhizosheath formation because they had longer (by 26 %) root hairs (Figure 2.7). Thus, the longer root hairs on the barley WT axile roots were more efficient at binding soil than the shorter root hairs on the barley lateral roots, while maize axile and lateral roots (with the same root hair length) bound the same amount of soil.

2.4.5. Root exudates

That root hairless mutants can bind some soil, albeit much less, shows that other root traits, such as root exudates, also determine rhizosheath development (Haling *et al.* 2014; George *et al.* 2014). However, their significance in root hairless mutants has hitherto not been evaluated. Overall, maize exudates were far more adhesive than barley exudates. Similarly, Naveed *et al*. (2017) found that barley root exudates initially act to weaken the soil, whereas maize roots more actively bind to soil. Root exudate adhesiveness cannot completely compensate for shorter root hairs between species, but becomes more important when root hairs are absent (Figure 2.4 and Figure 2.7). The increased adhesiveness of *rth3* root exudates meant it was 1.5 times more effective at binding soil than *brb* root systems of the same length. However, when root hairs were present, the increased adhesiveness of the maize WT did not outweigh the benefits of increased root hair development, as it bound 1.4 times less soil than the barley WT. While adhesive root exudates can aid rhizosheath formation, and even determine its extent in the absence of root hairs, the presence and abundance of root hairs are the main driving force behind rhizosheath development.

2.5. Conclusion

Variation in rhizosheath formation between different species, mutants and root types can most easily be explained by differences in root hair development. The presence of root hairs significantly enhances rhizosheath formation, but root mucilage becomes more prominent when root hairs are absent. Increasing root hair length and density further enhances rhizosheath formation, but further work is needed to disentangle their relative contributions. Additionally, the chemical composition of exudates derived from root hairs and the roots themselves should be measured, to better understand the mechanisms contributing to rhizosheath formation.

Chapter 3. Do root hairs reinforce soil under shear stress?

3.1. Introduction

When the frictional forces holding soil together are overcome by shearing forces, the consequential land wasting varies in both pace and scale. Soil instability can pose a multitude of economic problems ranging from small scale erosion that results in the sedimentation of waterways and the subsequent increased flood risk and reduction in water quality (Boardman and Poesen 2007; Pollen *et al.* 2013). Larger scale soil instability can result in the destruction of properties and loss of life (Petley 2012). Soils are inherently anisotropic and are weak under shear forces (Al-Karni and Al-Shamrani 2000). The fault line that occurs when the soil fails under shear stress is called the shear plane. Some soils are naturally susceptible to shear erosion due to a layer of weakness referred to as a failure plane, but most landslide events occur due to hydraulic pressures (Iverson 2000).

Soil shear strength is the ability of a soil to withstand these shear forces. Plant roots are widely understood to increase slope stability because they add tensile reinforcement to the soil, countering their natural susceptibility to shear forces (Wu and Sidle 1995; Simon and Collison 2002; Gyssels *et al.* 2005; Stokes *et al.* 2009, 2014). Fine roots penetrate laterally through the soil enmeshing and binding the surface soil together, whilst deeper reaching tap roots cross failure planes, pinning them together as well as anchoring the fine root matting (Simon and Collison 2002; Stokes *et al.* 2009; Fan and Chen 2010). A root's ability to reinforce the soil depends on its resistance to either being pulled out or breaking. If their tensile strength is greater than the friction of their anchorage, roots will slip from the soil at the shear plane, if it is less, then the root will break before being pulled out (Pollen 2007).

Root anchorage is achieved by forks and bends in the root system acting as soil pins and effectively increasing the area of soil which the root can engage and use to dissipate the traction forces (Stokes and Mattheck 1996; Bengough *et al.* 2011). For straight roots, without forks or bends, the length of the root determines how efficiently it is anchored; a root is anchored when there is sufficient root-soil contact to provide friction in excess of the root's tensile strength (Ennos 1990). Though tensile strength has an inverse relationship with root diameter (Nilaweera and Nutalaya 1999; Pollen and Simon 2005; Genet *et al.* 2005; Burylo *et al.* 2012), assumed to be caused by fine roots having greater cellulose concentrations (Genet *et al.* 2005; Indran *et al.* 2014), the force required to break a root increases with root diameter (Nilaweera and Nutalaya 1999; Pollen and Simon 2005; Tosi 2007; Docker and Hubble 2008; Yang *et al.* 2016), as does the force required to pull the root from the soil (Nilaweera and Nutalaya 1999; Norris 2005; Stokes *et al.* 2009). Although root diameter is widely recognised to strongly impact soil reinforcement, our understanding of how roots reinforce the soil is predominantly driven by tree roots and woody shrubs, and fine roots have frequently been homogenised into one synonymous category (Pregitzer *et al.* 2002; Reubens *et al.* 2007; Hishi 2007). For this reason the function of small scale root traits, such as root hairs, have yet to be associated with soil reinforcement on a larger scale.

This thesis focuses on assessing the ability of root hairs to reinforce the soil. Chapter 2 showed that root hairs heavily influence how much soil a root system can bind, but it is not known whether this trait translates to a capacity to reinforce the soil under shear stress. Previous studies have found that root hairs aid root anchorage. Root hairs start to grow just behind the root elongation zone anchoring the root tip to enabling the root tip to penetrate the soil (Bengough *et al.* 2011; Haling *et al.* 2013) whilst preventing

the growth force from deforming the rest of the root or pushing the plant out of the soil (Bengough *et al.* 2016). Several other studies have also noted the force by which root hairs bond the root to the soil (Czarnes et al., 1999; Ennos, 1989; Stolzy and Barley, 1968) and their importance for root anchorage (Waldron and Dakessian 1981; Handley and Davy 2002), to the extent that root anchorage is believed to be a primary function of root hairs (Gilroy and Jones 2000; Bengough *et al.* 2011). However, whether this capacity to anchor the root to the soil enhances soil anchorage under shear stress is, as yet, unknown.

This chapter aims to measure the contribution of root hairs to a root system's ability to reinforce soil by measuring the shear resistance exerted by soil columns permeated with root systems with and without root hairs in a laboratory shearing box. Other root characteristics, such as root length density (RLD), average root diameter, and root surface area density (RSAD), were also measured, as well as the tensile strength of individual roots. Root reinforcement of the soil was calculated by observing the increased force required to shear rooted soil columns in comparison to soil columns void of roots.

3.2. Materials and methods

3.2.1. Germination and growth

For this experiment, root hairless mutants of barley (*brb*) and maize (*rth3*) were compared to their respective WTs. The same germination and growth environments were used as in Chapter 2.2.2. The pots for this experiment, however, were constructed out of two sections of 68 mm diameter guttering down pipe (FloPlast Ltd) cut into 125 mm sections, making the total height of each pot 250 mm. The two sections were held together with gaffer tape. The bottom of each pot was sealed with a

section of woven wire mesh (0.70 mm Aperture, 0.36 mm Wire Diameter, SS304 Grade) to allow water to drain but retain the soil. Each pot was filled with a set weight (dependant on the initial water content) of a sandy loam topsoil (as used in Chapter 2) which provided an approximate bulk density of 1.3 g cm^3. Eighteen plants per genotype were harvested over 3 periods. For barley these were 35, 49 and 54 days after germination (DAG) and for maize they were 23, 35, and 49 DAG. Due to limited growing space, the barley harvests were grown consecutively, but all plants were grown under the same environmental conditions (as detailed in Chapter 2.2.2.).

3.2.2. The shearing rig

This experiment utilised a laboratory shearing box rig designed by Gould (2014). The shearing rig comprises a metal frame that supports two wooden inserts each

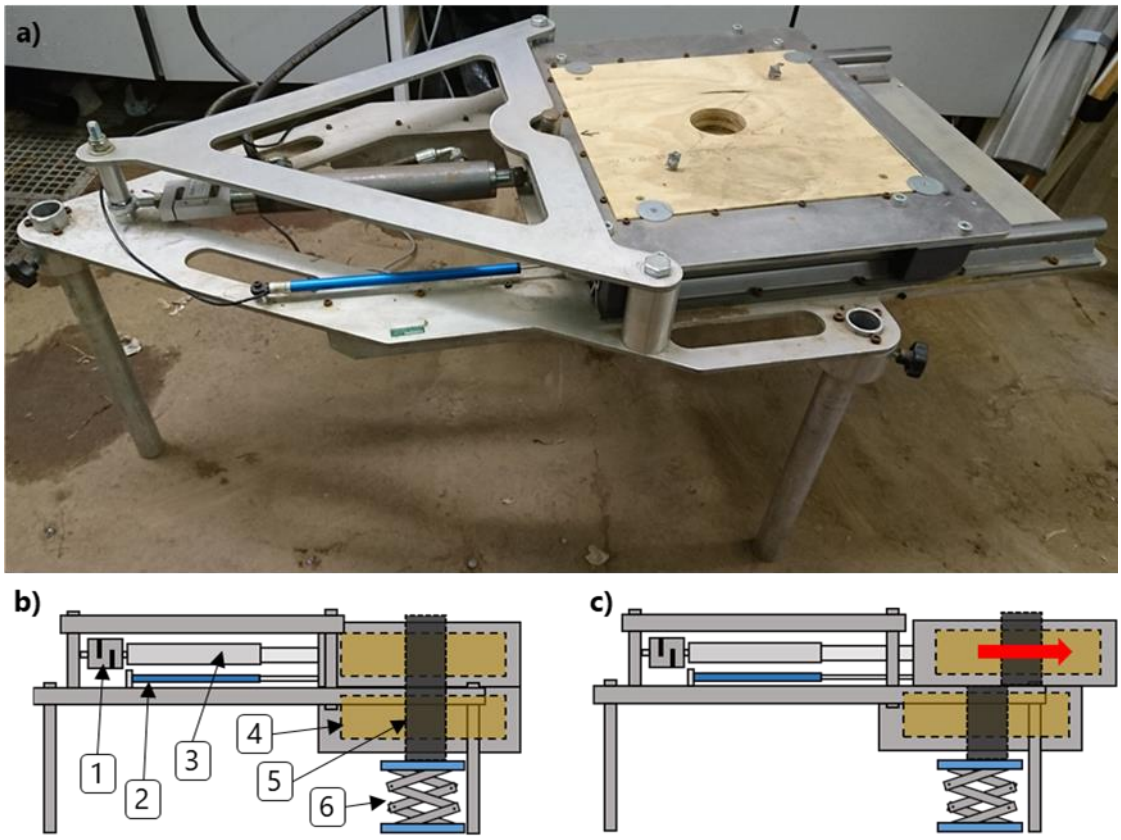

Figure 3.1. Depicts the shearing rig used in this experiment (a). The parts of the rig are numbered in their stationary position (a); 1. Load cell, 2. Transducer, 3. Hydraulic arm, 4. Wooden inserts, 5. Pot, 6. Adjustable platform to support the pot at the correct height so that the seam of the pot lines up with the shearing plane of the rig. The top section of the rig then extends over the bottom section shearing the pot (c).

containing a hole for the experimental pots (Figure 3.1). The top part of the frame is moved laterally on metal runners powered by a hydraulic pump. The top section is moved over the bottom section at a rate of 8-9 mm sec^{-1}, depending on the sample resistance, and extends the whole width of the pot allowing for a full displacement profile. The displacement of the top section was measured by a linear potentiometric displacement transducer (PD13, LCM Systems Ltd, UK) and the displacement force was measured at a resolution of 0.02 kg by an S type compression load cell (STA-1-300, LCM Systems Ltd, UK). All data were recorded by a CR800 data logger (Campbell Scientific, Inc., USA) programmed to sample every 200 milliseconds.

3.2.3. Sampling

Pots were stood in water overnight to achieve a consistent soil moisture content and, just prior to shearing, the gaffer tape was cut with a razor blade. Once sheared, the soil from the bottom half of the pot was weighed and then dried at 105 °C to establish soil bulk density (BD) and soil water content (WC). The top half was sealed in a plastic bag and stored in a fridge until the roots could be harvested, usually the day after the experiment. Only the bottom 3 cm of this section was used for root measurement as it was assumed that the root mass directly adjacent to the shear plane would most influence the soil's shear resistance. The 3 cm was measured and then cut with a razor blade. The roots were then washed out and stored at approximately 4 °C in a 50 % ethanol and DI water solution until they could be scanned (as in Chapter 2.2.2.). Due to the sizes of root used in this study it was not possible to measure root area ratio (percentage of total cross sectional area of roots per the soil cross sectional area at the shearing plane) so root length density (RLD) and root surface area density (RSAD) were used instead and are calculated as follows:

$$RLD = \frac{RL}{V_s}$$

$$RSAD = \frac{(\pi D) \times RL}{V_s} = \frac{RSA}{V_s}$$

Where RL is the total length of live roots (cm) and V_s is the volume of soil sampled (cm^3). Root surface area (RSA, cm^2) is calculated assuming the root is cylindrical.

3.2.4. Root tensile strength

To test the tensile strength of roots, four of each barley and maize genotypes were grown in 4 litre pots; pot dimensions, germination procedure, soil type and density, and growth environment are as mentioned in Chapter 2.2.2. After 35 days of growth, the roots were washed out of the soil and stored in approximately 4 °C in a 50 % ethanol and DI water solution for two days. The roots were kept in this solution until immediately before testing to ensure a consistent moisture content. Five, 3 cm segments of lateral and axile roots were randomly selected from each plant and scanned using an Epson Perfection V700 at 600 DPI, later to be analysed using WinRHIZO (as in Chapter 2.2.2). Each segment of root was then attached to a small plastic tab using a combination of superglue and gaffer tape (Figure 3.2), overlapping the plastic by 1 cm at each end; leaving a 1 cm length of unobstructed root. The plastic tabs were pre-tested to ensure their tensile strength far exceeded that of the roots and

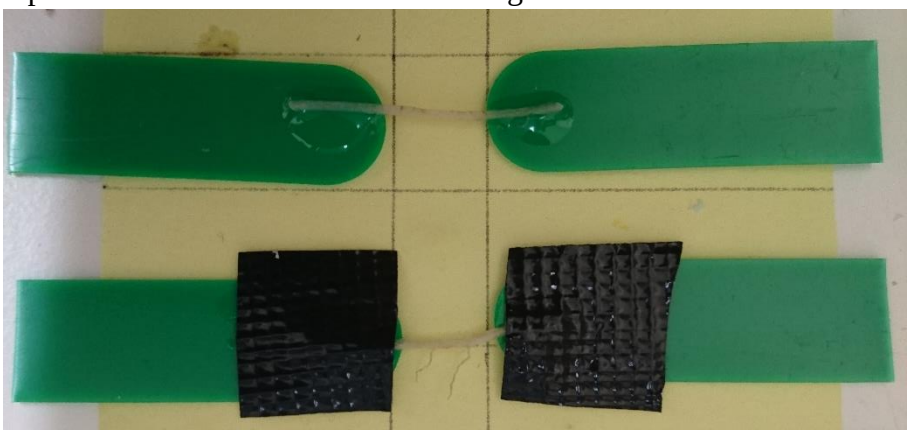

Figure 3.2. Root segments being attached to the plastic tabs with superglue (top) and then a strip of gaffer tape (bottom) to quicken the setting of the superglue.

that their deformation was negligible. The plastic tabs with the roots attached were then secured into the clamps of a Single Column Table-top Testing Machine (series 5944, Istron, UK). The clamps were then moved apart at a displacement rate of 10 mm min^{-1} and the force was recorded every 20 ms by a 100 N load cell at a resolution of 0.5 mN (Instron, UK). Any root that broke at the joint of the plastic tabs was discarded.

3.2.5. Data and statistical analysis

The data were normally distributed for both barley and maize so a repeated measures analysis of variance (ANOVA) assessed whether the treatments (pots containing WT roots, root hairless mutant roots, and the control with no roots) exerted a different force over the same distance of displacement. However, the data violated the sphericity assumption of this method so the p value is corrected using Greenhouse-Geisser. Pairwise comparisons with a Bonferroni correction was used as a post-hoc test. This analysis was carried out in SPSS (Version 25).

The ANOVA function and multiple comparison procedures in MATLAB (R2017b) were used to estimate the means across the genotypes for peak force and the displacement distance in order to assess which treatments statistically differed. This method was also used to assess whether the root parameters differed between genotype. The analysis of covariance (ANCOVA) function in MATLAB assessed whether the genotypes displayed differences in root tensile strength with increasing root diameter, as well as whether there was any genotypic difference in relative increase in peak displacement force (RPF) with increasing root measurement. RPF was calculated:

$$RPF = \left(\frac{PF_r - \overline{PF_c}}{\overline{PF_c}}\right) \times 100$$

Where PF_r is the peak force exerted by a rooted pot and $\overline{PF_c}$ is the mean root force exerted by the unplanted control pots (the maize and barley experiments were carried out at separate times so the controls are considered separately).

3.3. Results

3.3.1. Force over distance

Figure 3.3 shows that the force required to displace the plots changed significantly ($p < 0.001$) over the displacement profile for both barley and maize. The presence of roots significantly ($p < 0.05$) increased shear resistance in comparison to the unplanted pots. For each rooted treatment there is an initial build-up of force to a peak which then tapers off, whereas the unplanted pots had a more gradual build-up and peaked much later. For maize these differences were evident across the whole displacement profile, though for barley, the differences were restricted to between 6-24 mm and 6-48 mm of displacement for *brb* and its WT, respectively. The peak force for each treatment and the point at which they occurred on the displacement scale are recorded in Figure 3.4a and Figure 3.4b. There is a general trend for the peak shearing force to increase with harvest for each genotype, however, differences only became statistically significant ($p < 0.05$) at harvest 3.

There was no consistent genotypic effect for either harvest 1 or 2. Although all genotypes produced a greater mean peak force than their respective unplanted pots in harvest 1 (*brb* = 6.7 %, barley WT = 5.1 %, *rth3* = 8.0 %, and maize WT = 10.7 % increase from the mean of their respective unplanted pots), none of the increases were statistically significant. In harvest 2 all genotypes, again, produced a greater mean

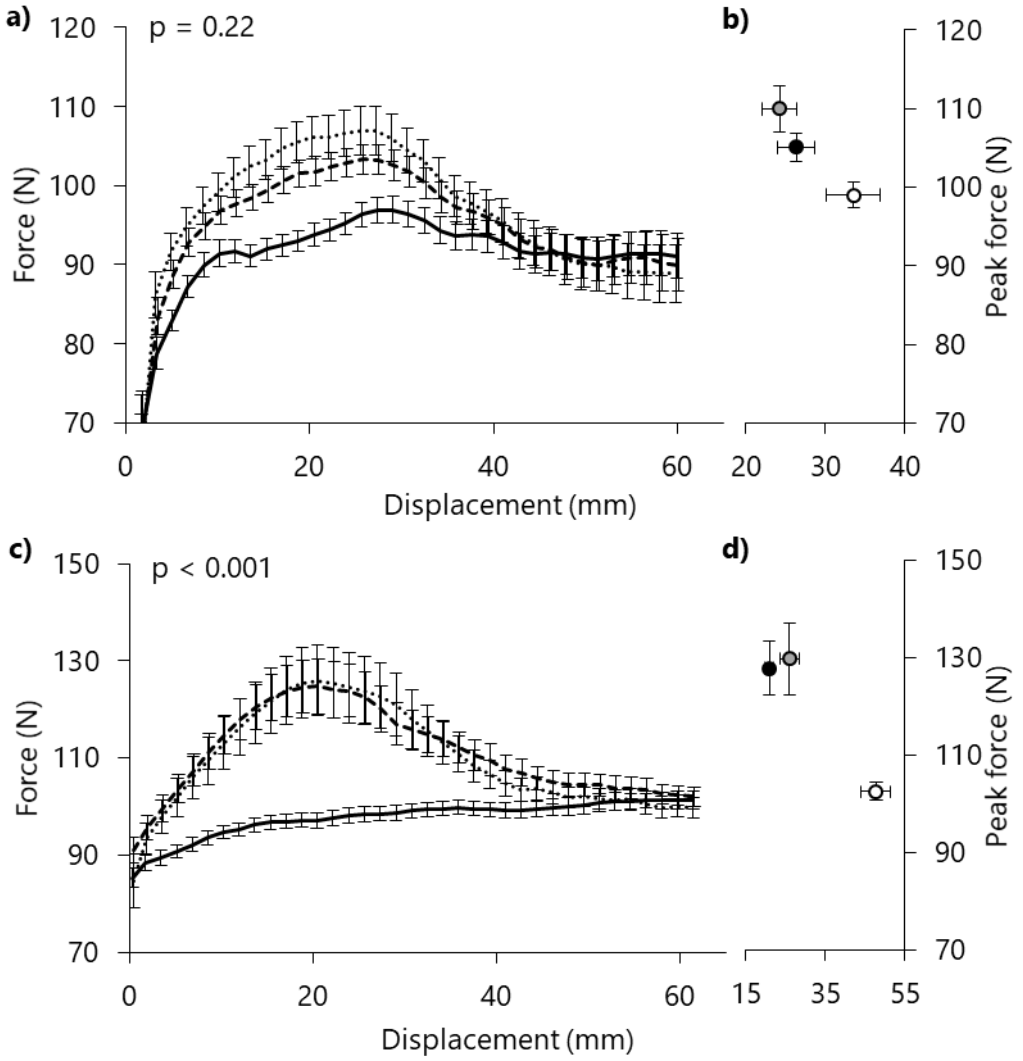

Figure 3.3. Displacement force (a, c) and peak displacement force (b, d) for barley (a, b) and maize (c, d) versus distance. Solid lines = unplanted control pots, dashed line = root hairless mutant, dotted line = WT. P value represents the genotype*displacement interaction with displacement force derived from repeated measures ANOVA. White marker = unplanted, black marker = root hairless mutant, grey marker = WT.
For all genotypes the data are means of 18 replicates, the barley and maize unplanted pots are means of 15 and 17 replicates respectively. Error bars are equal to 1 standard error.

peak force than their respective unplanted pots (*brb* = 3.7 %, barley WT = 10.4 %, *rth3* = 33.1 %, and maize WT = 15.5 % increase from the mean of their respective unplanted pots) but only *rth3* was statistically significant ($p < 0.05$). In harvest 1 *brb* produced a peak force 1.6 % greater than its WT but in harvest 2 the peak force required to shear the *brb* pots were 6.1 % less than its WT. For maize, *rth3* produced a peak force 2.5 % smaller than its WT in harvest 1 and in harvest 2 produced a peak force 13.2 % greater than its WT. At harvest 3, all treatments were statistically different with a consistent treatment effect across both species. Both the barley and maize WTs required significantly ($p < 0.05$ and $p < 0.01$, respectively) greater forces to shear than both their root hairless mutants (8.3 % and 13.0 % increase for barley and maize, respectively) and their respective unplanted pots (17.7 % and 52.6 % for barley and maize, respectively; $p < 0.001$). Both *brb* and *rth3* also required significantly ($p < 0.05$ and $p < 0.01$, respectively) more force to shear than their respective unplanted pots (7.9 % and 32.8 %, respectively). Thus, the presence of roots consistently (but not always significantly) increased peak force, but the presence of root hairs only showed a consistent and significant increase after the 3rd harvest for both species.

Peak displacement force was reached at a mean distance of 26.3 mm and 24.2 mm for barley *brb* and its WT, respectively, and of 20.9 mm and 26.0 mm for maize *rth3* and its WT, respectively. The corresponding unplanted pots peaked at 33.5 mm and 47.7 mm for the barley and maize unplanted pots, respectively (Figure 3.4c and Figure 3.4d). However, for barley, the only significant ($p < 0.05$) difference was recorded between the WT and unplanted pots in harvest 1 where the WT reached peak force at a mean displacement 55.6 % less than the unplanted pots. Barley *brb* reached peak force at a mean displacement 40.2 % less than the unplanted pots, but the difference

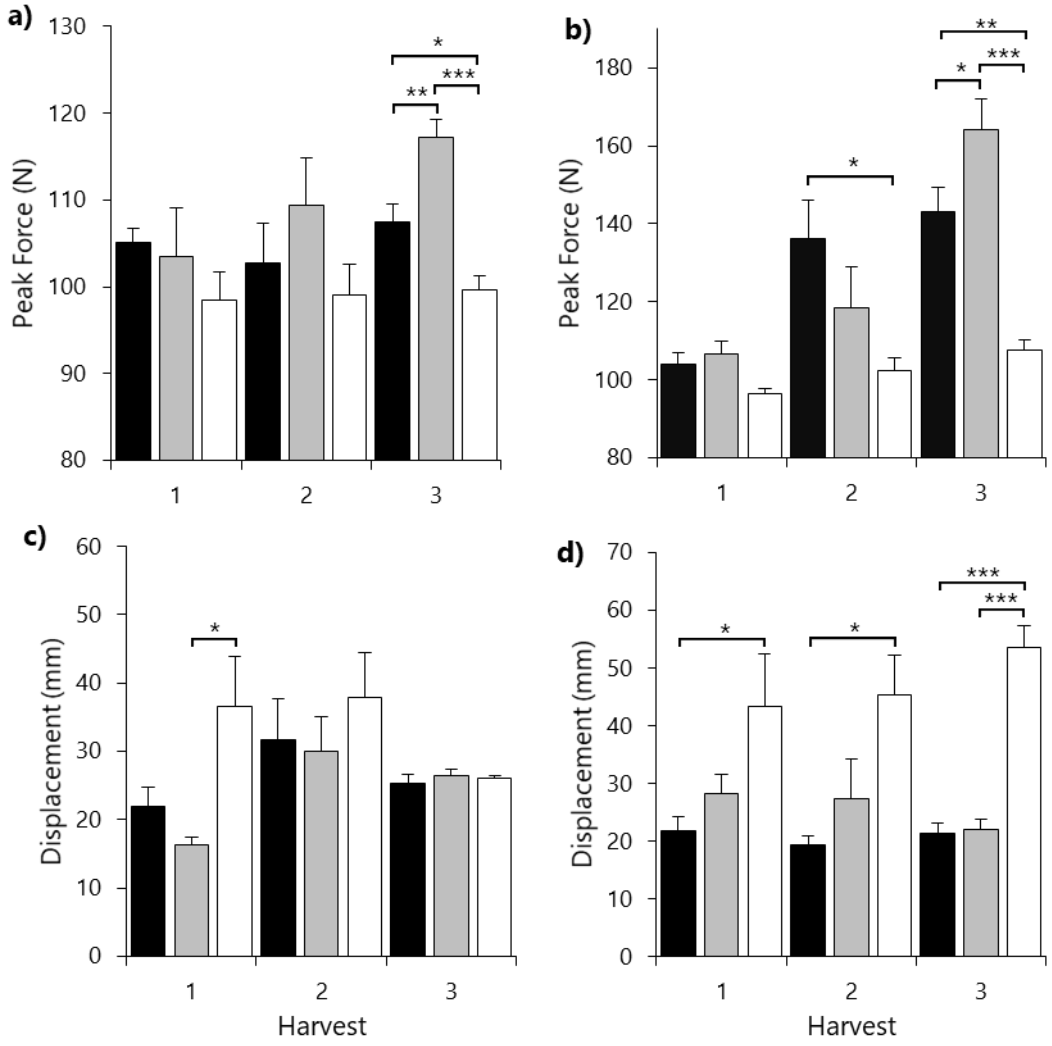

Figure 3.4. Peak force readings (a, b) and displacement distance (c, d) for barley (a, c) and maize (b, d) harvests (d). Black bars = root hairless mutants, grey bars = WT and white bars = unplanted control pots. Data are means of 6 replicates. Asterisks are derived from pairwise comparisons with a Bonferroni correction. * = $p < 0.05$, ** = $p < 0.01$, *** = $p < 0.001$. Error bars are equal to 1 standard error.

was not significant. For barley, the differences between the location of the peak force of the planted and the unplanted pots reduced with each successive harvest. In harvest 2, *brb* and its WT reached peak force 16.4 % and 20.7 % earlier than their unplanted pots and in harvest 3 *brb* pots reached peak force 2.7 % earlier, but WT pots reached peak force 1.3 % later than the unplanted pots. These differences were not statistically significant. Except for harvest 3 where WT pots tended to reach peak force before the *brb* pots and, like the unplanted pots, the differences (although not significant) decreased with successive harvests. Consequently, no consistent genotypic or harvest effect was observed in relation to where along the displacement profile the peak force was reached for barley.

For maize, *rth3* consistently reached its peak force before its WT and the corresponding unplanted pots were invariably last. For harvest 1, *rth3* and its WT reached peak force 49.7 % and 34.7 % earlier than the unplanted pots, for harvest 2 the difference increased to 57.1 % and 39.7 % for *rth3* and its WT respectively. For harvest 3 the differences increased again to 60.2 % and 58.7 % respectively. Although *rth3* consistently reached peak force before its WT at no point were the differences significant.

The presence of roots consistently (though not always significantly) decreased the mean displacement distance at which the peak force was reached for both species (except for barley harvest 3) in comparison to their respective unplanted pots. However, there was no consistent genotypic impact of root hairs as barley WT mostly reached peak force earlier than *brb* whereas the maize WT consistently reached peak force after *rth3*.

Table 3.1. Root parameters per genotype per harvest. Diameter = mean diameter of the whole root system, Lateral = the proportion of the root system made up of lateral roots, RLD = root length density and RSAD = root surface area density. Letters denote statistically different means ($p < 0.05$) than other harvests/genotypes within the species and are generated from a pairwise comparison with a Bonferroni correction. Data are means of 6 replicates ± 1 standard error.
* = $p < 0.05$, ** = $p < 0.01$, *** = $p < 0.001$

			Diameter (mm)	Lateral (%)	RLD (cm cm^{-3})	RSAD (cm^{-2} cm^{-3})
Barley	*brb*	1	0.146 ± 0.003^{a}	96.77 ± 0.69^{ab}	8.94 ± 1.37^{a}	0.408 ± 0.064^{a}
		2	0.143 ± 0.005^{a}	94.94 ± 0.84^{ab}	10.29 ± 0.81^{a}	0.461 ± 0.035^{a}
		3	0.165 ± 0.006^{ab}	93.35 ± 1.35^{b}	13.62 ± 3.80^{a}	0.692 ± 0.188^{a}
	WT	1	0.161 ± 0.003^{ab}	95.65 ± 0.38^{a}	11.18 ± 0.87^{a}	0.567 ± 0.049^{a}
		2	0.180 ± 0.002^{b}	91.89 ± 0.82^{ab}	16.41 ± 1.35^{a}	0.787 ± 0.074^{a}
		3	0.170 ± 0.008^{b}	93.77 ± 1.53^{ab}	15.66 ± 2.87^{a}	0.835 ± 0.079^{a}
Maize	*rth3*	1	0.236 ± 0.006^{a}	93.40 ± 0.82^{a}	4.14 ± 0.49^{a}	0.305 ± 0.033^{a}
		2	0.257 ± 0.010^{a}	94.43 ± 0.53^{a}	5.69 ± 0.69^{ab}	0.451 ± 0.040^{ab}
		3	0.255 ± 0.009^{a}	95.03 ± 0.80^{a}	7.18 ± 0.74^{ab}	0.572 ± 0.053^{b}
	WT	1	0.229 ± 0.012^{a}	93.58 ± 1.13^{a}	3.96 ± 0.80^{a}	0.271 ± 0.044^{a}
		2	0.240 ± 0.004^{a}	95.20 ± 0.77^{a}	6.47 ± 0.98^{ab}	0.489 ± 0.074^{ab}
		3	0.247 ± 0.012^{a}	94.66 ± 1.22^{a}	8.49 ± 0.77^{b}	0.649 ± 0.041^{b}

ANOVA	*F Value*	*F Value*	*F Value*	*F Value*
Species	333.71***	0.00	46.07***	10.79**
Genotype	0.88	0.80	4.33*	5.28*
Interaction	10.80**	1.48	2.06	3.13

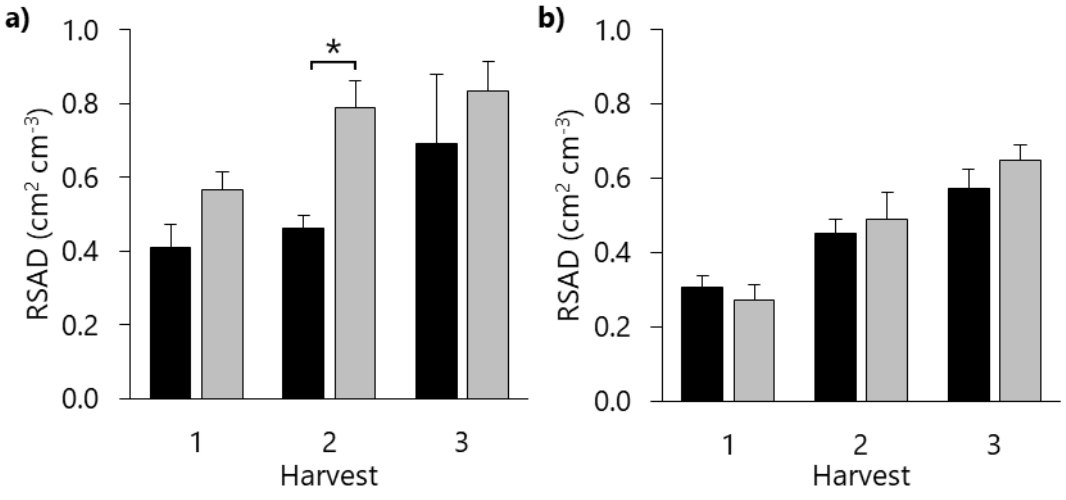

Figure 3.5. Root surface area density (RSAD) per harvest for barley (a) and maize (b). Black bars represent root hairless mutants and grey bars represent their respective WT. Data are means of 6 replicates and error bars are equal to 1 standard error. Asterisks is from a student t-test, * = < 0.05.

3.3.2. Root parameters

Not all parameters varied over time (Table 3.1). For root diameter, only the maize WT increased significantly with harvest. Proportional representation of lateral roots was also poorly and inconsistently correlated with harvest, with the percentage of lateral roots decreasing with each harvest in *brb* and tending to increase with each harvest in *rth3*. For all genotypes RLD increased with harvest, although RLD decreased from harvest 2 to harvest 3 in barley WT. Only RSAD increased with harvest for each genotype of each species (Figure 3.5), suggesting that RSAD is the most appropriate root trait for representing the growth stage of the harvests.

Across all harvests, the barley genotypes had significantly ($p < 0.001$) thinner roots (by 34.2%) than the maize genotypes. The percentage of lateral roots did not differ between species ($p = 0.99$), varying by only 0.01 %. Barley roots grew at a mean rate of 23.81 ± 1.46 and 31.34 ± 1.31 cm day^{-1} for *brb* and its WT, respectively, and maize roots grew at a slower rate of 16.22 ± 0.96 and 17.59 ± 0.41 cm day^{-1} for *rth3* and its WT, respectively. Thus, the RLD of maize root systems was 52.8 % less than in barley. However, though shorter, maize roots were significantly ($p < 0.001$, Table 3.1) thicker than barley, producing on a mean 34.2 % greater thickness than the barley roots. So, barley had longer roots, but maize had thicker roots, and as RSAD is more responsive to increases in length the RSAD of barley was significantly ($p < 0.001$) greater (by 27.1%) than maize.

Root hair presence/absence also affected root parameters. The maize WT and barley *brb* had consistently lower mean root diameter than their genotypic counterparts. The barley WT and maize *rth3* had the least percentage of lateral roots in their species at

Table 3.2. Pearson correlation coefficients for measured root parameters and displacement at which the peak force was recorded. RLD = root length density and RSAD = root surface area density.
* = $p < 0.05$, ** = $p < 0.01$, *** = $p < 0.001$

	Correlations	Diameter (mm)	Fine roots (%)	RLD (cm cm^{-3})	RSAD (cm^2 cm^{-3})
Barley	Fine roots (%)	0.05			
	RLD (cm cm^{-3})	0.13	0.22		
	RSAD (cm^2 cm^{-3})	0.34*	0.18	0.90***	
	Displacement (mm)	0.07	-0.07	-0.06	-0.08
Maize	Fine roots (%)	-0.66***			
	RLD (cm cm^{-3})	-0.18	0.54**		
	RSAD (cm^2 cm^{-3})	0.07	0.38*	0.97***	
	Displacement (mm)	-0.11	-0.19	-0.03	-0.06

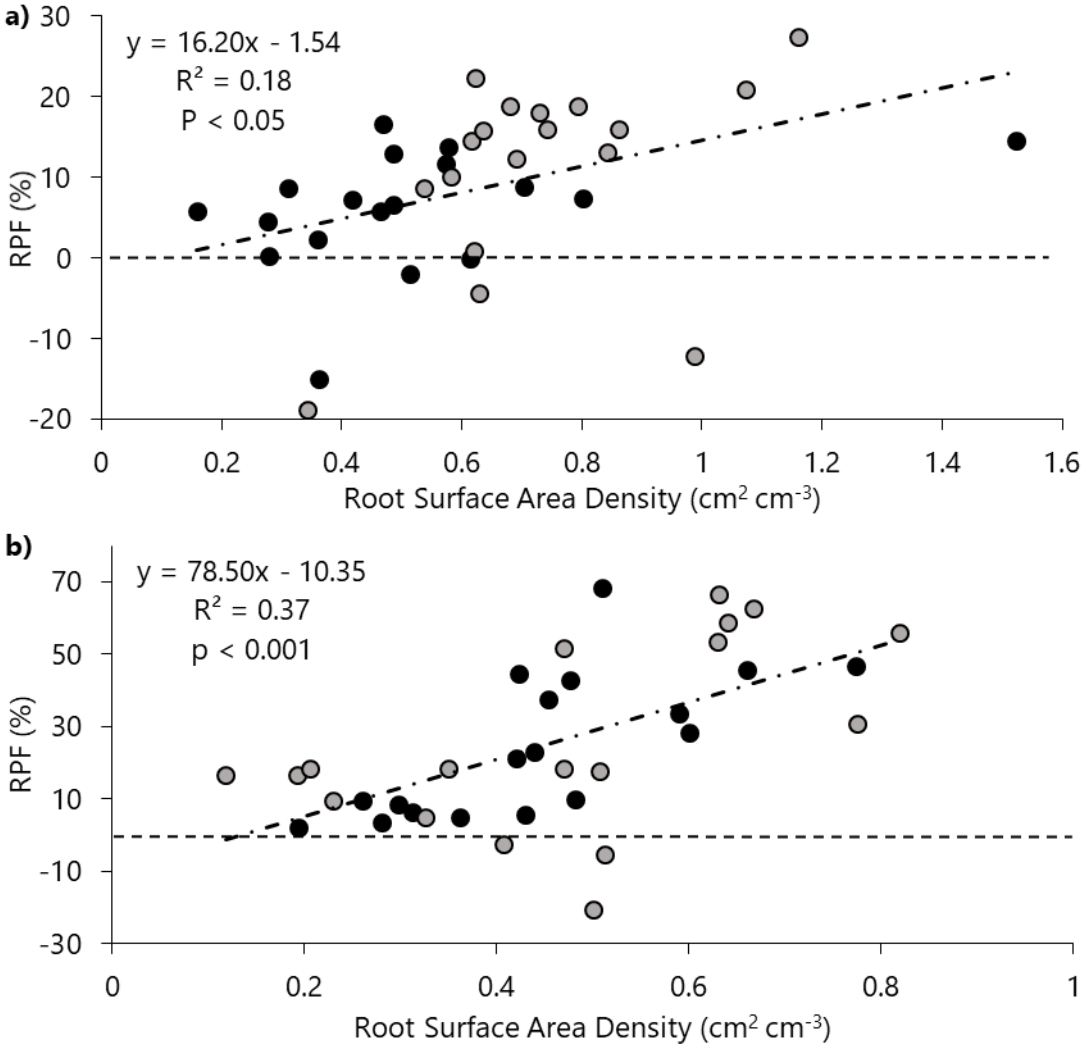

Figure 3.6. Relative increase in peak force (RPF) from the average unplanted pot against root surface area density (RSAD) for barley (a) and maize (b). Grey markers = WT and black markers = root hairless mutant. There was no significant genotypic effect so the dot and dash trend line represents the data from both root hairless mutant and its WT for both species.

harvests 1 and 2, but these genotypic effects were reversed at harvest 3. Root length density (RLD) was lowest in barley *brb* in all harvests. In maize, RLD was lowest in maize WT at harvest 1, but in *rth3* at harvests 2 and 3. The root hairless mutants had lower RSADs than their WT, except for the first maize harvest. RSAD showed the most consistent trends across the harvest and species.

3.3.3. Root effect on peak force

None of the root parameters for either species had a significant relationship with the distance at which the peak force occurred (Table 3.2). However, for both species the relative increase in peak force from their respective unplanted pots (RPF) significantly ($p < 0.05$ for barley and $p < 0.001$ for maize) increases with RSAD (Figure 3.6).

Although barley reached greater RSADs than maize (Figure 3.5 and Table 3.1), the rate at which one unit of RSAD increased RPF was significantly ($p < 0.001$) reduced in comparison to maize. For barley, RPF increased by 16.20 % with each unit increase of RSAD, whereas for maize the increase was at a rate 4.8 times greater, with one unit of RSAD increasing RPF by 78.5 %. During the tensile strength test, the peak force required to break the roots of both species increased significantly with root diameter ($p < 0.001$, Figure 3.7). Although maize roots reached thicknesses four times greater than barley, one unit increase in diameter significantly ($p < 0.001$) increases maize peak breaking force at a rate 2-fold more than barley roots (Figure 3.6). Thus, maize had a mean tensile strength 21.4 % greater than the barley roots. Barley pots produced a more extensive network of roots than the maize pots, but the increased diameter of the maize root systems were more effective at increasing the RPF, suggesting that root diameter is more influential at reinforcing soil than root proliferation.

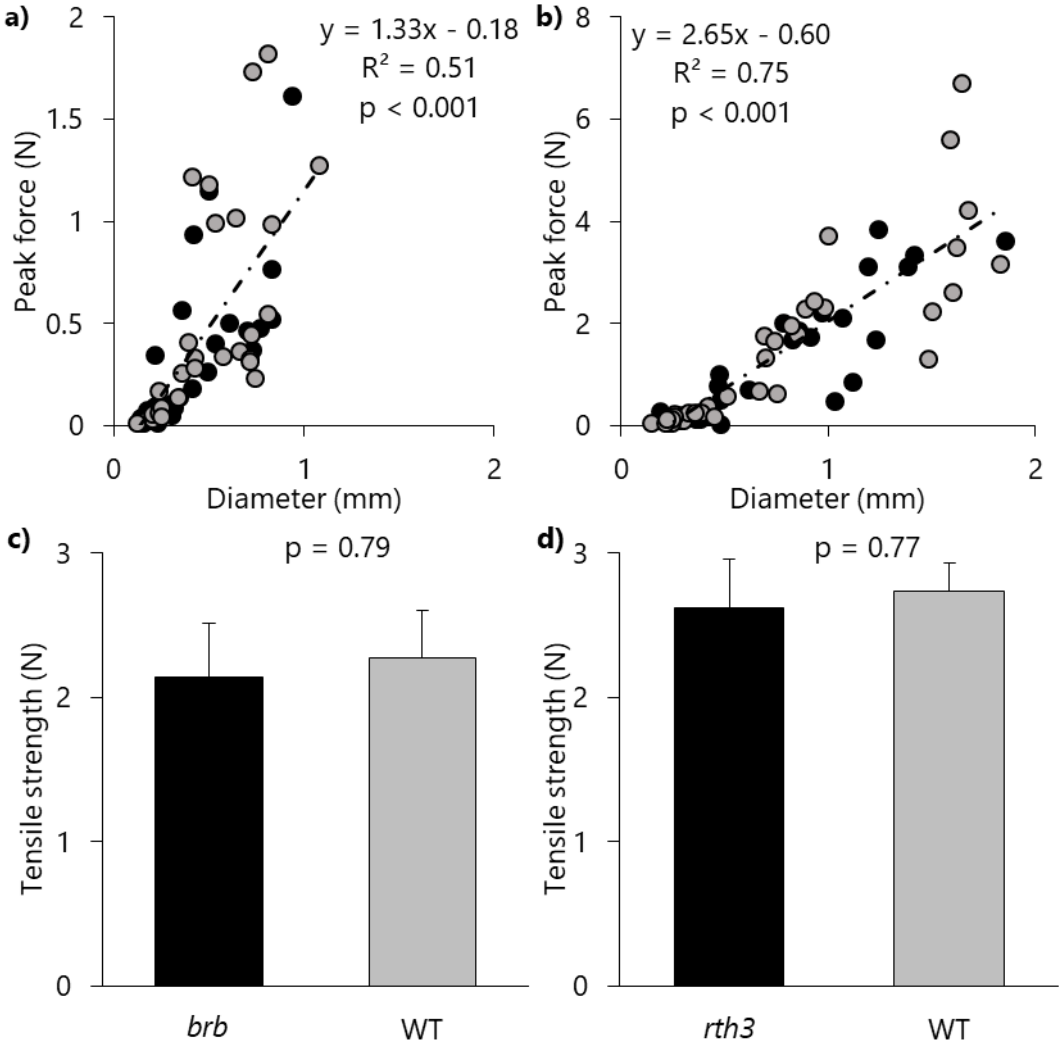

Figure 3.7. Peak breaking force against diameter of root for barley (a) and maize (b) and mean tensile strength of the barley (c) and maize (d). Grey = WT and black = root hairless mutant. For a and b, there was no genotypic effect so the dot and dash line is a trend line for both the WT and mutant data combined, p value is from an ANCOVA.
For graphs c and d, data are means of 32 measurements, error bars are equal to 1 standard error, and the p value is from an ANOVA.

Although barley WT roots and maize *rth3* roots were consistently thicker (Table 3.1) than their genotypic counterpart, both the barley and maize WTs and their respective root hairless mutants increased RPF at an equal rate (Figure 3.6). Additionally, the increase in peak breaking force with increasing root diameter (observed in the tensile strength test) was equal between root hairless mutants and WT plants (Figure 3.7). Thus mean root tensile strengths did not differ more than 5.8 % for barley and 4.1 % for maize, which were well within 1 standard error of the data's distribution. Since genotype did not affect root tensile strength ($p = 0.79$ and $p = 0.77$ for barley and maize respectively) or the relationship between diameter and RPF ($p = 0.60$ and $p = 0.94$ for barley and maize respectively), any variation in peak shearing force can be attributed to differences in root parameters and not due to the presence/absence of root hairs.

3.4. Discussion

3.4.1. Plant species affects root contribution to soil shear strength

Soil reinforcement by both barley and maize roots was measured under shear stress. As the top part of the pot is displaced, increasing tension is exerted on the roots. Roots subjected to increasing tension ultimately reach a point where they either break or are pulled out of the soil (Pollen, 2007). Rooted soil columns required considerably more force to shear than unplanted soil columns and the force required to shear the pots increased with increasing root presence, as previously observed (Jonasson and Callaghan 1992; Pollen and Simon 2005; Fan and Su 2008; Loades *et al.* 2010; Li *et al.* 2013). However, when roots are present, root diameter seems to be the determining trait for soil reinforcement.

As the pots are displaced, the force exerted increases to a peak (termed the peak shear force) and then tapers off. Peak shear force increased with increasing RSAD in each species, however not at the same rate. Although RSAD of barley roots was consistently greater (by 27.1 %) than maize (Figure 3.5), the force required to shear the maize pots increased at a rate 6.3 times greater than the barley pots resulting in peaks far greater in the maize pots than the barley pots (Figure 3.4). The peak tensile strength of a group of roots is less than the combined strength of each individual root because each root has a different peak breaking force and so they do not break in unison. When tension is initially exerted (assuming all roots are perpendicular to the shearing plane) the force is equally distributed, but when the force exceeds the strength of the weakest root, it will then break, compounding the force on the remaining roots (Pollen and Simon 2005). RLD of barley was much greater (by 52.8%) than maize, so it can be assumed that more roots crossed the shearing threshold in the barley pots than in the maize pots. However, the maize roots were significantly thicker than barley roots (an increase of 51.9 %). Root diameter determines the force needed to either break the root or cause it to be pulled from the soil (Pollen and Simon 2005; Norris 2005; Pollen 2007; Tosi 2007; Fan and Su 2008; Docker and Hubble 2008) and so, even though maize had less root mass, the individual roots were stronger than barley, due to their increased diameter. Taken together, the thinner, more numerous barley roots are not as effective at reinforcing the soil as the thicker but less numerous maize roots.

Although it is widely understood that tensile strength decreases as root diameter increases (Nilaweera and Nutalaya 1999; Pollen and Simon 2005; Genet *et al.* 2005; Burylo *et al.* 2012; Yang *et al.* 2016; Hudek *et al.* 2017), surprisingly the thicker maize roots had greater tensile strength than the thinner barley roots. Root tensile

strength can be changeable depending on the orientation of slope and prevailing wind direction (Stokes *et al.* 1995; Norris 2005). Taller plants have extra weight to anchor, so produce roots with greater tensile strength (Nilaweera and Nutalaya 1999; Ali 2010; Sun *et al.* 2011; Osman *et al.* 2011). It is therefore rational that maize roots have greater tensile strength per diameter and a greater breaking point, because they grow significantly taller and, thus, have more above-ground matter to support.

There is a general consensus in the literature that increasing soil water content decreases the soil shear strength (Vanapalli *et al.* 1996; Kayadelen *et al.* 2007; Fan and Su 2008; Hales and Miniat 2016; Yang *et al.* 2016). For the maize pots, there was no difference in WC between the treatments so this phenomenon is of no concern. In the barley experiment, unplanted pots had greater WC than both the *brb* and WT pots at each harvest by a mean of 5.3 % and 7.1 %, respectively. This suggests that the peak shearing force of the soil alone would have been reduced in the unplanted pots in comparison to the rooted pots and that the increased force required to shear the rooted pots may have resulted from both dryer soil and the presence of roots. The reduction in soil shear strength with increasing WC varies with soil type. Further experiments are needed to establish how much the variation in WC altered the shear strength of the soil before the root reinforcement from the barley roots can be properly quantified.

3.4.2. Impact of root hairs on soil shear strength

Although root hairs increased the resistance of seedling radicles to removal from the soil (Stolzy and Barley 1968; Ennos 1989; Czarnes *et al.* 1999; Bengough *et al.* 2011, 2016) and significantly increased the amount of soil bound to the root system (Figure 2.4), they did not improve soil reinforcement. The root systems of the root hairless mutants were equally as capable as their respective WT in reinforcing the soil as they

required equal forces to shear. Although barley WT roots had significantly longer and more numerous root hairs than the maize WT roots and thus, would form more rhizosheath (as concluded in Chapter 2.5), these differences in rhizosheath formation did not affect soil reinforcement. In contrast, barley roots consistently provided less soil reinforcement than the maize root systems.

A root's ability to withstand shear forces and contribute to a soil's shear strength is determined by its ability to withstand breaking. Root hairs are only single celled and have significantly smaller diameters than their parent roots, so their breaking force is estimated to be an order of magnitude less than that of a fine root (Bengough *et al.* 2011). Although root hairs can effectively reinforce singular roots (Handley and Davy 2002; Bengough *et al.* 2011, 2016; Haling *et al.* 2013), they do not reinforce a more complex root system because their contribution is overshadowed by the shear resistances exerted by the greater tensile strength and diameter of the roots themselves (Figure 3.8).

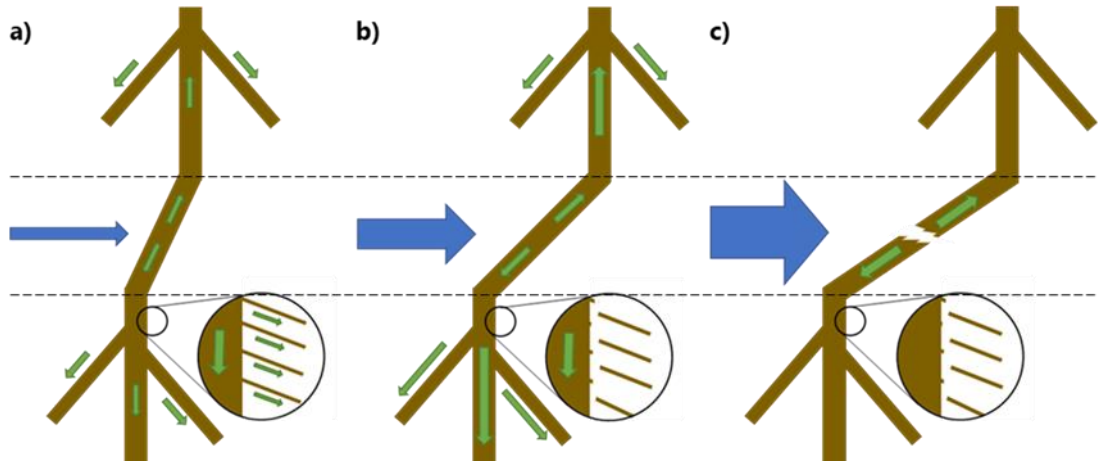

Figure 3.8. A conceptual diagram of the impact of root hairs on a roots ability to reinforce soil at the shearing plane (dashed lines). Under low stress (a) all roots including root hairs contribute to anchoring (green arrows) the root however as the shearing force increases (blue arrow) the breaking force of the root hairs is reached (b) long before the parent root breaks (c) thus root hairs have no effect on the ultimate soil reinforcement supplied by the root.

3.5. Conclusion

This study investigated which root traits most influenced a root system's ability to reinforce soil. Root hairless mutants of barley and maize were assessed for both their tensile strength and their contribution to soil shear resistance. Barley roots were more than twice as numerous as maize roots, but were almost half as thin, so broke under significantly less force than the maize roots. So, increased root diameter reinforced soil more effectively than increased root length density. Additionally, maize roots exhibited slightly elevated tensile strengths in comparison to barley roots, so withstood greater forces than barley roots of a similar diameter. Overall, maize root systems (with their increased diameter and tensile strength) were five times more efficient at reinforcing soil than the barley root systems. As for the impact of root hairs on soil reinforcement, since the WT and root hairless mutants showed no differences in soil reinforcement, it can be concluded that root hairs (with their minute diameter) have very little impact on soil reinforcement, as they cannot withstand the same forces resisted by the main root system.

Chapter 4. A mesocosm-based assessment of whether root hairs influence soil erosion under simulated rainfall.

4.1. Introduction

Erosion of agricultural soil is of global concern (Quinton *et al.* 2010; Borrelli *et al.* 2017) and has severe financial implications, but also threatens our food security (Verheijen *et al.* 2009; Posthumus *et al.* 2015). Soil can be eroded by both wind and water with water being the prominent cause in the UK (Verheijen *et al.* 2009). When the intensity of rainfall exceeds either the infiltration rate and/or capacity of the soil, water pools on the soil surface. If the surface is sloped, then the water will move with gravity to create surface flow. The velocity of the surface flow can vary depending on the angle of the slope and the quantity of water, with increasing velocity comes a greater erosive force (Nearing *et al.* 1997). The mechanisms that cause soil to erode via water are governed by the detachment force of water *versus* the cohesive and adhesive bonds between the soil particles (Laflen *et al.* 1991). For soil to erode the former must exceed the latter and the contrary is true for mitigating soil erosion. Soil strength, and thus, the soil's resistance to erosion, is mostly determined by properties such as aggregation and organic matter (Amézketa 1999).

Plants have long been known to reduce soil erosion (Acostasolis 1947; Singer *et al.* 1980). Although most research has focused on the impact of above-ground plant matter (such as canopy cover and stems), the relative contribution of roots to preventing soil erosion can outweigh the contribution of above-ground matter (Zhou and Shangguan 2007). Up to 95% of a plant's ability to reduce soil erosion, caused by overland flow, can be attributed to its root system (De Baets *et al.* 2006; Zhou and

Shangguan 2007; Burylo *et al.* 2012). Other studies report more conservative figures; 64% (Mamo and Bubenzer 2001a), and 35% (Prosser *et al.* 1995). Similar results were found when simulated rainfall (rather than overland flow) was the erosive force (Ghidey and Alberts 1997; Zhou and Shangguan 2007, 2008). Determining the quantitative variation in the contribution of the root system to ameliorate soil erosion requires an understanding of the mechanisms by which roots mediate erosivity.

Plant roots influence soil erosivity in different ways. They can increase soil porosity and decrease soil bulk density (Zhou and Shangguan 2007; Shinohara *et al.* 2016) thus increasing infiltration and reducing surface flow. Moreover, root exudates fortify soil by chemically facilitating the bonds between particles and can increase the number, size, and durability of water stable aggregates (Jastrow *et al.* 1998; Amézketa 1999; Zhou and Shangguan 2007; Wang *et al.* 2017). Soil organic carbon is strongly associated with aggregate stability (Tisdall and Oades 1982; Annabi *et al.* 2007) and roots can contribute up to 2.3 times more soil organic carbon than above-ground plant matter (Kätterer *et al.* 2011). Thus, roots provide biological, chemical, and physical support to the soil.

Previous studies looking at the impact of roots on soil erosion found a variety of root parameters are significantly negatively correlated with sediment yield including: root surface area (Li *et al.* 1991; Prosser *et al.* 1995; Zhou and Shangguan 2005, 2007, 2008), root length density (Bui and Box 1993; Ghidey and Alberts 1997; Mamo and Bubenzer 2001a; b; De Baets *et al.* 2006, 2007), root density (Tengbeh 1993; Gyssels and Poesen 2003), and diameter (Li *et al.* 1991), and a combination of the above (Shit and Maiti 2012). Further to this, Burylo *et al.* (2012) carried out a multi-species analysis on nine functional root traits, including all of the above, and found that soil

detachment rate was most strongly correlated with root diameter (positively) and percentage of fine roots (negatively).

At just a cell thick, root hairs are only just visible to the naked eye but have been associated with some of the characteristics attributed to aiding the rest of the root system in reducing soil loss. For example, their abundance throughout the root system means that over 90% of root surface area can be attributed to the presence of root hairs (Gilroy and Jones 2000). This increased surface area is one of the reasons why root hairs are considered the main vector for water uptake by the root system (Segal *et al.* 2008; White and Kirkegaard 2010; Wasson *et al.* 2012). Root hairs can grow as long as 1.5 mm (Brown *et al.* 2017) and their total length can be 20 times that of the rest of the root system (Wulfsohn and Nyengaard 1999). Due to their small diameter, root hairs can physically penetrate and enmesh soil aggregates (Rasse *et al.* 2005; Keyes *et al.* 2013). Further to this, White and Kirkegaard (2010) show that roots actively increase root hair density to increase soil contact. So, root hairs exhibit traits suggesting that they are beneficial to soil reinforcement.

Though not directly linked to soil erosion, some studies have shown an association between root hairs and soil strength. Czarnes *et al.* (1999) and Ennos (1989) show that root hairs play a role in anchoring the plant to the soil. Logically, this conclusion can be reversed to suggest that root hairs also play a role in anchoring the soil to the root. Root hairs are seen as one of the key requirements for binding soil to the root through the formation of the rhizosheath (Watt *et al.* 1994; McCully 2005; Brown *et al.* 2017; Pang *et al.* 2017). In addition, George *et al*. (2014) and Delhaize *et al*. (2015) found that root hair length is positively correlated with the amount of soil secured in the

rhizosheath. However, no studies looking at the impact of root hairs on soil erosion were found.

Although root hairs strongly influence a number of traits associated with a plant's ability to reduce soil erosion, such as increased surface area and the binding of soil to the root, it has not yet been established if the soil binding abilities of root hairs have any impact on soil erosion mitigation. This chapter aims to investigate whether the presence of root hairs and their increased ability to bind soil ameliorates soil erosion. Root hair traits and their interactions with the soil (Chapter 2) strongly suggest that they should affect a plant's ability to reduce soil erosion. This experiment will compare root hairless mutants to their wild type in mesocosms under simulated rainfall to better understand how the root system mitigates soil erosion.

4.2. Materials and methods

4.2.1. Mesocosm construction

The mesocosms were constructed out of 21 litre plastic containers (Euro Container ref. 9230001, Schoeller Allibert Ltd, UK), with an internal area of 55.5 cm length x 3.6 cm width x 11.5 cm height (Figure 4.1). Drainage holes were drilled in the base in a 5 cm grid to aid drainage. The top 2.5 cm of the front edge was removed so that the surface of the soil would be above the edge of the plastic, with 1 cm leeway, to remove any obstacles to drainage. The detached section was temporarily re-attached during the growth stage to maintain the front edge of the soil profile. Guttering was constructed out of 40 mm pipe with a 90° bend, which was solvent welded to one end and affixed to the box with small nuts and bolts, with silicone sealant used to prevent leakage. The whole box was then affixed to a piece of 18 mm thick marine plywood, cut with corresponding drainage holes and oversized to allow handles to be attached to

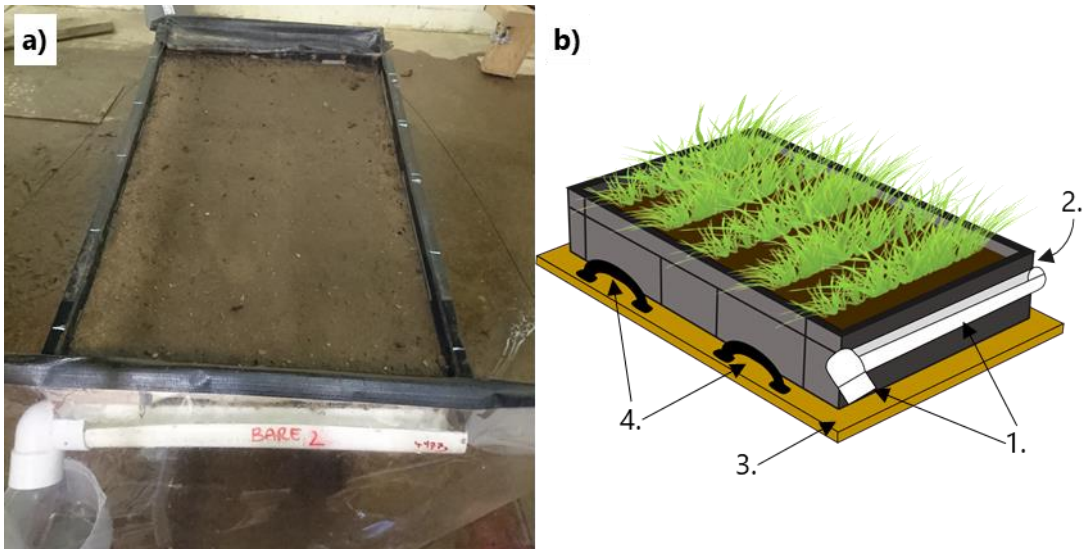

Figure 4.1. A mesocosms under the rainfall simulator with the cover over the outlet drainpipe and the collection container (a) and a schematic of the boxes (b) showing; 1. Gutter and U-bend spout, 2. Removable box section that is kept in place during the growth stage to support the soil, 3. Plywood base for reinforcement and 4. Lifting handles.

either side of the box. The plywood and handles were necessary to minimise any disturbance to the soil structure whilst moving the mesocosms. The mesocosms had a layer of 20 mm gravel lining the bottom to aid drainage and then filled with a sandy loam textured top soil (as detailed in Chapter 2.2.2). The soil was packed to a bulk density of 1.4 g cm^{-3} and filled in 3 cm increments to achieve a uniform profile.

4.2.2. Germination and growth

Each block (5 in total) consisted of 3 mesocosm treatments, a barley root hairless mutant (*brb*), its wild type (WT, as described in Chapter 2) and an unplanted control. Seeds were placed in five trenches dug, approximately 1 cm deep, across the width of the mesocosm and spaced at 11.5 cm intervals (assuming an 80 % germination rate, this equated to 12 seeds per row and a density of 245 seeds m^{-2}). The trenches were then filled in and the surface smoothed over. For continuity, this process was also carried out on the unplanted mesocosms (minus the seeds). The mesocosm was then wetted until a film of water appeared on the surface using a watering can with a spray rose attached (this was sufficient water for the barley to grow, any more resulted in

excessive movement of surface soil). The mesocosms were kept in a walk-in controlled environment room (as described in Chapter 2) and watered, as stated above, every 2–3 days for 35 days until harvest.

4.2.3. Rainfall simulator

This experiment used a gravity-fed rainfall simulator (Armstrong *et al.* 2012), approximately 3 m above the mesocosm surface (Figure 4.2). The simulator consisted of 958 hypodermic needles (25G x 25 mm, BD Microlance™ 3, Fisher Scientific, UK) in 27 staggered rows of 35 and 36 needles in a grid 47.25 x 72.00 cm, producing a rainfall rate of approximately 23 mm h^{-1} (CU = 86.6). A 2 mm mesh was suspended approximately 20 cm below the needles to disperse the water droplets and make them less uniform in size and distribution on the mesocosm surface. The simulator was run with tap water and there is a weir and outlet pipe in the chamber above the needles to ensure a consistent water pressure through the needles.

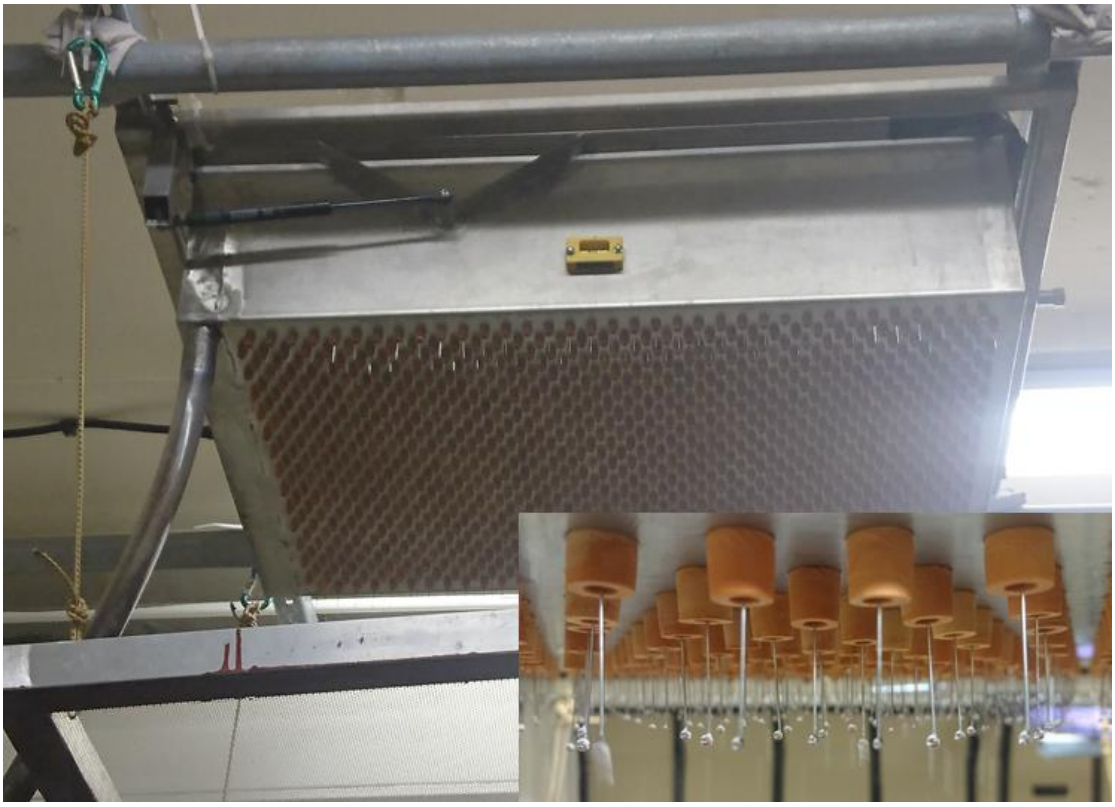

Figure 4.2. Gravity-fed rainfall simulator and the mesh hanging below with a close up of the droplets on the needle points.

4.2.4. Harvest

The day before harvest, the mesocosms were left standing in approximately 5 cm of water overnight to pre-wet from the base to achieve a consistent soil water content (soil moisture measurements made before each experiment proved that this method was effective). The rainfall simulator was turned on 1–2 hours before the experiment, to give time for the needle reservoir chamber to fill. The shoots and leaves were removed with care so as not to disturb the surface soil immediately prior to each test. Any large gaps (approx. > 3 mm) which formed as a result of soil shrinkage or movement of the temporary barrier were filled with plumber's putty (Plumbers Mait, Evo–Stik, UK), this also served to reinforce the front edge of the soil, preventing it from slumping. Each mesocosm was then placed on a 6 % slope under the rainfall simulator for 1 hour. Sediment and runoff were continually collected in a beaker, at 5 minute intervals the contents of the gutter was washed into the beaker using a measured amount of water from a 60 ml syringe and the beaker replaced with an empty one. The beaker contents were weighed and then washed into a metal tray to be dried in an oven at 105 ℃. The amount of erosion for each interval was equal to the weight of the dry soil and is displayed as soil detachment rate (SDR). The amount by which the presence of roots reduced the quantity of eroded soil in comparison to their respective unplanted mesocosms (relative soil detachment reduction rate, RSDR) is calculated as a percentage decrease from the unplanted mesocosms:

$$RSDR = \left(\frac{E_c - E_r}{E_c}\right) \times 100$$

where E_c is the sum of the erosion from the control unplanted mesocosm and E_r is the sum of the erosion from the rooted mesocosm. The amount of runoff was calculated from the weight of the beaker's initial content, minus the weight of soil and beaker.

Roots were harvested from the top 1.5 cm of soil using a guillotine, then washed out of the soil. The roots were stored in a 50 % ethanol and DI water solution and kept at approximately 4 ℃ until they were measured. The roots were then scanned at 600 DPI using an Epson expression 11000 XL pro scanner, analysed using WinRHIZO (2013a Pro, Regent, Canada), as described in Chapter 2. Root length density (RLD) was calculated as follows:

$$RLD = \frac{RL}{V_s}$$

where RL is the total length of live roots (cm) and V_s is the volume of soil sampled (cm^3). Root surface area density was similarly calculated:

$$RSAD = \frac{(\pi D) \times RL}{V_s} = \frac{RSA}{V_s}$$

where D is the diameter (cm) of the root and RSA is the root surface area (cm^2) is under the assumption that the root is cylindrical. Percentage of fine roots is calculated using the diameter threshold described in Chapter 2 (Figure 1.2). The quantity of rhizosheath for each species was calculated using the data from Chapter 2 (*brb* = 13.3 mg cm^{-1}, WT = 41.2 mg cm^{-1}) and the average rhizosheath in each mesocosm for the two genotypes was assumed to be 91.5 ± 34.0 g for *brb* and 125.0 ± 48.0 g for WT.

4.2.5. Statistical analysis

The erosion data were non-normally distributed so a repeated measures Friedman's Test and a Wilcoxon ranked sum post-hoc test with Bonferroni correction were used to assess the difference in the erosion and runoff rates. Pearson's Correlation and ANOVA were used to assess the root data.

4.3. Results

4.3.1. Erosion

The impact of roots on SDR was initially delayed (Figure 4.3). It took 25 minutes of rainfall for the mean of the unplanted mesocosms to exceed that of both the rooted treatments. For this reason, 25 minutes was taken as the threshold for root impact. The average amount of erosion at 25 mins, before roots became influential, was 27.1 ± 4.1 g for unplanted, 29.6 ± 10.1 g for *brb* and 22.2 ± 4.8 g for WT mesocosms and all treatment were statistically equivalent to each other ($p = 0.069$). Assuming erosion occurred uniformly across the mesocosms, this would equate to an average eroded depth of 0.061 ± 0.009 mm across all treatments. Due to the lack of discernible root influence, the first 25 minutes of erosion are discarded from further erosion analysis.

In the subsequent 35 minutes, the rate of erosion in the *brb* and WT is significantly different from the unplanted mesocosms ($Z = -4.39$, $p < 0.001$ and $Z = -4.17$, $p < 0.001$ respectively). Although the erosion rate from *brb* and WT mesocosms did not significantly differ ($Z = -1.25$, $p = 0.383$), WT most frequently yielded less soil than both the unplanted and *brb* mesocosms, resulting in the greatest overall reduction in SDR with an average decrease of 40.4 ± 15.0 % from their respective unplanted mesocosms (Table 4.1). Barley *brb* consistently yielded the second least soil with an average of 32.2 ± 12.6 % less soil than their corresponding unplanted mesocosms. This translates to an eroded depth of 0.07 ± 0.02 mm for the planted mesocosms in comparison to the eroded depth of 0.12 ± 0.02 mm from the unplanted mesocosms.

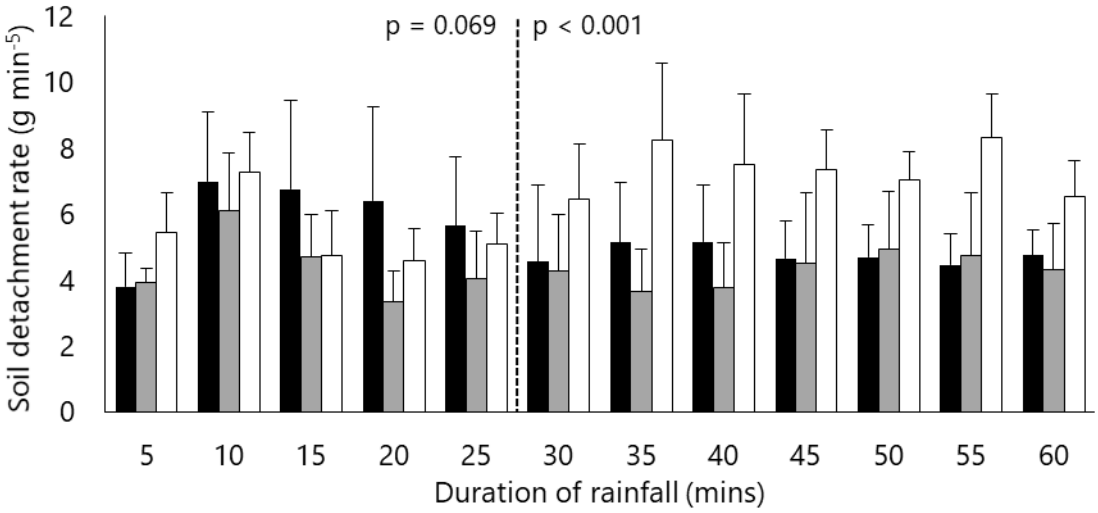

Figure 4.3. The total erosion per each 5 minute interval. The dashed line depicts the threshold where erosion from unplanted mesocosms begins to consistently surpass those of rooted mesocosms. P values are from the Friedman's Test for the first 25 mins of rainfall and the subsequent 35 mins of rainfall. The solid black bars = *brb*, grey bars = WT and the white bars = unplanted. Bars are means + SE of 5 replicates.

Table 4.1. Lists the mean ranks produced by the Friedman's Test from Figure 4.3 and the median and interquartile range of the soil detachment rate for all 5 replicates of the unplanted, *brb* and WT mesocosms.

	First 25 mins			Last 35 mins		
	Mean rank	Median	Quartile	Mean rank	Median	Quartile
Fallow	2.08	4.79	3.19	2.57	6.70	4.09
brb	2.28	4.83	5.46	1.89	4.03	2.73
WT	1.64	3.58	3.30	1.54	3.37	3.14

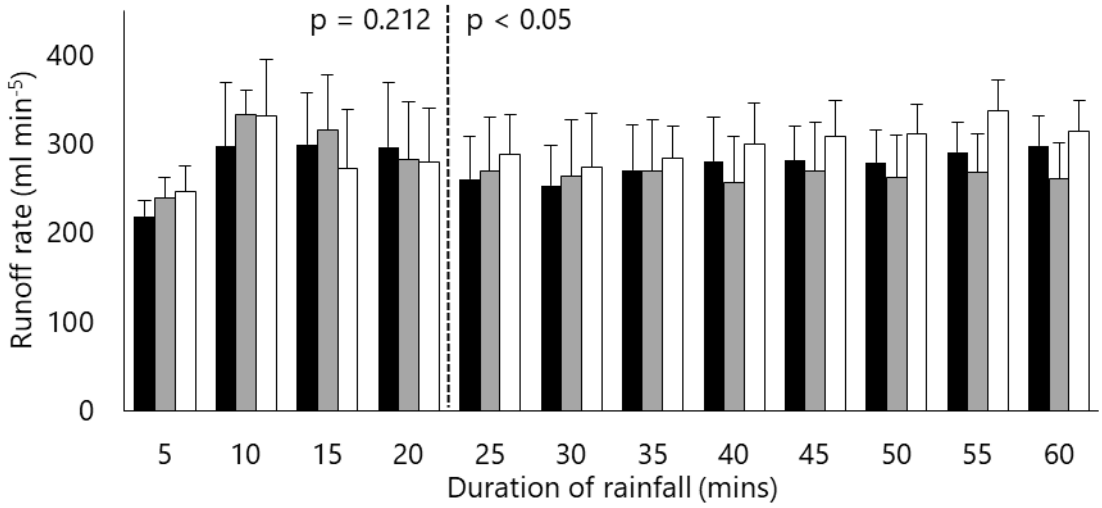

Figure 4.4. The runoff per each 5 minute interval. The dashed line depicts the threshold of root influence. P values are from the Friedman's Test for the first 25 mins of rainfall and the subsequent 35 mins of rainfall. The solid black bars = *brb*, grey bars = WT and the white bars = unplanted. Bars are means + 1SE of 5 replicates.

Table 4.2. Lists the mean ranks produced by the Friedman's Test from Figure 4.4 and the median and interquartile range of the runoff rate for all 5 replicates of the unplanted, *brb* and WT mesocosms.

	First 20 mins			Last 40 mins		
	Mean rank	Median	Quartile	Mean rank	Median	Quartile
Fallow	2.05	281.49	159.64	2.35	306.90	155.96
brb	1.70	259.99	125.01	1.88	242.58	96.89
WT	2.25	304.11	146.82	1.78	278.62	164.85

4.3.2. Runoff

Unlike erosion rates, runoff rates were much less susceptible to temporal fluctuations. After a brief peak 10 minutes into the experiment, the runoff rates remained relatively steady for the rest of the hour (Figure 4.4). However, as with erosion rates, there was a delay in the observable difference between rooted and unplanted mesocosms. The mean of the unplanted mesocosms consistently exceeded both the rooted treatments after the first 20 minutes of rainfall, in comparison to the first 25 minutes with erosion rates. In the last 40 minutes, the mean amount of runoff from the rooted mesocosms were consistently ($p < 0.05$) less than the unplanted mesocosms, though not every block followed this trend. For the 2nd and 4th block, the unplanted mesocosms produced more runoff than rooted mesocosms making the overall decrease from the unplanted mesocosms 9.5 ± 6.6 %. The WT mesocosms most frequently yielded the least runoff (Table 4.2), followed by *brb*, with unplanted mesocosms most frequently yielding the most runoff in the last 40 mins. The runoff rates (RR) for *brb* and WT both significantly differed from the unplanted mesocosms ($Z = -2.70$, $p < 0.05$ and $Z = -2.61$, $p < 0.05$, respectively) but were not significantly different from each other ($Z = -0.94$, $p = 1.041$).

4.3.3. Root parameters

As in previous chapters, *brb* grew faster than WT, resulting in a 66% greater root length density in the top 1.5 cm of the mesocosms (Table 4.3). Only root diameter and percentage of fine roots statistically differed between the genotypes. For WT, fine roots made up 11.8 ± 1.4 % less of the root system than in *brb* largely because WT root systems had a greater average diameter by 15.9 ± 3.0 %. Table 4.4 illustrates the correlation coefficients between measured root parameters. Root length density is the

Table 4.5. Summary statistics for the measured root parameters. RLD = root length density, RSAD = root surface area density, Est. R = estimated rhizosheath (as calculated from results in Chapter 2). F-statistic is from a one-way ANOVA, * = $p < 0.05$, ** = $p < 0.005$.

	Averages		
	brb	WT	F-statistic
Diameter (mm)	0.188 ± 0.009	0.223 ± 0.004	12.579*
Fine roots (%)	89.35 ± 1.55	79.93 ± 1.30	21.58**
RLD (cm cm^{-3})	2.54 ± 0.70	1.53 ± 0.59	1.21
RSAD (cm2 cm^{-3})	0.14 ± 0.04	0.11 ± 0.04	0.44
Volume (cm^3)	1.91 ± 0.44	1.74 ± 0.69	0.04
Est. Rhizosheath (g)	100.25 ± 27.75	187.10 ± 72.36	—

Table 4.4. A list of Pearson's Correlation Coefficients for all measured root parameters. RLD = root length density, RSAD = root surface area density. Units are as stated in Table 4.5.
* = $p < 0.05$, ** = $p < 0.005$, *** = $p < 0.001$.

	Diameter	Fine roots	RLD	RSAD
Fine roots	−0.96***			
RLD	−0.70*	0.71*		
RSAD	−0.55	0.59	0.98***	
Volume	−0.36	0.43	0.90***	0.97***

Table 4.3. Pearson's Correlation coefficients between the measures root parameters and RSDR with and without the anomalous 2nd replicate. RLD = root length density, RSAD = root surface area density. Units are as reported in Table 4.5. * = $p < 0.05$, ** = $p < 0.005$, *** = $p < 0.001$.

	With 2nd rep		2nd rep removed	
	brb	WT	*brb*	WT
Diameter	-0.63	-0.89	-0.86	-0.89
Fine roots	0.62	0.62*	0.82	0.82
RLD	0.48	0.49	0.99**	0.97*
RSAD	0.37	0.25	1.00**	0.90
Volume	0.29	0.19	0.99**	0.92

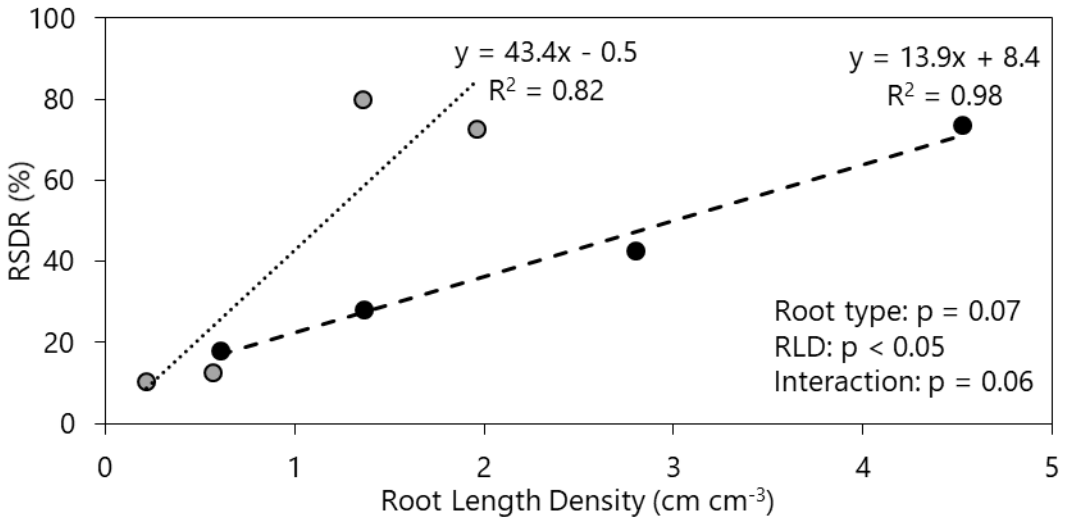

Figure 4.5. Shows the linear relationships between root length density and relative soil detachment rate (RSDR) for both *brb* (black markers with dashed line) and WT (grey markers with dotted line). A 50 % RSDR would mean that the planted mesocosm produced half as much erosion as the unplanted mesocosms, whereas a 0 % RSDR would mean it produced the same amount.
P values are derived from ANCOVA analysis.

chosen parameter for further analysis as it is the only parameter that is correlated with all other root parameters and shows no significant genotypic variation.

With an anomalously low erosion rate (Table 4.5) from one block removed, all the measured root parameters (except root diameter and percentage fine roots) were positively correlated with RSDR for *brb*. Less soil was detached in comparison to the unplanted mesocosms with increasing RLD for both genotypes (Figure 4.5) and although not significant, the interaction term ($p = 0.06$) suggests that increasing length of WT roots are more effective at reducing erosion (in comparison to unplanted soil) than increasing length of *brb* roots. These findings suggest that root hairs have the capacity to diminish soil erosion.

4.4. Discussion

Mesocosms containing three treatments, *brb* roots (lacking root hairs), WT roots (with root hairs), and unplanted soil (with no roots), were subjected to simulated rainfall under a laboratory gravity fed rainfall simulator. The presence of roots significantly decreased soil loss from both rooted treatments as the unplanted mesocosms produced

significantly greater concentration of soil in the runoff (Figure 4.3). The unplanted mesocosms also yielded more runoff though the differences in runoff (14.6 ± 5.5 % for *brb* and 11.8 ± 7.5 % for WT) were slight in comparison to the differences in soil loss (32.2 ± 12.6 % for *brb* and 40.4 ± 9.3 % for WT). Additionally, RLD significantly reduced the amount of soil eroded in comparison to their respective unplanted mesocosms (Figure 4.5). The presence of root hairs, however, seemed to limit soil erosion, with WT roots appearing to reduce soil erosion at a greater rate than *brb* roots, but comparing the genotypes at a higher range of RLDs and with additional measurements is required to substantiate this conclusion.

The presence of roots significantly decreased SDR (Figure 4.3 and Figure 4.5). This phenomena is well documented in the literature, even though the RLDs reported in this study are near the lower end of the range reported (0.04 cm cm^{-3} to 622.9 cm cm^{-3}) in previous studies (Vannoppen *et al.* 2015). Previous studies with similar RLD ranges have also found linear relationships between root parameters and RSDR (Zhou and Shangguan 2007, 2008) though most studies suggest the relationship is exponential (Gyssels *et al.* 2005; Vannoppen *et al.* 2015). However, this study shows that even at a relatively low root abundance, root systems can still significantly reduce soil erosion.

One of the mechanisms by which roots aid in decreasing soil erosion is by increasing soil shear strength (Prosser and Dietrich 1995; De Baets *et al.* 2008; Fattet *et al.* 2011). Tangentially, root masses increase surface roughness and provide physical barriers that capture loose soil (Prosser *et al.* 1995). Increased surface roughness also decreases the speed and density of the drainage network, which in turn reduces its speed and scourability (Römkens *et al.* 2002). However, these traits rely on the roots

withstanding the pressure of the sediment and water it is holding in place. Root hairs, and their ability to bind soil, have been strongly linked to anchoring the roots in the soil and resisting a pull out force (Ennos 1989; Bailey *et al.* 2002) and in facilitating root tip penetration of the soil (Jaunin and Hofer 1986; Bengough *et al.* 2011). Since no roots were visible above the surface of the soil, there is no evidence to suggest this was the mechanism reducing soil erosion.

Root systems of both genotypes decreased SDR, however, when the soil eroded from the planted mesocosms is expressed as a function of that from the unplanted mesocosms (RSDR), the data suggests that roots with root hairs could reduce erosion by rates up to three times greater than those without root hairs (Figure 4.5). Even though *brb* mesocosms produced a mean total root length more than twice that of WT mesocosms (1.2-fold; Table 4.3), this phenomenon would explain why less soil was eroded from the WT mesocosms (5.7 %) than the *brb* mesocosms. However, there are too few data points to certain of this putative effect.

The primary way in which root hairs reinforce the soil is by binding it in a rhizosheath and barley rhizosheaths are strong enough to withstand submersion in a sonic bath for 5 minutes (Brown *et al.* 2017). Barley WT and *brb* roots can form 41.2 mg cm^{-1} and 13.3 mg cm^{-1} of rhizosheath, respectively (as calculated from Chapter 2.3.1). When considering the volume of the mesocosms, this rhizosheath soil accounts for a mean of 2.3 ± 1.0 % for *brb* and 3.1 ± 1.2 % for WT of the top 1.5 cm. The WT roots are estimated to have 34.8 % more rhizosheath than the *brb* roots. However, considering the amount of soil eroded from each treatment with respect to the volume of soil sampled (which equates to 0.87 ± 0.30 % for *brb* and 0.82 ± 0.36 % for WT), WT is

only 5.7 % more efficient than *brb*. This suggests that the capacity to form a rhizosheath far exceeds the relative capacity to mitigate erosion.

4.5. Conclusion

In the absence of above-ground plant matter, this study showed that root systems with and without root hairs can reduce soil erosion, and increasing root length density (especially in *brb*) clearly enhanced this. The impact of root hairs, however, was less obvious. Even though *brb* tended to have greater RLD, it was less able to reduce erosion than WT roots, suggesting that WT roots could better mitigate soil erosion, even though the trend was not statistically significant ($p = 0.06$). Additionally, due to their greater rhizosheath development, WT root systems should have been able to fortify significantly more soil than *brb*, but the reduction in soil erosion was only slight in comparison. The mechanisms by which root hairs support the soil is still relatively poorly understood and further study is required to fully understand the contribution of root hairs and their rhizosheaths to soil reinforcement.

Chapter 5. Root hairs do not affect soil erosion from plots under rainfall simulation in the field.

5.1. Introduction

An estimated 17 % of the UK's 18.3 million hectares of agricultural land is affected by soil erosion (Posthumus *et al.* 2015), a phenomena that is observed worldwide (Quinton *et al.* 2010; Amundson *et al.* 2015). Soil is arguably a finite resource and is being eroded at rates several orders of magnitude greater than the rate it is being produced (Verheijen *et al.* 2009). Soil erosion is estimated to cost the UK an average of £248-£469 million (Posthumus *et al.* 2015) every year. Some costs are wrought as erosion preferentially acts on the top fertile layer of soil, reducing the productivity of agricultural fields, as well as causing damage to crops and causing difficult field working conditions. Furthermore, most of the costs are incurred off-site as a consequence of flood damage, siltation and eutrophication of watercourses and lakes.

Soil erosion is a type of physical degradation that results from a decline in the soil structure (Lal 2015). Overland flow (water) is the predominant driver of erosion in European countries (Verheijen *et al.* 2009). It can be categorised as inter-rill, rill, and gully erosion. Inter-rill erosion is defined as sheet erosion that preferentially transports smaller particles, whereas rill and gully erosion is when flow is concentrated and forms eroded channels, thus, eroding larger soil particles non-selectively (Shi *et al.* 2012). Although some soils are naturally prone to erosion, due to properties like their physical texture, organic matter content, and water holding capacity (Adhikari and Hartemink 2016), various agricultural practices can exacerbate the degradation of soil structure, thus intensifying soil erosion. These practices include tillage (Van Oost *et al.* 2006; Mehra *et al.* 2018), crop harvesting (Ruysschaert *et al.* 2004), and the

movement of farm equipment and livestock (Batey 2009). However, agricultural fields, independent of their soil structure or properties, are most at risk of soil erosion when they are left (completely or partially) bare (Anache *et al.* 2017). This can occur immediately after planting of tilled fields, in row crops prior to canopy closure or when fields are left unplanted between crops.

It is well understood that vegetation can protect soils from eroding (Durán Zuazo and Rodríguez Pleguezuelo 2008) and in time even reverse degradation (Gerhardt *et al.* 2009). Most research has concerned above-ground plant material. The size and shape of leaves, as well as their inclination and orientation, affect the plant's ability to reduce soil erosion by dampening the force of rain drops (Elwell and Stocking 1976; Foot and Morgan 2005; Nearing *et al.* 2005; Frasson and Krajewski 2013). When raindrops impact the soil surface, their force dislodges and disperses smaller particles, resulting in a particle sorting that can lead to surface crusting (Armenise *et al.* 2018; Carmi *et al.* 2018), which aggravates erosion. The stems of plants also dampen concentration flow, which in turn reduces soil erosion; with their diameter, abundance, and rigidity all determining their effectiveness (Fasching and Bauder 2001; Melville and Morgan 2001; Xiao *et al.* 2011; Lambrechts *et al.* 2014; Mekonnen *et al.* 2016; Li and Pan 2018). While the effects of above-ground plant material in mitigating soil erosion has been relatively well documented, plant roots can have as much, if not more, impact (Gyssels and Poesen 2003; De Baets *et al.* 2006; Zhou and Shangguan 2007; Zhang *et al.* 2012; Burylo *et al.* 2012; Katuwal *et al.* 2013; Zhao *et al.* 2017; Li and Pan 2018).

Most research into root effects on soil erosion have used controlled laboratory conditions (Vannoppen *et al.* 2015), with root length (Mamo and Bubenzer 2001a;

Shit and Maiti 2012; Burylo *et al.* 2012; Niu and Nan 2017), root surface area density (Zhou and Shangguan 2005, 2007, 2008; Shit and Maiti 2012; Burylo *et al.* 2012), root area ratio (De Baets *et al.* 2006), diameter (Li *et al.* 1991), and weight of both live (Katuwal *et al.* 2013; Zhang *et al.* 2013) and dead (Ghidey and Alberts 1997) roots all positively correlated with erosion mitigation. Furthermore, some studies have compared the contribution of various root traits to soil erosion reduction, including some architectural features such as maximum rooting depth, maximum lateral spread, and apportionment of fine roots in a root system (Burylo *et al.* 2012; Chau and Chu 2017). However, these traits have generally been ignored in field studies under simulated rainfall, instead using the simple acknowledgement that roots were present (Zhang *et al.* 2014; Li and Pan 2018) or determinations of root weight (Spaeth *et al.* 2003; Cogo and Streck 2003; Volk and Cogo 2008) and length (Bui and Box 1993; Mekonnen *et al.* 2016). While the knowledge gap pertaining to the impact of roots on soil erosion is closing, there is still a dearth of studies investigating the impact of roots on erosion at a field scale.

Previous chapters have shown that root hairs greatly affect the binding of soil to the roots (Chapter 2). The presence of root hairs can increase the amount of soil a root system can bind by up to 400 %. Additionally, the presence of root hairs increase a root system's ability to mitigate soil erosion in a laboratory mesocosm experiment (Chapter 4). The amount of soil erosion reduced in comparison to unplanted mesocosms increases at a three times greater in the presence of root hairs than when they are absent. To further upscale these observations, this chapter will assess the impact of root hairs on soil erosion under simulated rainfall in field-grown plants.

5.2. Materials and methods

5.2.1. Site description

The field site is located close to Preston, UK (Figure 5.1) in a field used to grow cattle fodder the previous season. At the time of this experiment (26th April – 31st July, 2018), the field was planted with a spring crop of barley. The experimental plots were treated the same as the rest of the field; first ploughed (20th March) then power harrowed (21st April) before the crops were planted (26th April for the plots, the exact date for the rest of the field is not known but precedes the experimental plots by less than 1 week). A pre-emergence weed killer was then sprayed across the field on the 28th April and a granular fertilizer on the 14th May (nitrogen; 27 %, sulphur; 9 %), The soil is of a fine loamy texture with impeded drainage classified as Salop (711 m) (Cranfield University 2019).

Figure 5.1. Location of the field site (generated by Digimap n.d.).

5.2.2. Erosion plots

This experiment consisted of 15 adjacent plots, 1 m long and 0.7 m wide; 0.5 m was left between each plot for access. The average slope of the plots was 4.2 ± 0.3 % with a SSE aspect. There were three treatments, barley with root hairs (WT), barley without root hairs (*brb*), and unplanted plots. Treatments were designated to each plot in a randomized block design. Rows of barley, 7 per plot, were spaced at 15 cm across the slope and sown, by hand (approximately 1 inch deep), at a density of 245 seeds m^{-1} (31 seeds per row, assuming an 80% germination rate). The plots were left to grow for 3 months under natural environmental conditions.

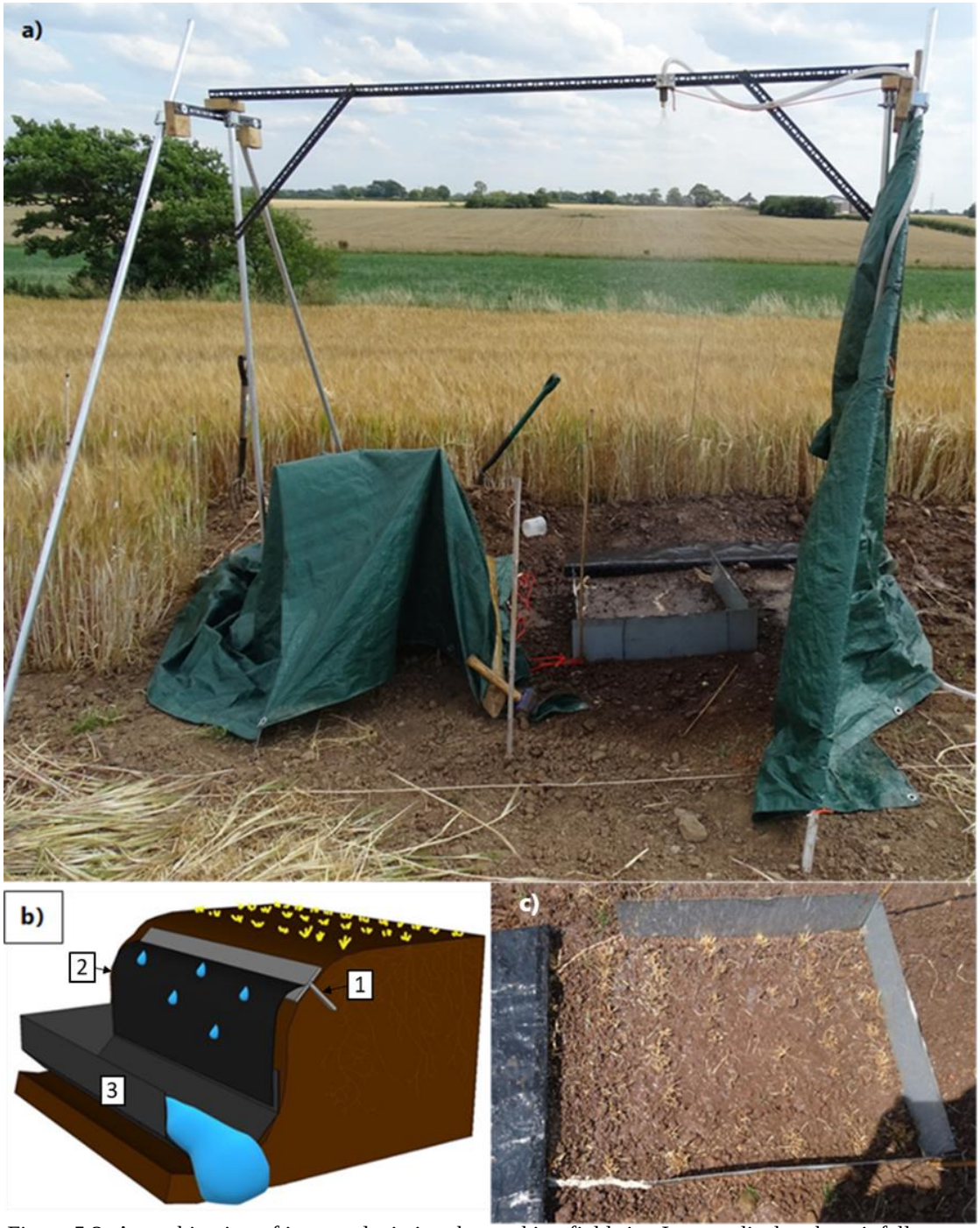

Figure 5.2. A combination of images depicting the working field site. Images display the rainfall simulator structure with tarpauling covering adjacent plot (a), a diagram of the runoff collection system (b), and an image of a plot being rained on with barrier isolating the extent of the plot and a cover over the drainage ditch to ensure only runoff from the plot is collected (c).

5.2.3. Rainfall simulator

The rainfall simulator consisted of one brass full cone nozzle (Spraying Systems Fulljet® 3/8HH–9.5) which had a drop size distribution of 1000 to 5000 µm. The frame is constructed out of angled iron and supported 2 m above the plot by six 2" aluminium poles (Figure 5.2a); the angled poles had 1" telescopic extensions to contend with uneven ground. Each pole was affixed to the frame using a 2" flag pole foot. The water supply for this experiment was tap water contained in a metal bowser near the plots that was refilled before each test day. Water was pumped from the bowser through a pressure reducing valve set at 1 bar, using a 12 V pump, resulting in a rainfall intensity of 273.6 mm h^{-1} (Christiansen uniformity coefficient = 52 %). The period at which the harvest was carried out was during a heatwave with the area receiving less than 100 mm of rainfall throughout the whole growth period and temperatures reaching in excess of 22 ℃ for extended periods of time (Met Office) so the high intensity rainfall was chosen to ensure runoff and erosion in the given allotted time span of one hour.

5.2.4. Sampling period

The plots were harvested sequentially in blocks over five days, 24-27th and 31st July 2018. Plots remained untouched until it was their turn to be harvested. In preparation for the plots being subjected to rainfall, the above-ground plant matter was harvested, taking care not to disturb the soil. Metal boards were inserted into the ground to form a physical barrier to the plots (Figure 5.2c). A trench was dug at the downhill edge of the plot, deep enough to hold a drainpipe slanting down to a larger hole, and big enough for a beaker to be held level under the drain pipe and collect the runoff. A piece of angled aluminium with a sheet of plastic attached to it was hammered into the cut edge of the trench so all runoff entered the gutter (Figure 5.2b). The upwards edge

of this along with any other large visible cracks in the surface were sealed with plumber's putty. Putty was also used to continue the metal barrier to the gutter lip. During rainfall, the whole trench was covered so that the only water entering the gutter and subsequently the sampling beaker was runoff from the plot.

Before the simulator was turned on, it was centred over the plot using a plumb-line. Tarpaulins were placed over the adjacent unharvested plot to keep them dry (Figure 5.2a). If it was windy, another tarpaulin was secured upwind to dampen the gusts. Rainfall was applied long enough to create runoff for 1 hour (if runoff didn't start until the 20th minute of rainfall, 80 mins of rainfall was applied). Samples were collected every 5 minutes, producing 12 runoff samples. Runoff was then collected in a 600 ml capacity beaker until full and the time taken to fill the beaker was recorded. The runoff was then transferred into a clean 1 litre plastic bottle.

After the hour of rainfall five soil cores were taken at random from each plot and combined into one plastic bag, for subsequent root density measurements. A FieldScout SC 900 Soil Compaction Meter (Spectrum Technologies, Inc) was then used in replicates of five, again randomly distributed (if a stone was struck, that record was deleted and redone) to gauge soil compaction up to 5 cm deep.

The runoff was left to settle in the plastic bottle until the water had cleared, for about a week. The supernatant was then carefully discarded, and the bottle cut open to rinse the sediment into pre-weighed metal trays. The metal trays were then placed in an oven at 105 °C until they reached a constant weight. This weight (minus the weight of the tray) was used to represent the soil eroded during the time period taken to fill the beaker.

Runoff rate (RR) is calculated:

$$RR = \left(\frac{R_v}{T}\right)$$

Where R_v = total volume of liquid runoff in beaker and T = amount of time in seconds taken to fill the beaker.

Soil concentration (SC) is calculated by:

$$SC = \left(\frac{\left(\frac{S_m}{R_v}\right)}{T}\right)$$

Where S_m = total mass eroded soil in beaker.

Root density of the plots was established using the five soil cores (53 mm diameter x 37 mm height) taken from each plot. The roots were washed out of the soil and stored in 50 % ethanol at 4 °C until analysed. Digital images of the roots were produced in 8 bit greyscale using an Epson Expression 11000XL Pro with transparency lid at 600 DPI. Root length was analysed using WinRHIZO (2013e, Regent Instruments Inc.), debris with a width x length ratio less than 4 was excluded (as stated in Chapter 2.2.2).

Not all vegetation could be removed without excessively disturbing the soil surface, so the remaining vegetation was recorded in a photograph of each plot taken prior to the application of rainfall. These images were then analysed using a MATLAB app called Canopeo (Patrignani and Ochsner 2015). This program cannot discriminate senescent (yellow) vegetation, so before analysis the vegetation had to be colour adjusted to green using the image software GIMP (version 2.8.2.2, The GIMP Team). Vegetation cover is displayed as a percentage of the soil area.

5.2.5. Statistical analysis

Variations in the root traits of WT and *brb* were investigated using one-way analysis of variance (ANOVA). Due to the non-normal distribution of the data and the missing data points (a result of delayed runoff from some plots), the Skilling-Mack test (Chatfield and Mander 2009), a non-parametric version of a repeated measures ANOVA that can account for missing data points, assessed whether runoff and erosion concentrations from the three treatments differed over time, followed by a Wilcoxon post-hoc test with a Bonferroni correction. The Kruskal-Wallis test was used to determine whether there were differences between the soil compaction of the three treatments.

Relative soil detachment rate (RSDR) is calculated as the mean percentage decrease of the rooted plots from the unplanted plots:

$$RSDR = \overline{\left(\frac{(E_{Bi} - E_{Ri})}{E_{Bi}}\right)} * 100$$

Where E_{Bi} = the total erosion from the unplanted plot of a block and E_{Ri} = total erosion from a rooted plot of a block. Relative runoff is calculated in the same way as RSDR.

5.3. Results

5.3.1. Runoff

The unplanted plots produced more runoff than the rooted plots (Figure 5.3). Runoff from two *brb* plots did not commence until after the first 15 minutes and a further *brb* and WT plot did not produce any runoff for the first 25 minutes. For this reason the data after 65 minutes of rainfall does not reliably indicate any trend as there are few

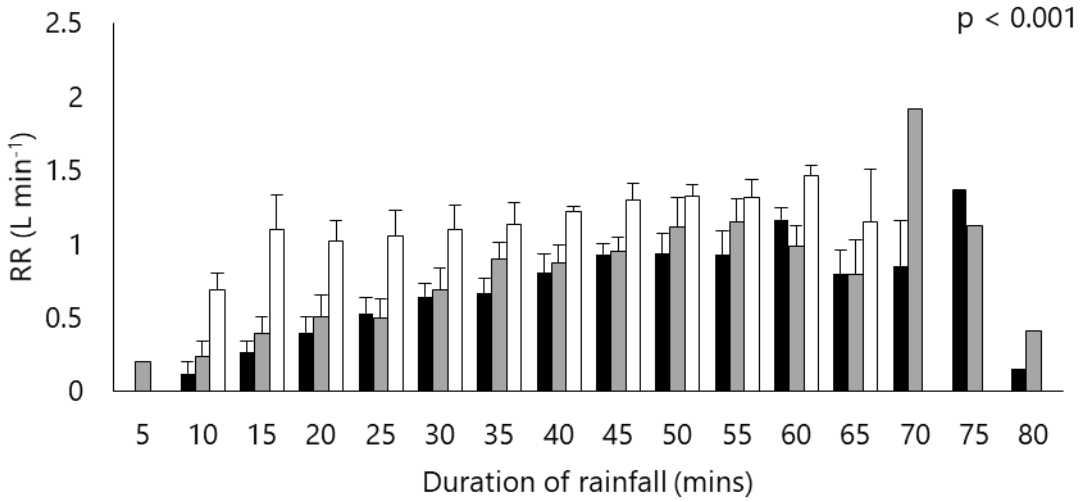

Figure 5.3. The runoff rate for the duration of the experiment. P value is from the Skilling-Mack Test. The solid black bars = *brb*, grey bars = WT and the white bars = unplanted. The bars are equal mean of 5 replicates ± 1 Standard Error.

Table 5.1. Shows the medians and interquartile ranges (IQR) for the rate of runoff (RR) for each treatment. Letters indicate that the medians are from different distributions, p values < 0.001.

	Median	IQR	Mean ranks
Fallow	1.21a	0.47	41.51
brb	0.76b	0.47	24.31
WT	0.76b	0.57	26.68

replicates. In attempting to increase the number of overlapping data points, but restricting the number of samples collected, all but one WT plot were given 10 minutes of rainfall before initiating the first sample. For this reason, it cannot be confidently said that runoff was absent in the first 10 minutes. On the contrary, all unplanted plots produced runoff after the first 10 minutes, at such a rate that runoff likely commenced in the unplanted plots far sooner than in the rooted plots. The rapid increase meant that runoff from the unplanted plots was most frequently greater than that of the rooted plots (Table 5.1), resulting in a total mean runoff of 69.2 ± 5.9 L, 43.9 ± 4.3 L and 47.1 ± 7.1 L for the unplanted, *brb* and WT plots, respectively. The runoff from the two genotypes are so similar that their medians differ only slightly in comparison to that of the unplanted plots (). Thus, the presence/absence of root hairs did not influence the volume of runoff yielded from the plots.

5.3.2. Sediment

The concentration of sediment in the runoff (SC) was far greater in the unplanted than in the rooted plots. The SC from the unplanted plots was already twice that of the rooted plots after 10 minutes, suggesting that erosion started occurring before the first 10 minutes and that any subsequent increase in SC was much slower (Figure 5.4). The initial SC from the *brb* and WT plots are both much less than the unplanted plots (by 95.9 % and 89.5 % for *brb* and WT, respectively), but increase more rapidly. Initial runoff from the unplanted plots most frequently produced the greatest SC (Table 5.2), such that unplanted plots were statistically greater than both *brb* ($Z = 5.95$, $p < 0.001$) and WT ($Z = 4.45$, $p < 0.001$), resulting in a mean total sediment yield of 1.60 ± 0.43 kg/m^2, 0.49 ± 0.14 kg/m^2, and 0.75 ± 0.26 kg/m^2 for the unplanted, *brb* and WT plots, respectively.

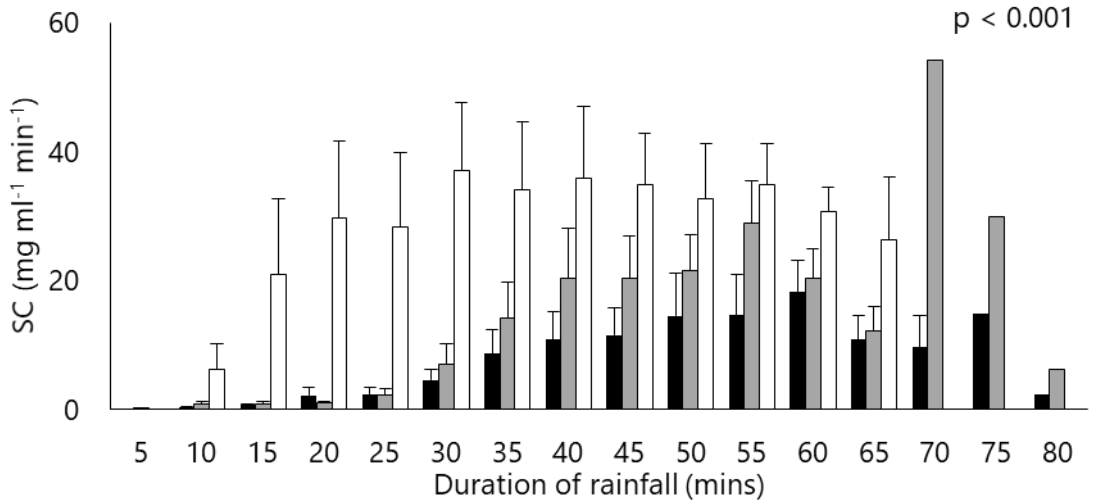

Figure 5.4. The sediment concentration per ml of runoff for the duration of the experiment. P value is from the Skilling-Mack Test. The solid black bars = *brb*, grey bars = WT and the white bars = unplanted. The bars are equal mean of 5 replicates ± 1 Standard Error.

Table 5.2. Shows the medians and interquartile ranges (IQR) for the soil concentration in runoff (SC) for each treatment. Letters indicate that the medians are different distributions, p values < 0.001.

	Median	IQR	Mean ranks
Bare	25.38a	36.95	40.97
brb	5.28b	14.08	22.56
WT	9.89b	17.99	28.97

As with RR, the SC from *brb* and WT plots was equivalent ($Z = -1.56$, $p = 0.118$). Both genotypes show a very slow rate of increase for the first 30 minutes of rainfall and then begin to increase more rapidly. The similar behaviour is reflected in the summary statistics with the medians and ranges varying only slightly in comparison (Table 5.2). So, the presence of roots decreased the yield of eroded soil, but the presence of root hairs had no discernible impact.

5.3.3. Vegetation cover

The amount of residual vegetation cover did not differ between genotypes (Table 5.3). As with the root parameters, percentage vegetation cover did not explain why some rooted plots yielded more erosion and runoff than their respective unplanted plots. Additionally, low levels of vegetation cover was not responsible for the some plots yielding more soil/runoff than their respective unplanted plots. Although there was a general trend for increasing vegetation cover to decrease RSDR and RR, these correlations were not significant (Table 5.4). This suggests that vegetation cover is not the cause of the difference observed in the erosion and runoff data.

5.3.4. Compaction

Soil within the unplanted plots was significantly ($p < 0.01$) more compact than the rooted plots (Figure 5.5). Penetrometer resistance of the unplanted plots was 497 ± 51 kPa, whereas values for *brb*

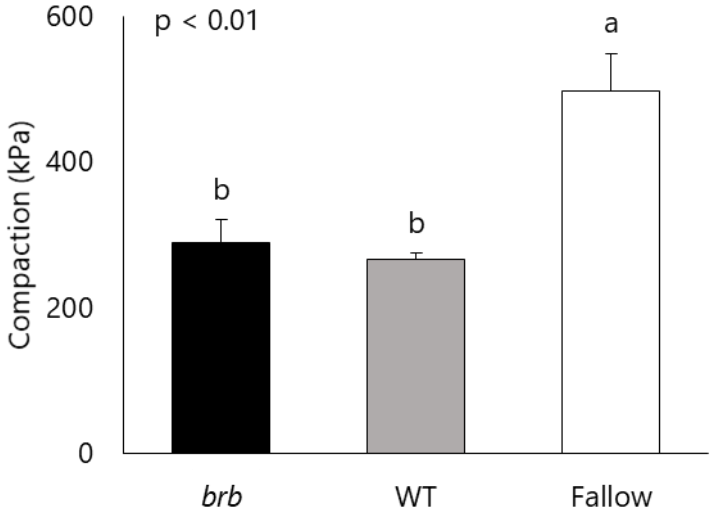

Figure 5.5. Average soil compaction from all three treatments. The p value is from a Kruskal-Wallis test and the letters indicate statistically different distributions from a Bonferroni pairwise comparison. Bars are means of 25 replicates + 1 standard error.

and WT plots were almost half at 289.2 ± 30.8 kPa and 266.1 ± 8.7 kPa, respectively, resulting in the unplanted plots being 72.1 % and 87.0 % more compact than the *brb* are WT plots, respectively. However, the *brb* and WT plots did not differ. Therefore, the presence of roots decreased soil compaction, but the presence of root hairs had no discernible effect.

5.3.5. Roots

There was no significant genotypic difference between root diameter, percentage of fine roots, root length density (RLD), or root volume density (RVD). Unlike previous chapters, WT produced more root length than *brb*, resulting in an RLD 33.4 % greater (Table 5.3). Also, root surface area density (RSAD) from WT plots was statistically ($p < 0.05$) higher than the *brb* plots. Although most root parameters did not differ between the genotypes, WT is assumed to have more root-soil contact.

No root traits correlated with either RR or RSDR (Table 5.4). Most rooted plots yielded less soil and runoff than their respective unplanted plots, however, reduced root presence was not a determining factor for the rooted plots that produced a positive RSDR as these occur in the middle of the range of root parameters. Although soil compaction was significantly lower in WT and brb plots than the unplanted plots, it was also not correlated to any of the root parameters. Neither was compaction correlated with RSDR or RR. The changes in soil and runoff yield as well as changes in compaction do not seem to be driven by increasing root presence.

Table 5.3. Summary statistics for the measured root parameters: root length density (RLD), root surface area density (RSAD), and root volume density (RVD). F-statistic is from a one-way anova, * = $p < 0.05$.

	brb	WT	F-statistic
Diameter (mm)	0.25 ± 0.02	0.26 ± 0.02	0.02
Fine roots (%)	76.00 ± 3.24	74.12 ± 4.96	0.10
RLD (cm cm^{-3})	7.08 ± 1.70	10.63 ± 1.37	2.66
RSAD (cm^2 cm^{-3})	0.48 ± 0.11	0.98 ± 0.15	7.07*
RVD (m^3 m^{-3})	51.11 ± 9.19	47.33 ± 20.00	0.03
Vegetation cover (%)	10.96 ± 2.07	10.07 ± 1.72	0.11

Table 5.4. Pearson's correlation coefficients for; average root diameter (D), percentage of fine roots (% FR), root length density (RLD), root surface area density (RSAD), root volume density (RVD), vegetation cover (VC), relative soil detachment rate (RSDR), relative runoff (RR) and compaction (C). * = $p < 0.05$, ** = $p < 0.001$, *** = $p < 0.001$

	Diameter (mm)	Fine roots (%)	RLD (cm cm^{-3})	RSAD (cm^2 cm^{-3})	RVD (m^3 m^{-3})	VC (%)	RSDR (%)	RR (%)	C (kPa)
D									
% FR	-0.99***								
RLD	-0.43	0.37							
RSAD	-0.45	0.40	0.94***						
RVD	0.80**	-0.74*	-0.35	-0.38					
VC	0.05	-0.02	-0.06	-0.17	0.10				
RSDR	0.14	-0.10	-0.54	-0.48	0.06	0.18			
RR	-0.06	0.07	-0.10	-0.11	0.00	0.41	0.77**		
C	-0.40	0.38	0.17	0.03	-0.37	0.04	-0.55	-0.45	

5.4. Discussion

The presence of roots significantly decreased runoff (Figure 5.3). Previous studies have attributed the initial delay in runoff to an initial increase in infiltration from an unsaturated surface (Zhou and Shangguan 2007). It took the *brb* and WT plots more than 35 and 30 minutes, respectively, to achieve the same rate of runoff the unplanted plots achieved within the first 10 minutes, resulting in the unplanted plots producing a mean total runoff 57.5 % greater than the *brb* plots and 46.9 % greater than the WT plots. This suggests that roots may have increased infiltration.

Roots and the mucilage they produce are only indirectly responsible for facilitating infiltration. The root mucilage promotes aggregation and roots themselves physically enmesh the soil, adding stability to the soil structure. These features combined promote and maintain pathways for water movement (McCully and Boyer 1997). Although this study did not directly measure infiltration, roots significantly decreased soil compaction (Figure 5.5). With increasing compaction, there is a reduction in soil porosity due to the compression of the soil structure and the collapse of soil pores that act as water pathways and therefore a reduction in hydraulic conductivity (Lipiec *et al.* 2006; Strudley *et al.* 2008; Cambi *et al.* 2015). As roots grow, they can create or expand existing soil pores and reinforce them to such an extent that they can long outlive the original root (Williams and Weil 2004). By decreasing compaction and increasing soil porosity, roots amplify a soil's ability to transport water away from the surface effectively reducing runoff.

Few publications have attempted to investigate the impact of roots on erosion under simulated rainfall in the field and the conclusions are varied. Various root parameters (number and mass) were positively, exponentially correlated to RSDR (Li *et al.* 1991;

Cogo and Streck 2003). These findings are consistent with most analogous laboratory experiments with broader ranges of species (Gyssels *et al.* 2005; Vannoppen *et al.* 2015). However, Bui and Box (1993) reported that maize roots had no significant impact on soil erosion when compared to unplanted plots. Thus, there is no consensus in the literature about the impacts of roots on erosion in the field. This experiment found that the presence of roots significantly reduced erosion (Figure 5.4); resulting in the unplanted plots produced a mean total sediment yield 3.3 and 2.1 times greater than the *brb* and WT plots, respectively. However, neither above-ground nor below-ground plant matter could explain variations in SDR or RR, which does not contribute greatly to the consensus in the literature and makes attributing reactions to the presence or absence of root hairs impossible.

A soil's erodibility can be influenced by many factors that were not accounted for or measured in this experiment, including but not restricted to, surface roughness (Kamphorst *et al.* 2000; Darboux *et al.* 2002; Le Bissonnais *et al.* 2005), presence of rocks (Poesen *et al.* 1999), and antecedent soil moisture (Luk 1985; Poesen *et al.* 1999; Singh and Thompson 2016). Wind further disturbed the results by reducing consistency of the rainfall distribution and intensity. These uncontrolled variables are suspected to influence RSDR and RR, thereby masking any significant relationship(s) between measurable plant traits and soil erosion. However the design of the rainfall simulator may also have contributed to obscuring the root impact.

The intensity of simulated rainfall experiments normally range between 30 mm hr^{-1} to 120 mm hr^{-1}, rarely exceeding 200 mm hr^{-1} (Zhou and Shangguan 2007; Cournane *et al.* 2011; Armstrong *et al.* 2011; Shinohara *et al.* 2016). These intensities are aimed to replicate moderate to intense rainstorms, however, the intensity of the rainfall

produced by the rainfall simulator in this experiment is equal to three times that of the peak rainfall intensity for a period of one hour recorded in the UK which was 92 mm hr^{-1} (Met Office). It is not uncommon for rainfall to reach in excess of 200 mm throughout the duration of a day, however, rainfall intensities exceeding 200 mm hr^{-1} are only recorded for the duration of a couple of minutes every couple of hundred years (Arup *et al.* 2002). Rainfall intensity strongly influences the erosivity of the rainfall event. As rainfall intensity increases infiltration rates decrease resulting in more water remaining at the surface to form surface/concentration flow (Dunne *et al.* 1991). So rainfall intensity has a power relationship with erosion rates (Meyer 1981; Panagos *et al.* 2017). Roots are able to contribute to soil erosion mitigation at surface flow intensities in excess of 35 L min^{-1} (Mamo and Bubenzer 2001a; b), however, the more kinetic energy an erosive force exerts the more potential it has to erode, thus reducing the ability of roots to mitigate soil erosion (Ghidey and Alberts 1997). The rainfall intensities exerted in this experiment would have produced large amounts of erosive force which could explain why there was no response of root hairs and no correlation with increasing root presence.

5.4.1. Improvements to experimental design

This experiment had constraints on time, space, availability of volunteers, and seed stocks which influenced the experimental design. These limiting factors controlled the number of plots and the number of days available to harvest the plots. Additionally, the soil was so dry that, even with the high intensity rainfall, several plots did not start producing runoff until after 20 minutes of rainfall. In an ideal repeat of this experiment, the soil would be pre-wetted to saturation prior to the erosion experiment. A lower, more realistic, rainfall intensity could then be applied that would reduce the severity of the erosion event and potentially expose a clearer root response. With a

visible root response, the presence/lack of impact from root hairs would also become evident. Ideally the experiment would also have a greater number of replicates. As with increased replication, increased resolution of root sampling would also capture more of the variation in root development. Capturing more of the variations in the data allow more accurate extrapolations and can ultimately strengthen trends.

5.4.2. Successes of the experimental design

Although aspects of the experimental design were lacking and should be addressed in later work, there were aspects that were hugely successful. The light and portable design of the rainfall simulator was extremely quick and easy to construct on site, but durable/minimalist enough to withstand the wind. Another aspect of the experiment that worked well was the drainage method. The plastic sheet attached to some angled metal that was then hammered into the side of the drainage ditch was a very effective way of capturing and channelling the runoff into the guttering. Additionally, the use of plumbers putty was integral to isolating the plot and channelling the runoff into the drainage system.

5.5. Conclusion

This experiment shows that the presence of roots significantly decreased soil erosion and runoff in comparison to the unplanted plots. The presence of roots significantly decreased the compaction of the soil, which ultimately lead to a reduction in runoff. There was no observable impact of root hairs on either compaction, runoff or erosion due to the lack of correlation between increasing root presence and either compaction or soil erosion reduction. Thus, it can be concluded that if root hairs affect soil erosion in a field setting, their influence was negated by the erosive forces applied here and/or it is minimal compared to the natural variability of the soil and environmental features

(such as micro-topography) that also influence soil erosion. The lessons learned from this simulation experiment are that more is not always better with respect to rainfall intensity. Further experiments are needed that quantify and account for the uncontrolled variables at a field scale (such as cracks and micro-topography) at a lower intensity rainfall before the contribution of root hairs can either be validated or dismissed.

Chapter 6. General Discussion.

Although the ability of roots to reinforce soil and mitigate soil erosion is well known, most studies examining the impact of plant roots on soil erosion or shear resistance have focused on root systems as a whole or on classes of roots distinguished as homogeneously as coarse (> 1, 2 or 3 mm diameter) or fine (< 1, 2 or 3 mm diameter). For this reason, the impact of individual root traits on root mitigation of soil erosion and shear reinforcement are poorly understood. While root hairs and mucilage can bind soil and anchor the root system, their contribution to root reinforcement of soil has hitherto not been considered. The aim of this thesis was to investigate which root traits reinforced soil at a small scale and then increase the scale to see if their impact was continuous. Thus, the traits of root hairs and exudates within different root classes (axile, lateral) of three WT species (barley, maize and *L. japonicus*) and their root hairless mutants were assessed for their relative contribution to rhizosheath formation in pot trials (Chapter 2). These experiments were scaled up to examine the impact of these genotypes on soil responses to shear forces (Chapter 3) and simulated rainfall in the laboratory (Chapter 4) and field (Chapter 5), to see if genotypic differences in the ability to reinforce soil had any wider implications.

6.1. Rhizosheath formation

Rhizosheath formation is known to depend on both root hairs and mucilage as well as other processes such as wetting and drying cycles. However, the effectiveness of these different root traits in contributing to rhizosheath formation has not yet been quantified. A further impedance to experimentally evaluating the interplay between root hairs and mucilage is the difficulties involved in obtaining sufficient root mucilage. Studies often use commercially available polysaccharides or chia seed

mucilage and extrapolate the effects of root mucilage. Although these alternatives provide valuable insight into the function and behaviours of mucilage more generally, they may misrepresent how root exudates affect rhizosheath formation. Chapter 2 compared the relative ability of root hair traits and root derived exudates to facilitate rhizosheath formation.

6.1.1. Mucilage

Although generally considered to bind soil particles together and to the root, Chapter 2 found that mucilage is not the main component contributing to rhizosheath formation. When root hairs were present, the increased adhesiveness of the maize root exudates (Figure 2.9) were not as effective at binding soil as the increased root hair development (length and length density) of the barley root systems (Figure 2.4). However, when root hairs were absent, the more adhesive exudate of the maize root hairless mutant *rth3* was more effective at binding soil than the much less adhesive exudate from the barley root hairless mutant *brb*. Alternative explanations could be that the barley WT roots produced greater quantities of exudates than the maize WT roots allowing for them to compensate for the reduced adhesiveness. However, barley exudates are known to bind soil less effectively than maize due to differences in exudate composition (Naveed *et al.* 2017).

The composition of root exudates determines how efficient they are at binding soil. Root exudates comprise many compounds, some with no apparent function except as waste products of internal metabolic processes and others that aid external processes such as root lubrication and facilitation of nutrient uptake (Bertin et al., 2003). Polysaccharide rich mucilage is highly adhesive and binds soil particles, producing hydrophobic barriers that aid water retention (Morel *et al.* 1991; Piccolo and Mbagwu

1999; Czarnes, Hallett, *et al.* 2000; Galloway *et al.* 2018). Conversely organic acid secretion from roots is predominantly associated with weathering soil particles to mobilise otherwise inaccessible nutrients (Oades 1984; Goldberg *et al.* 1990; Ström 1997; Landeweert *et al.* 2001; Dakora and Phillips 2002; Read *et al.* 2003). Naveed *et al.* (2017) show that barley exudates are predominantly composed of organic acids and have a very small quantity of sugars (derived from polysaccharides) whereas maize exudates have proportionally less organic acids and proportionally more sugars than barley. This could explain why barley exudates were much less adhesive than maize exudates. The composition and consequent adhesiveness of exudates suggest that barley roots prioritise nutrient uptake over water retention, whereas the reverse is true for maize. These assumptions about the relative effects of barley and maize roots may reflect differences in shoot behaviour (Tomaz *et al.* 2017). It would be interesting to investigate if similar differences are observed in a wider range of C3 (barley) and C4 (maize) species.

6.1.2. Root hairs

The presence of root hairs significantly increases the amount of rhizosheath a root system can form (Figure 6.1). Root hairs greatly increase the total root surface area as they extend into and enmesh soil aggregates, thus, physically binding them to the root. The contribution of root hairs to rhizosheath formation has been noted previously (Watt *et al.* 1994; Haling *et al.* 2014; George *et al.* 2014; Delhaize *et al.* 2015; Adu *et al.* 2017). Indeed, species with greater root hair development bound more soil than species with shorter and less dense root hairs. In Chapter 2, it was not possible to differentiate the contribution of root hair length and root hair length density (RHLD; length of root hairs on a given length of root) to rhizosheath formation and there is no available literature on the topic. However, many studies have noted that root hair

Figure 6.1. The difference in rhizosheath formation of a root hairless mutant (left) and its WT (right) of *L. japonicus*.

length and rhizosheath development are positively correlated, and root hair length is deemed to determine the radial extent of the rhizosheath (Pang *et al.* 2017), though the impact of RHLD is rarely mentioned.

Interestingly, the correlation between root hair length and rhizosheath size weakens with increasing root hair length in comparisons across multiple species (Brown *et al.* 2017). As root hairs extend into an increasing circumference of soil (thereby decreasing the number of root hairs per area ratio), other root hair traits, such as diameter and density, may become more dominant in rhizosheath formation with increasing root hair length. However, the trade-offs between the effects of different root hair traits on rhizosheath formation is still poorly understood and more species comparisons (than the ones of Chapter 2) are needed to fully understand thresholds by which root hair traits, affect rhizosheath development.

Different root types only expressed divergent rhizosheath formation if root hair development differed, with the root type exhibiting the greatest root hair development (in this case barley WT axile roots, as reported in Figure 2.6) also having the greatest rhizosheath development. This phenomenon may be exaggerated with increasing age of the root system, since lateral roots are relatively ephemeral in comparison to the axile roots that have a slower turnover rate. However, some studies suggest that the rhizosheath bonds can far outlast the lifespan of the root and provide channels of passage for water and other roots long after the original root has died (Williams and Weil 2004). This suggests that the structural rhizosheath may remain intact, just no longer bound to the root due to the lack of root hairs. This argument could be extended to root hairless mutants. It is possible that root hairless mutants form as comprehensive a rhizosheath as their WT (due to the bonds provided by mucilage), but just lacking the ability to retain the root-soil bond after extraction from the soil. High-resolution synchrotron imaging has been used to assess the porosity of rhizosphere soil, and found that soil remained adhered to the root when the soil shrinks (Koebernick *et al.* 2017). The same methodology could be used to assess whether the "rhizosheath" of root hairless mutants behaves in a similar manner as soil shrinks (in response to drying). If soil at the root-soil interface of root hairless mutants behaves similarly to the rhizosheath soil of WT roots when still in the soil, the definition of what a rhizosheath is, and the methods used to assess rhizosheath formation, would need to be altered.

6.2. Shear resistance

The contribution of root hairs to soil reinforcement under shear stress was quantified using a hydraulic shearing box. Soil permeated by roots of genotypes with and without root hairs were compared to an unplanted soil column. Both rooted treatments

required more shear force to displace than the unplanted soil columns (Figure 3.3) and the difference increased with increasing root surface area density (Figure 3.6). However, the presence/absence of root hairs did not influence the root system's ability to reinforce the soil as the force required to shear both rooted treatments increased equally with root surface area density. Soil reinforcement by a root system was more accurately determined by its average diameter, as larger diameter roots withstood greater forces before breaking.

Previous studies have found that root hairs significantly increase anchorage of seedling radicles (Stolzy and Barley 1968; Ennos 1989; Czarnes *et al.* 1999; Bengough *et al.* 2011, 2016). However, Chapter 3 shows that for more developed and complex root systems, the main roots contribute much more anchorage than root hairs. The peak resistance of a seedling radicle is determined by its length, peak breaking resistance, and quality of the root-soil bond (Ennos 1990), with the lateral protrusions of root hairs adding to the latter. A more complex root system has a network of lateral roots of much greater diameter and peak breaking resistance. The peak resistance of multiple roots is not equal to the peak breaking force of the sum of each root and is largely determined by the strongest root. Multiple weaker roots may not be able to resist as much force as fewer, stronger roots (Ennos 1990). Although the breaking force of root hairs has not been measured, it is assumed to be magnitudes less than an average lateral root (Bengough *et al.* 2011). Thus, root hairs would break long before the lateral roots break and so do not influence the force required to shear a root-permeated soil column.

That root hairs do not affect overall peak shear resistance of a soil does not mean they do not influence soil reinforcement under shear stress. Root hairs may affect other

aspects of shear resistance such as elasticity (the ability to return to the original state after deformation) and plasticity (the ability to deform, irreversibly, before failure), or on root scale shear stresses such as macro-fissures. Further, studies are needed to determine whether root hairs affect the full range of processes that aid soil reinforcement.

6.3. Soil erosion

6.3.1. Laboratory erosion event

Chapter 4 investigated the impact of root hairs on soil erosion by growing a root hairless mutant of barley (*brb*) and its WT in mesocosms modified to collect eroded soil under controlled conditions. After removing above-ground plant matter, rooted soils were compared to unplanted soils under simulated rainfall, with eroded soil collected and quantified. Both rooted treatments yielded less soil than the unplanted soils (Figure 4.3 and Table 4.1), and the amount decreased with increasing root presence (Figure 4.5). However, the data suggests the presence of root hairs could reduce soil losses per unit of root length in comparison to unplanted soil, though only minimally.

The *brb* mesocosms produced, on average, more prolific root systems than WT, but overall more soil was eroded from their mesocosms, suggesting that root hairs could compensate for the lesser root length. Additionally, when considering soil erosion reduction (RSDR) with increasing root length, WT root growth was up to three times more efficient at reducing soil erosion than *brb*, but due to the difference in total root length, this only equated to a 5.7 % difference in erosion reduction. Further to this, the reduction in eroded soil was much less than the estimated quantity of rhizosheath soil, suggesting that root hairs are relatively inefficient at reinforcing soil at the root:soil

interface against water erosion, or these figures would be more closely aligned. The resistance of rhizosheath soil to erosion is very poorly understood with a dearth of literature on the topic. Brown *et al*. (2017) found that both maize and barley rhizosheaths could withstand submission in a sonic bath for 5 minutes however, this study suggests that neither rhizosheaths can withstand more extensive wetting.

Previous studies looking at the impact of crop roots on soil erosion have used several methodologies: measuring the splash erosion from raindrops, the eroded soil from surface flow without raindrops and a combination of raindrops and surface flow. All methodologies have yielded results concluding that root presence reduces the amount of soil eroded in comparison to unplanted soil. However, to further understand the mechanisms by which root hairs mitigate soil erosion, different methodologies that emphasise different soil erosion processes should be compared.

6.3.2. Field erosion event

To assess whether the ability of root hairs to bind soil (Chapter 2) and potentially mitigate soil erosion (Chapter 4) affects soil losses under more "natural" conditions, a field experiment was conducted (Chapter 5). A root hairless barley mutant (*brb*) and its WT were grown in an agricultural field under the same conditions as a commercial crop of spring barley. After 3 months of growth, the above-ground plant matter was removed and the rooted plots were subjected to simulated rainfall. The eroded soil yield was quantified and compared to that of the paired unplanted plots. Again, both rooted treatments yielded significantly less soil than the unplanted treatment (Figure 5.3 and Table 5.4). The variability in trends inevitably increases from laboratory experiment to field experiments (Mamo and Bubenzer 2001a; b), however, unlike the laboratory experiment, increasing root presence showed no correlation with the

reduction in soil yield (Table 5.3) and WT showed no discernible difference in comparison to the root hairless mutant.

There is a range of possible reasons why increasing root presence was not correlated with soil erosion reduction. Firstly, the impedance of surface flow caused by the remaining vegetation (plant stems could not be completely removed without excessively disturbing the top soil) may have had the major effect on soil losses. However, the remaining vegetation cover was not correlated with erosion reduction. Another explanation could be that there was not enough variation in root growth, as all plots were harvested after the same length of growth period, though this did not prove to be a problem for the laboratory experiment that also consisted of only one length of growth period. Additionally, the intensive rainfall rate of the field rainfall simulator was far in excess of what could be classed as "natural" rainfall so would have exerted an unnaturally high erosive force. As the influence of roots on erosion mitigation decreases with increasing erosive force, this would have obscured the relationship between the roots and their ability to reduce soil erosion. Many other factors that influence a soils propensity to erode were deliberately not controlled, unlike the laboratory experiment. Ultimately, although the presence of roots was a dominant feature in erosion reduction, unmeasured variables (such as the interplay between surface roughness and flow impedance or variations in infiltration capacity that altered the quantity of surface runoff) and the high intensity rainfall likely determined any variation between individual plots. Since root development and soil erosion were not correlated, the impact of root hairs cannot be wholly disproved. Root hairs may have contributed to the overall ability of roots to reduce soil erosion, however, their impact was not sufficiently large enough to detect at a field scale.

6.4. The impact of root hairs on soil reinforcement and erosion mitigation

Root hairs are one of the most effective traits at reinforcing soil at the root-soil interface (Figure 6.2a). They are able to increase the amount of soil bound in a rhizosheath by up to 4-fold (Figure 2.4). The resulting bonds are not easily water soluble (Brown *et al.* 2017) and can outlive their origin root (Williams and Weil 2004). Root hairs possess traits that suggest they may also reinforce soil and mitigate soil erosion, such as increased root-soil contact and a proven ability to anchor roots, but their effectiveness on a greater scale had not been evaluated.

Through the binding capabilities associated with rhizosheath formation, root hairs have been shown to significantly increase the stability of a single root (Czarnes *et al.* 1999; Bengough *et al.* 2011, 2016). However, this study found that their influence does not extend to anchorage of a complex root system (Figure 6.2b). For reinforcement against shear stress, the soil needs an expansive network of roots that

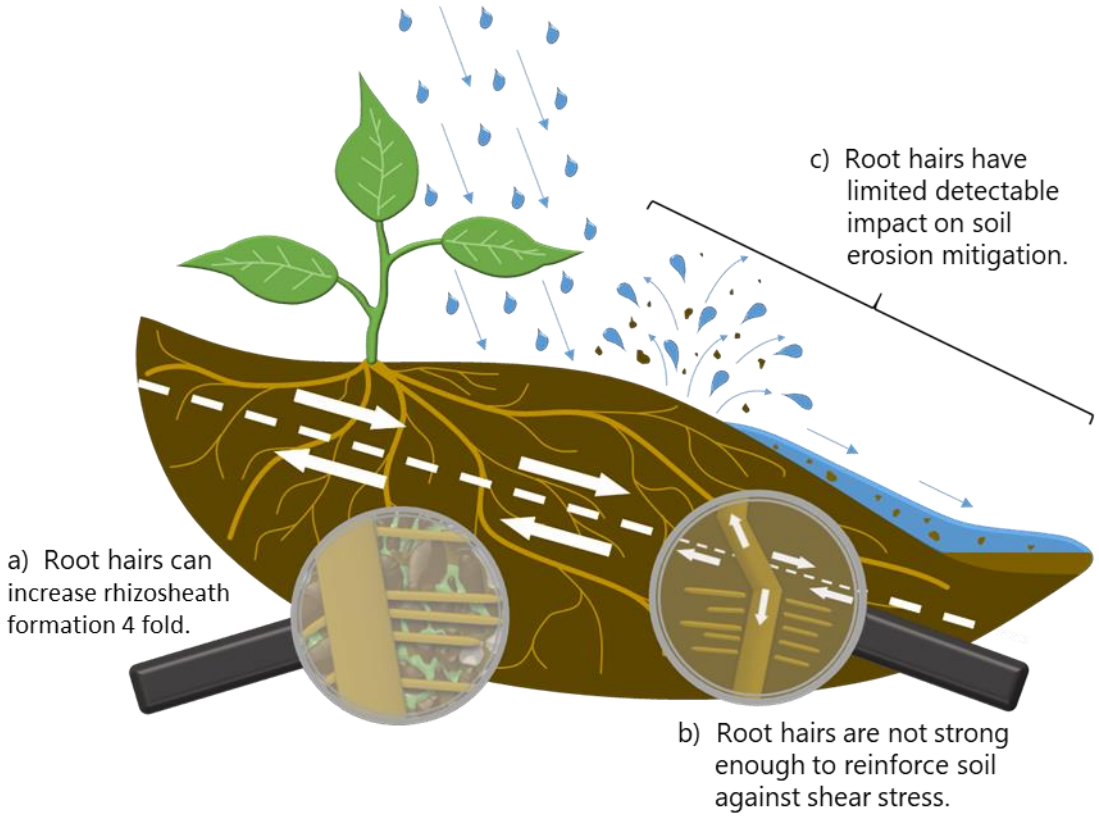

Figure 6.2. A conceptual diagram of the impact root hairs have on soil reinforcement at the root-soil interface as rhizosheath (a), under shear stress (b), and against erosion by rainfall and surface flow (c).

can engage as much of the soil as possible in order to effectively dissipate the shear force. Their prolific length means that root hairs greatly increase the roots contact with the soil, however, this area of influence is confined to the root-soil interface and has limited impact on soil further than a few millimetres from the root. An assumption could be made that, despite their limited radial influence, their ubiquity throughout the root system and the resulting cumulative soil contact provided by their associated rhizosheath soil, would bolster the anchorage provided by other roots. In reality, root diameter and tensile strength proved the most beneficial for boosting shear resistance, and root hairs were too weak to maintain the root-soil contact under increasing shear force, rendering any beneficial anchorage associated with rhizosheath development inconsequential.

Proliferation of roots is frequently reported to be correlated with increased soil erosion mitigation (Vannoppen *et al.* 2015), as such, the increased length and surface area provided by root hairs suggest they would be associated with a root systems ability to mitigate soil erosion. Further, the influence root hairs have on the formation of a rhizosheath, show that they are heavily involved in the root systems ability to bind soil. The rhizosheath is reportedly strong enough to withstand submersion in water, however, when subjected to the high impact force of rainfall and/or surface flow, rhizosheath soil proves less resistant. In controlled, small-scale experiments, root hairs appear to have a limited impact on soil erosion (Figure 4.5), though, this equates to only a slight decrease in soil yield that becomes completely lost when more uncontrolled variables are present (Figure 5.4). Similarly with shear resistance, the strength of the root hairs and/or their bond to the soil is not capable of withstanding the forces able to transport soil, and thus they have very little impact on soil erosion mitigation.

6.5. Conclusion

Root hairs efficiently facilitate plant functions, such as nutrient and water uptake, and can contribute to root anchorage that supports root elongation and above-ground growth, however, they do not seem to be of much importance to soil reinforcement. The contribution of root hairs to soil reinforcement has, thus far, been assumed to extend only to the boundaries of the rhizosheath soil, and is hampered by the assumption that all fine roots contribute equally to soil reinforcement. Root hairs indeed heavily influence the amount of soil bound at the root-soil interface in the form of a rhizosheath, but their impact on soil reinforcement is localised to the immediate proximity of the parent root. With increasing scale and heterogeneity, the strength and influence of root hairs on both soil reinforcement and erosion mitigation can be overshadowed by more dominant features such as increasing root diameter (soil reinforcement) as well as soil topography and rainfall intensity (erosion mitigation). To conclude, root hairs can readily reinforce soil at the root-soil interface, but, due to their limited radial influence and relatively negligible strength, their contribution easily becomes imperceptible compared to other, more dominant factors. Thus, root hairs have a limited application in soil reinforcement and erosion mitigation.

References

Acostasolis M. **1947**. The Soil Erosion in the Agricultural Highlands of Ecuador and Suggestions for Their Protection by Appropriate Plants, Principally by Setaria Cernua Hbk. *American Journal of Botany* **34**: 608–608.

Adhikari K, Hartemink AE. **2016**. Linking soils to ecosystem services: A global review. *Geoderma* **262**: 101–111.

Adu MO, Asare PA, Yawson DO, *et al.* 2017. Quantifying variations in rhizosheath and root system phenotypes of landraces and improved varieties of juvenile maize. *Rhizosphere* **3**: 29–39.

Ahmed MA, Zarebanadkouki M, Kaestner A, Carminati A. **2015**. Measurements of water uptake of maize roots: the key function of lateral roots. *Plant and Soil* **398**: 59–77.

Akhtar J, Galloway AF, Nikolopoulos G, Field KJ, Knox P. **2018**. A quantitative method for the high throughput screening for the soil adhesion properties of plant and microbial polysaccharides and exudates. *Plant and Soil* **428**: 57–65.

Albalasmeh AA, Ghezzehei TA. **2013**. Interplay between soil drying and root exudation in rhizosheath development. *Plant and Soil* **374**: 739–751.

Ali F. **2010**. Use of vegetation for slope protection: Root mechanical properties of some tropical plants. *International Journal of Physical Sciences* **5**: 496–506.

Al-Kaisi M, Licht M. **2005**. Reduce potential soil erosion early in the spring. *Integrated Crop Management News* **494**: 57–58.

Al-Karni AA, Al-Shamrani MA. **2000**. Study of the effect of soil anisotropy on slope stability using method of slices. *Computers and Geotechnics* **26**: 83–103.

Amézketa E. **1999**. Soil aggregate stability: A review. *Journal of Sustainable Agriculture* **14**: 83–151.

Amundson R, Berhe AA, Hopmans JW, Olson C, Sztein AE, Sparks DL. **2015**. Soil and human security in the 21st century. *Science* **348**: 647–653.

Anache JAA, Wendland EC, Oliveira PTS, Flanagan DC, Nearing MA. **2017**. Runoff and soil erosion plot-scale studies under natural rainfall: A meta-analysis of the Brazilian experience. *CATENA* **152**: 29–39.

Anderson CJ, Coutts MP, Ritchie RM, Campbell DJ. **1989**. Root extraction force measurements for Sitka spruce. *Forestry* **62**: 127–137.

Annabi M, Houot S, Francou C, Poitrenaud M, Bissonnais YL. **2007**. Soil aggregate stability improvement with urban composts of different maturities. *Soil Science Society of America Journal* **71**: 413–423.

Armenise E, Simmons RW, Ahn S, *et al.* 2018. Soil seal development under simulated rainfall: Structural, physical and hydrological dynamics. *Journal of Hydrology* **556**: 211–219.

Armstrong A, Quinton JN, Francis B, Heng BCP, Sander GC. **2011**. Controls over nutrient dynamics in overland flows on slopes representative of agricultural land in North West Europe. *Geoderma* **164**: 2–10.

Armstrong A, Quinton JN, Maher BA. **2012**. Thermal enhancement of natural magnetism as a tool for tracing eroded soil. *Earth Surface Processes and Landforms* **37**: 1567–1572.

Arup O, Partners, Davies E. **2002**. Physical considerations in site selection In: Snow DA, ed. *Plant Engineer's Reference Book (Second Edition)*. Oxford: Butterworth-Heinemann, 1/1-1–23.

Bai ZG, Dent DL, Olsson L, Schaepman ME. **2008**. Proxy global assessment of land degradation. *Soil use and management* **24**: 223–234.

Bailey PHJ, Currey JD, Fitter AH. **2002**. The role of root system architecture and root hairs in promoting anchorage against uprooting forces in Allium cepa and root mutants of Arabidopsis thaliana. *Journal of Experimental Botany* **53**: 333–340.

Banwart S. **2011**. Save our soils. *Nature* **474**: 151–152.

Batey T. **2009**. Soil compaction and soil management: A review. *Soil Use and Management* **25**: 335–345.

Baveye PC, Rangel D, Jacobson AR, *et al.* 2011. From dust bowl to dust bowl: Soils are still very much a frontier of science. *Soil Science Society of America Journal* **75**: 2037–2048.

Beach T, Dunning N, Luzzadder-Beach S, Cook DE, Lohse J. **2006**. Impacts of the ancient Maya on soils and soil erosion in the central Maya Lowlands. *CATENA* **65**: 166–178.

Benard P, Kroener E, Vontobel P, Kaestner A, Carminati A. **2016**. Water percolation through the root-soil interface. *Advances in Water Resources* **95**: 190–198.

Bengough AG, Loades K, McKenzie BM. **2016**. Root hairs aid soil penetration by anchoring the root surface to pore walls. *Journal of Experimental Botany* **67**: 1071–1078.

Bengough AG, McKenzie BM, Hallett PD, Valentine TA. **2011**. Root elongation, water stress, and mechanical impedance: A review of limiting stresses and beneficial root tip traits. *Journal of Experimental Botany* **62**: 59–68.

Bergmann D, Zehfus M, Zierer L, Smith B, Gabel M. **2009**. Grass rhizosheaths: Associated bacterial communities and potential for nitrogen fixation. *Western North American Naturalist* **69**: 105–114.

Bertin C, Yang X, Weston LA. **2003**. The role of root exudates and allelochemicals in the rhizosphere. *Plant and Soil* **256**: 67–83.

Boardman J, Poesen J. **2007**. *Soil Erosion in Europe*. John Wiley & Sons.

Borrelli P, Robinson DA, Fleischer LR, *et al.* 2017. An assessment of the global impact of 21st century land use change on soil erosion. *Nature Communications* **8**: No. 2013.

Bresson L-M, Boiffin J. **1990**. Morphological characterization of soil crust development stages on an experimental field. *Geoderma* **47**: 301–325.

Bridge P, Spooner B. **2001**. Soil fungi: diversity and detection. *Plant and Soil* **232**: 147–154.

Bristow CE, Campbell GS, Wullstein LH, Neilson R. **1985**. Water uptake and storage by rhizosheaths of Oryzopsis hymenoides: a numerical simulation. *Physiologia Plantarum* **65**: 228–232.

Bronick CJ, Lal R. **2005**. Soil structure and management: A review. *Geoderma* **124**: 3–22.

Brown LK, George TS, Neugebauer K, White PJ. **2017**. The rhizosheath: A potential trait for future agricultural sustainability occurs in orders throughout the angiosperms. *Plant and Soil* **418**: 115–128.

Brown LK, George TS, Thompson JA, *et al.* 2012. What are the implications of variation in root hair length on tolerance to phosphorus deficiency in combination with water stress in barley (Hordeum vulgare)? *Annals of Botany* **110**: 319–328.

Bui EN, Box JE. **1993**. Growing corn root effects on interrill soil erosion. *Soil Science Society of America Journal* **57**: 1066–1070.

Burylo M, Rey F, Mathys N, Dutoit T. **2012**. Plant root traits affecting the resistance of soils to concentrated flow erosion. *Earth Surface Processes and Landforms* **37**: 1463–1470.

Cahn MD, Zobel RW, Bouldin DR. **1989**. Relationship between root elongation rate and diameter and duration of growth of lateral roots of maize. *Plant and Soil* **119**: 271–279.

Cambi M, Certini G, Neri F, Marchi E. **2015**. The impact of heavy traffic on forest soils: A review. *Forest Ecology and Management* **338**: 124–138.

Carmi G, Abudi I, Berliner P. **2018**. An experimental study to assess the effect of the energy and the electrolyte concentration of rain drops on the infiltration properties of naturally crusted soils. *Journal of Arid Environments* **152**: 69–74.

Carminati A. **2013**. Rhizosphere wettability decreases with root age: a problem or a strategy to increase water uptake of young roots? *Frontiers in Plant Science* **4**.

Carminati A, Benard P, Ahmed MA, Zarebanadkouki M. **2017**. Liquid bridges at the root-soil interface. *Plant and Soil* **417**: 1–15.

Carminati A, Moradi AB, Vetterlein D, *et al.* 2010. Dynamics of soil water content in the rhizosphere. *Plant and Soil* **332**: 163–176.

Caspari T, van Lynden G, Bai Z. **2015**. *Land degradation neutrality: An evaluation of methods*. Dessau-Rosslau : Umweltbundesamt: ISRIC - World Soil Information.

Chan KY, Mullins CE. **1994**. Slaking characteristics of some Australian and British soils. *European Journal of Soil Science* **45**: 273–283.

Chatfield M, Mander A. **2009**. The Skillings–Mack test (Friedman test when there are missing data). *The Stata journal* **9**: 299–305.

Chau NL, Chu LM. **2017**. Fern cover and the importance of plant traits in reducing erosion on steep soil slopes. *CATENA* **151**: 98–106.

Chertkov VY, Ravina I. **1999**. Tortuosity of crack networks in swelling clay soils. *Soil Science Society of America Journal* **63**: 1523–1530.

Chibowski E. **2011**. Flocculation and dispersion phenomena in soils In: Gliński J, Horabik J, Lipiec J, eds. *Encyclopedia of Agrophysics*. Dordrecht: Springer Netherlands, 301–304.

Cogo NP, Streck EV. **2003**. Surface and subsurface decomposition of a desiccated grass pasture biomass related to erosion and its prediction with RUSLE. *Revista Brasileira de Ciência do Solo* **27**: 153–164.

Cournane FC, McDowell R, Littlejohn R, Condron L. **2011**. Effects of cattle, sheep and deer grazing on soil physical quality and losses of phosphorus and suspended sediment losses in surface runoff. *Agriculture, Ecosystems & Environment* **140**: 264–272.

Cranfield University. **2019**. *The Soils Guide*. www.landis.org.uk. 15 May 2019.

Czarnes S, Dexter AR, Bartoli F. **2000**. Wetting and drying cycles in the maize rhizosphere under controlled conditions. Mechanics of the root-adhering soil. *Plant and Soil* **221**: 253–271.

Czarnes S, Hallett PD, Bengough AG, Young IM. **2000**. Root- and microbial-derived mucilages affect soil structure and water transport. *European Journal of Soil Science* **51**: 435–443.

Czarnes S, Hiller S, Dexter AR, Hallett PD, Bartoli F. **1999**. Root:soil adhesion in the maize rhizosphere: the rheological approach. *Plant and Soil* **211**: 69–86.

Dakora FD, Phillips DA. **2002**. Root exudates as mediators of mineral acquisition in low-nutrient environments. *Plant and Soil* **245**: 35–47.

Darboux F, Davy Ph, Gascuel-Odoux C, Huang C. **2002**. Evolution of soil surface roughness and flowpath connectivity in overland flow experiments. *CATENA* **46**: 125–139.

Datta S, Kim CM, Pernas M, *et al.* 2011. Root hairs: development, growth and evolution at the plant-soil interface. *Plant and Soil* **346**: 1–14.

De Baets S, Poesen J, Gyssels G, Knapen A. **2006**. Effects of grass roots on the erodibility of topsoils during concentrated flow. *Geomorphology* **76**: 54–67.

De Baets S, Poesen J, Knapen A, Galindo P. **2007**. Impact of root architecture on the erosion-reducing potential of roots during concentrated flow. *Earth Surface Processes and Landforms* **32**: 1323–1345.

De Baets S, Poesen J, Reubens B, Wemans K, De Baerdemaeker J, Muys B. **2008**. Root tensile strength and root distribution of typical Mediterranean plant species and their contribution to soil shear strength. *Plant and Soil* **305**: 207–226.

Degens BP. **1997**. Macro-aggregation of soils by biological bonding and binding mechanisms and the factors affecting these: A review. *Soil Research* **35**: 431–460.

Delhaize E, James RA, Ryan PR. **2012**. Aluminium tolerance of root hairs underlies genotypic differences in rhizosheath size of wheat (Triticum aestivum) grown on acid soil. *New Phytologist* **195**: 609–619.

Delhaize E, Rathjen TM, Cavanagh CR. **2015**. The genetics of rhizosheath size in a multiparent mapping population of wheat. *Journal of Experimental Botany* **66**: 4527–4536.

Dexter AR. **2004**. Soil physical quality: Part I. Theory, effects of soil texture, density, and organic matter, and effects on root growth. *Geoderma* **120**: 201–214.

Dietrich WE, Reiss R, Hsu M-L, Montgomery DR. **1995**. A process-based model for colluvial soil depth and shallow landsliding using digital elevation data. *Hydrological Processes* **9**: 383–400.

Dittmer HJ. **1949**. Root hair variations in plant species. *American Journal of Botany* **36**: 152–155.

Docker BB, Hubble TCT. **2008**. Quantifying root-reinforcement of river bank soils by four Australian tree species. *Geomorphology* **100**: 401–418.

Dolan L. **1997**. The role of ethylene in the development of plant form. *Journal of Experimental Botany* **48**: 201–210.

Dolan L, Costa S. **2001**. Evolution and genetics of root hair stripes in the root epidermis. *Journal of Experimental Botany* **52**: 413–417.

Doran JW. **2002**. Soil health and global sustainability: translating science into practice. *Agriculture, Ecosystems & Environment* **88**: 119–127.

Doussan C, Pagès L, Vercambre G. **1998**. Modelling of the hydraulic architecture of root systems: An integrated approach to water absorption — Model description. *Annals of Botany* **81**: 213–223.

Drew MC. **1975**. Comparison of the effects of a localized supply of phosphate, nitrate, ammonium and potassium on the growth of the seminal root system, and the shoot, in barley. *The New Phytologist* **75**: 479–490.

Drew MC, Saker LR. **1975**. Nutrient supply and the growth of the seminal root system in barley II. Localized, compensatory increases in lateral root growth and rates of nitrate uptake when nitrate supply is restricted to only part of the root system. *Journal of Experimental Botany* **26**: 79–90.

Dunne T, Zhang W, Aubry BF. **1991**. Effects of rainfall, vegetation, and microtopography on infiltration and runoff. *Water Resources Research* **27**: 2271–2285.

Durán Zuazo VH, Rodríguez Pleguezuelo CR. **2008**. Soil-erosion and runoff prevention by plant covers. A review. *Agronomy for Sustainable Development* **28**: 65–86.

Edwards AP, Bremner JM. **1967**. Microaggregates in soils. *Journal of Soil Science* **18**: 64–73.

Ehrlich J, Bartz QR, Smith RM, Joslyn DA. **1947**. Chloromyeetin: A new antibiotic from a soil actinomycete. *Science (Washington)*: 417.

Elwell HA, Stocking MA. **1976**. Vegetal cover to estimate soil erosion hazard in Rhodesia. *Geoderma* **15**: 61–70.

Engel OG. **1955**. Waterdrop collisions with solid surfaces. *Journal of Research of the National Bureau of Standards* **54**: 281.

Ennos AR. **1989**. The mechanics of anchorage in seedlings of sunflower, Helianthus annuus L. *New Phytologist* **113**: 185–192.

Ennos AR. **1990**. The anchorage of leek seedlings: the effect of root length and soil strength. *Annals of Botany* **65**: 409–416.

Evans R, Nortcliff S. **1978**. Soil erosion in north Norfolk. *The Journal of Agricultural Science* **90**: 185–192.

Evenson RE, Gollin D. **2003**. Assessing the Impact of the Green Revolution, 1960 to 2000. *Science* **300**: 758–762.

Fan C-C, Chen Y-W. **2010**. The effect of root architecture on the shearing resistance of root-permeated soils. *Ecological Engineering* **36**: 813–826.

Fan TW-M, Lane AN, Shenker M, Bartley JP, Crowley D, Higashi RM. **2001**. Comprehensive chemical profiling of gramineous plant root exudates using high-resolution NMR and MS. *Phytochemistry* **57**: 209–221.

Fan C-C, Su C-F. **2008**. Role of roots in the shear strength of root-reinforced soils with high moisture content. *Ecological Engineering* **33**: 157–166.

Fasching RA, Bauder JW. **2001**. Evaluation of agricultural sediment load reductions using vegetative filter strips of cool season grasses. *Water Environment Research* **73**: 590–596.

Fattet M, Fu Y, Ghestem M, *et al.* 2011. Effects of vegetation type on soil resistance to erosion: Relationship between aggregate stability and shear strength. *CATENA* **87**: 60–69.

Foot K, Morgan RPC. **2005**. The role of leaf inclination, leaf orientation and plant canopy architecture in soil particle detachment by raindrops. *Earth Surface Processes and Landforms* **30**: 1509–1520.

Foster RC. **1982**. The fine structure of epidermal cell mucilages of roots. *New Phytologist* **91**: 727–740.

Frasson RP de M, Krajewski WF. **2013**. Rainfall interception by maize canopy: Development and application of a process-based model. *Journal of Hydrology* **489**: 246–255.

Gahoonia TS, Nielsen NE, Joshi PA, Jahoor A. **2001**. A root hairless barley mutant for elucidating genetic of root hairs and phosphorus uptake. *Plant and Soil* **235**: 211–219.

Galloway AF, Pedersen MJ, Merry B, *et al.* 2018. Xyloglucan is released by plants and promotes soil particle aggregation. *New Phytologist* **217**: 1128–1136.

Gans J, Wolinsky M, Dunbar J. **2005**. Computational Improvements Reveal Great Bacterial Diversity and High Metal Toxicity in Soil. *Science* **309**: 1387–1390.

Gärdenäs AI, Hopmans JW, Hanson BR, Šimůnek J. **2005**. Two-dimensional modeling of nitrate leaching for various fertigation scenarios under micro-irrigation. *Agricultural Water Management* **74**: 219–242.

Genet M, Stokes A, Salin F, *et al.* 2005. The influence of cellulose content on tensile strength in tree roots. *Plant and Soil* **278**: 1–9.

George TS, Brown LK, Ramsay L, *et al.* 2014. Understanding the genetic control and physiological traits associated with rhizosheath production by barley (Hordeum vulgare). *New Phytologist* **203**: 195–205.

Gerhardt KE, Huang X-D, Glick BR, Greenberg BM. **2009**. Phytoremediation and rhizoremediation of organic soil contaminants: Potential and challenges. *Plant Science* **176**: 20–30.

Ghidey F, Alberts EE. **1997**. Plant root effects on soil erodibility, splash detachment, soil strength, and aggregate stability. *Transactions of the ASAE* **40**: 129–135.

Gibbs HK, Salmon JM. **2015**. Mapping the world's degraded lands. *Applied Geography* **57**: 12–21.

Giller KE, Beare MH, Lavelle P, Izac A-MN, Swift MJ. **1997**. Agricultural intensification, soil biodiversity and agroecosystem function. *Applied Soil Ecology* **6**: 3–16.

Gilroy S, Jones DL. **2000**. Through form to function: root hair development and nutrient uptake. *Trends in Plant Science* **5**: 56–60.

Goldberg S, Kapoor BS, Rhoades JD. **1990**. Effects of aluminum and iron oxides and organic matter on flocculation and dispersion of arid zone soils. *Soil Science* **150**: 588–593.

Gould IJ. **2014**. *The influence of plant diversity on soil physical properties in grasslands*. Lancaster: Lancaster University.

Guérif J, Richard G, Dürr C, Machet JM, Recous S, Roger-Estrade J. **2001**. A review of tillage effects on crop residue management, seedbed conditions and seedling establishment. *Soil and Tillage Research* **61**: 13–32.

Guo JH, Liu XJ, Zhang Y, *et al.* 2010. Significant acidification in major chinese croplands. *Science* **327**: 1008–1010.

Gupta R, Seth A. **2007**. A review of resource conserving technologies for sustainable management of the rice-wheat cropping systems of the Indo-Gangetic plains (IGP). *Crop Protection* **26**: 436–447.

Gyssels G, Poesen J. **2003**. The importance of plant root characteristics in controlling concentrated flow erosion rates. *Earth Surface Processes and Landforms* **28**: 371–384.

Gyssels G, Poesen J, Bochet E, Li Y. **2005**. Impact of plant roots on the resistance of soils to erosion by water: a review. *Progress in physical geography* **29**: 189–217.

Hales TC, Miniat CF. **2016**. Soil moisture causes dynamic adjustments to root reinforcement that reduce slope stability: Dynamic slope stability due to roots. *Earth Surface Processes and Landforms* **42**: 803–813.

Haling RE, Brown LK, Bengough AG, *et al.* 2013. Root hairs improve root penetration, root–soil contact, and phosphorus acquisition in soils of different strength. *Journal of Experimental Botany* **64**: 3711–3721.

Haling RE, Brown LK, Bengough AG, *et al.* 2014. Root hair length and rhizosheath mass depend on soil porosity, strength and water content in barley genotypes. *Planta* **239**: 643–651.

Haling RE, Richardson AE, Culvenor RA, Lambers H, Simpson RJ. **2010**. Root morphology, root-hair development and rhizosheath formation on perennial grass seedlings is influenced by soil acidity. *Plant and Soil* **335**: 457–468.

Haling RE, Simpson RJ, Delhaize E, Hocking PJ, Richardson AE. **2010**. Effect of lime on root growth, morphology and the rhizosheath of cereal seedlings growing in an acid soil. *Plant and Soil* **327**: 199–212.

Hall RL, Calder IR. **1993**. Drop size modification by forest canopies: Measurements using a disdrometer. *Journal of Geophysical Research: Atmospheres* **98**: 18465–18470.

Handley RJ, Davy AJ. **2002**. Seedling root establishment may limit Najas marina L. to sediments of low cohesive strength. *Aquatic Botany* **73**: 129–136.

Hartnett DC, Wilson GWT, Ott JP, Setshogo M. **2013**. Variation in root system traits among African semi-arid savanna grasses: Implications for drought tolerance. *Austral Ecology* **38**: 383–392.

Hazell PB. **2009**. *The Asian Green Revolution*. International Food Policy Research Institute (IFPRI).

Heimsath AM, Dietrich WE, Nishiizumi K, Finkel RC. **2001**. Stochastic processes of soil production and transport: erosion rates, topographic variation and cosmogenic nuclides in the Oregon Coast Range. *Earth Surface Processes and Landforms* **26**: 531–552.

Hillel D. **2008**. Soil Physical Attributes In: Hillel D, ed. *Soil in the Environment*. San Diego: Academic Press, 55–77.

Hinsinger P. **2001**. Bioavailability of soil inorganic P in the rhizosphere as affected by root-induced chemical changes: A review. *Plant and Soil* **237**: 173–195.

Hinsinger P, Bengough AG, Vetterlein D, Young IM. **2009**. Rhizosphere: biophysics, biogeochemistry and ecological relevance. *Plant and Soil* **321**: 117–152.

Hinsinger P, Gobran GR, Gregory PJ, Wenzel WW. **2005**. Rhizosphere geometry and heterogeneity arising from root-mediated physical and chemical processes. *New Phytologist* **168**: 293–303.

Hishi T. **2007**. Heterogeneity of individual roots within the fine root architecture: causal links between physiological and ecosystem functions. *Journal of Forest Research* **12**: 126–133.

Horst WJ, Härdter R. **1994**. Rotation of maize with cowpea improves yield and nutrient use of maize compared to maize monocropping in an alfisol in the northern Guinea Savanna of Ghana. *Plant and Soil* **160**: 171–183.

Horton RE. **1945**. Erosional development of streams and their drainage basins; Hydrophysical approach to quantitative morphology. *GSA Bulletin* **56**: 275–370.

Huang B, North GB, Nobel PS. **1993**. Soil sheaths, photosynthate distribution to roots, and rhizosphere water relations for Opuntia ficus-indica. *International Journal of Plant Sciences* **154**: 425–431.

Hudek C, Sturrock CJ, Atkinson BS, Stanchi S, Freppaz M. **2017**. Root morphology and biomechanical characteristics of high altitude alpine plant species and their potential application in soil stabilization. *Ecological Engineering* **109**: 228–239.

Hund A, Trachsel S, Stamp P. **2009**. Growth of axile and lateral roots of maize: I development of a phenotying platform. *Plant and Soil* **325**: 335–349.

Indran S, Edwin Raj R, Sreenivasan VS. **2014**. Characterization of new natural cellulosic fiber from Cissus quadrangularis root. *Carbohydrate Polymers* **110**: 423–429.

Itoh S, Barber SA. **1983**. A numerical solution of whole plant nutrient uptake for soil-root systems with root hairs. *Plant and Soil* **70**: 403–413.

Iverson RM. **2000**. Landslide triggering by rain infiltration. *Water Resources Research* **36**: 1897–1910.

Janaiah A, Otsuka K, Hossain M. **2005**. Is the productivity impact of the green revolution in rice vanishing? Empirical evidence from TFP analysis. *Economic and Political Weekly* **40**: 5596–5600.

Jankauskas B, Jankauskienė G, Fullen MA. **2008**. Soil erosion and changes in the physical properties of Lithuanian Eutric Albeluvisols under different land use systems. *Acta Agriculturae Scandinavica, Section B - Plant Soil Science* **58**: 66–76.

Jastrow JD, Miller RM, Lussenhop J. **1998**. Contributions of interacting biological mechanisms to soil aggregate stabilization in restored prairie1The submitted manuscript has been created by the University of Chicago as operator of Argonne National Laboratory under Contract No. W-31-109-ENG-38 with the U.S. Department of Energy.1. *Soil Biology and Biochemistry* **30**: 905–916.

Jaunin F, Hofer R-M. **1986**. Root hair formation and elongation of primary maize roots. *Physiologia Plantarum* **68**: 653–656.

Jenny H. **1941**. *Factors of soil formation: a system of quantitative pedology*. New York: McGraw-Hill.

Jobbágy EG, Jackson RB. **2004**. Groundwater use and salinization with grassland afforestation. *Global Change Biology* **10**: 1299–1312.

Jonasson S, Callaghan TV. **1992**. Root mechanical properties related to disturbed and stressed habitats in the Arctic. *New Phytologist* **122**: 179–186.

Kamphorst EC, Jetten V, Guérif J, *et al.* 2000. Predicting depressional storage from soil surface roughness. *Soil Science Society of America Journal* **64**: 1749–1758.

Karas B, Murray J, Gorzelak M, *et al.* 2005. Invasion of Lotus japonicus root hairless 1 by Mesorhizobium loti involves the nodulation factor-dependent induction of root hairs. *Plant Physiology* **137**: 1331–1344.

Kätterer T, Bolinder MA, Andrén O, Kirchmann H, Menichetti L. **2011**. Roots contribute more to refractory soil organic matter than above-ground crop residues, as revealed by a long-term field experiment. *Agriculture, Ecosystems & Environment* **141**: 184–192.

Katuwal S, Vermang J, Cornelis WM, Gabriels D, Moldrup P, de Jonge LW. **2013**. Effect of root density on erosion and erodibility of a loamy soil under simulated rain. *Soil Science* **178**: 29–36.

Kayadelen C, Tekinsoy MA, Taşkıran T. **2007**. Influence of matric suction on shear strength behavior of a residual clayey soil. *Environmental Geology* **53**: 891.

Kays SJ, Nicklow CW, Simons DH. **1974**. Ethylene in relation to the response of roots to physical impedance. *Plant and Soil* **40**: 565–571.

Keesstra S, Geissen V, Mosse K, *et al.* 2012. Soil as a filter for groundwater quality. *Current Opinion in Environmental Sustainability* **4**: 507–516.

Kesler SE, Simon AC, Simon AF. **2015**. *Mineral Resources, Economics and the Environment*. Cambridge University Press.

Keyes SD, Daly KR, Gostling NJ, *et al.* 2013. High resolution synchrotron imaging of wheat root hairs growing in soil and image based modelling of phosphate uptake. *New Phytologist* **198**: 1023–1029.

Koebernick N, Daly KR, Keyes SD, *et al.* 2017. High-resolution synchrotron imaging shows that root hairs influence rhizosphere soil structure formation. *New Phytologist* **216**: 124–135.

Laflen JM, Elliot WJ, Simanton JR, Holzhey CS, Kohl KD. **1991**. WEPP: Soil erodibility experiments for rangeland and cropland soils. *Journal of Soil and Water Conservation* **46**: 39–44.

Lagaly G, Ziesmer S. **2003**. Colloid chemistry of clay minerals: the coagulation of montmorillonite dispersions. *Advances in Colloid and Interface Science* **100–102**: 105–128.

Lal R. **2003**. Soil erosion and the global carbon budget. *Environment International* **29**: 437–450.

Lal R. **2009**. Soils and food sufficiency. A review. *Agronomy for Sustainable Development* **29**: 113–133.

Lal R. **2015**. Restoring soil quality to mitigate soil degradation. *Sustainability* **7**: 5875–5895.

Lal R, Stewart BA. **2012**. *Advances in Soil Science: Soil Degradation*. Springer Science & Business Media.

Lambin EF, Geist HJ, Lepers E. **2003**. Dynamics of land-use and land-cover change in tropical regions. *Annual Review of Environment & Resources* **28**: 205–241.

Lambrechts T, François S, Lutts S, Muñoz-Carpena R, Bielders CL. **2014**. Impact of plant growth and morphology and of sediment concentration on sediment retention efficiency of vegetative filter strips: Flume experiments and VFSMOD modeling. *Journal of Hydrology* **511**: 800–810.

Landeweert R, Hoffland E, Finlay RD, Kuyper TW, van Breemen N. **2001**. Linking plants to rocks: ectomycorrhizal fungi mobilize nutrients from minerals. *Trends in Ecology & Evolution* **16**: 248–254.

Le Bissonnais Y. **1996**. Aggregate stability and assessment of soil crustability and erodibility: I. Theory and methodology. *European Journal of Soil Science* **47**: 425–437.

Le Bissonnais Y, Cerdan O, Lecomte V, Benkhadra H, Souchère V, Martin P. **2005**. Variability of soil surface characteristics influencing runoff and interrill erosion. *CATENA* **62**: 111–124.

Lehmann J, Kleber M. **2015**. The contentious nature of soil organic matter. *Nature* **528**: 60–68.

Li J, He B, Chen Y, Huang R, Tao J, Tian T. **2013**. Root distribution features of typical herb plants for slope protection and their effects on soil shear strength. *Transactions of the Chinese Society of Agricultural Engineering* **29**: 144–152.

Li P, Li Z. **2011**. Soil reinforcement by a root system and its effects on sediment yield in response to concentrated flow in the loess plateau. *Agricultural Sciences* **02**: 86–93.

Li C, Pan C. **2018**. The relative importance of different grass components in controlling runoff and erosion on a hillslope under simulated rainfall. *Journal of Hydrology* **558**: 90–103.

Li Y, Zhu XM, Tian JY. **1991**. Effectiveness of plant roots to increase the anti-scourability of soil on the Loess Plateau. *Chinese Science Bulletin* **36**: 2077–2082.

Lipiec J, Kuś J, Słowińska-Jurkiewicz A, Nosalewicz A. **2006**. Soil porosity and water infiltration as influenced by tillage methods. *Soil and Tillage Research* **89**: 210–220.

Loades KW, Bengough AG, Bransby MF, Hallett PD. **2010**. Planting density influence on fibrous root reinforcement of soils. *Ecological Engineering* **36**: 276–284.

Loch RJ. **1994**. A method for measuring aggregate water stability of dryland soils with relevance to surface seal development. *Soil Research* **32**: 687–700.

Luk S. **1985**. Effect of antecedent soil moisture content on rainwash erosion. *CATENA* **12**: 129–139.

Ma Z, Bielenberg DG, Brown KM, Lynch JP. **2001**. Regulation of root hair density by phosphorus availability in Arabidopsis thaliana. *Plant, Cell & Environment* **24**: 459–467.

Ma W, Li X-X, Li C-J. **2011**. Modulation of soil particle size and nutrient availability in the maize rhizosheath. *Pedosphere* **21**: 483–490.

Mackay AD, Barber SA. **1984**. Comparison of root and root hair growth in solution and soil culture. *Journal of Plant Nutrition* **7**: 1745–1757.

Maeder P, Fliessbach A, Dubois D, Gunst L, Fried P, Niggli U. **2002**. Soil fertility and biodiversity in organic farming. *Science* **296**: 1694–1697.

Mamo M, Bubenzer GD. **2001a**. Detachment rate, soil erodibility, and soil strength as influenced by living plant roots part I: Laboratory study. *Transactions of the ASAE* **44**: 1167.

Mamo M, Bubenzer GD. **2001b**. Detachment rate, soil erodibility, and soil strength as influenced by living plant roots part II: Field study. *Transactions of the ASAE* **44**.

Marshall JS, Palmer WMK. **1948**. The distribution of raindrops with size. *Journal of Meteorology* **5**: 165–166.

Martens DA, Frankenberger WT. **1992**. Modification of infiltration rates in an organic-amended irrigated. *Agronomy Journal* **84**: 707.

McBratney A, Field DJ, Koch A. **2014**. The dimensions of soil security. *Geoderma* **213**: 203–213.

McCully M. **1995**. How do real roots work? (Some new views of root structure). *Plant Physiology* **109**: 1–6.

McCully ME. **1999**. ROOTS IN SOIL: Unearthing the complexities of roots and their rhizospheres. *Annual Review of Plant Physiology and Plant Molecular Biology* **50**: 695–718.

McCully M. **2005**. The rhizosphere: The key functional unit in plant/soil/microbial interactions in the field. Implications for the understanding of allelopathic effects. In: Centre for Rural Social Research, Charles Sturt University, 43–49.

McCully ME, Boyer JS. **1997**. The expansion of maize root-cap mucilage during hydration. 3. Changes in water potential and water content. *Physiologia Plantarum* **99**: 169–177.

McNally G. **2017**. *Soil and Rock Construction Materials*. CRC Press.

Mehra P, Baker J, Sojka RE, *et al.* 2018. A review of tillage practices and their potential to impact the soil carbon dynamics In: Sparks DL, ed. *Advances in Agronomy*. Academic Press, 185–230.

Mekonnen M, Keesstra SD, Ritsema CJ, Stroosnijder L, Baartman JEM. **2016**. Sediment trapping with indigenous grass species showing differences in plant traits in northwest Ethiopia. *CATENA* **147**: 755–763.

Melville N, Morgan RPC. **2001**. The influence of grass density on effectiveness of contour grass strips for control of soil erosion on low angle slopes. *Soil Use and Management* **17**: 278–281.

Met Office. *UK actual and anomaly maps*. https://www.metoffice.gov.uk/climate/uk/summaries/anomacts. 28 May 2019a.

Met Office. *UK climate*. https://www.metoffice.gov.uk/public/weather/climate-extremes. 27 May 2019b.

Meyer LD. **1981**. How rain intensity affects interrill erosion. *Transactions of the ASAE* **24**: 1472–1475.

Mills A j., Fey M v. 2004. Effects of vegetation cover on the tendency of soil to crust in South Africa. *Soil Use and Management* **20**: 308–317.

Misra RK, Alston AM, Dexter AR. **1988**. Root growth and phosphorus uptake in relation to the size and strength of soil aggregates. I. Experimental studies. *Soil and Tillage Research* **11**: 103–116.

Misra RK, Gibbons AK. **1996**. Growth and morphology of eucalypt seedling-roots, in relation to soil strength arising from compaction. *Plant and Soil* **182**: 1–11.

Mohammad AG, Adam MA. **2010**. The impact of vegetative cover type on runoff and soil erosion under different land uses. *CATENA* **81**: 97–103.

Montgomery DR. **2007**. Soil erosion and agricultural sustainability. *Proceedings of the National Academy of Sciences* **104**: 13268–13272.

Moore RJ. **2007**. The PDM rainfall-runoff model. *Hydrology and Earth System Sciences* **11**: 483–499.

Morel JL, Habib L, Plantureux S, Guckert A. **1991**. Influence of maize root mucilage on soil aggregate stability. *Plant and Soil* **136**: 111–119.

Moreno-Espíndola IP, Rivera-Becerril F, de Jesús Ferrara-Guerrero M, De León-González F. **2007**. Role of root-hairs and hyphae in adhesion of sand particles. *Soil Biology and Biochemistry* **39**: 2520–2526.

Morgan RPC. **2005**. *Soil erosion and conservation*. Malden, MA: Blackwell Publishing.

Muszyński A, O'Neill MA, Ramasamy E, *et al.* 2015. Xyloglucan, galactomannan, glucuronoxylan, and rhamnogalacturonan I do not have identical structures in soybean root and root hair cell walls. *Planta* **242**: 1123–1138.

Naveed M, Brown LK, Raffan AC, *et al.* 2017. Plant exudates may stabilize or weaken soil depending on species, origin and time: Effect of plant exudates on rhizosphere formation. *European Journal of Soil Science* **68**: 806–816.

Nearing MA, Bradford JM. **1985**. Single waterdrop splash detachment and mechanical properties of soils. *Soil Science Society of America Journal* **49**: 547–552.

Nearing MA, Jetten V, Baffaut C, *et al.* 2005. Modeling response of soil erosion and runoff to changes in precipitation and cover. *CATENA* **61**: 131–154.

Nearing MA, Norton LD, Bulgakov DA, Larionov GA, West LT, Dontsova KM. **1997**. Hydraulics and erosion in eroding rills. *Water Resources Research* **33**: 865–876.

Nestler J, Keyes SD, Wissuwa M. **2016**. Root hair formation in rice (Oryza sativa L.) differs between root types and is altered in artificial growth conditions. *Journal of Experimental Botany* **67**: 3699–3708.

Nielsen UN, Osler GHR, Campbell CD, Neilson R, Burslem DFRP, van der Wal R. **2010**. The enigma of soil animal species diversity revisited: The role of small-scale heterogeneity. *PLoS ONE* **5**: e11567.

Nilaweera NS, Nutalaya P. **1999**. Role of tree roots in slope stabilisation. *Bulletin of Engineering Geology and the Environment* **57**: 337–342.

Niu X, Nan Z. **2017**. Roots of cleistogenes songorica improved soil aggregate cohesion and enhance soil water erosion resistance in rainfall simulation experiments. *Water, Air, & Soil Pollution* **228**: 109.

Norris JE. **2005**. Root reinforcement by hawthorn and oak roots on a highway cut-slope in southern england. *Plant and Soil* **278**: 43–53.

North GB, Nobel PS. **1997**. Drought-induced changes in soil contact and hydraulic conductivity for roots of Opuntia ficus-indica with and without rhizosheaths. *Plant and Soil* **191**: 249–258.

Oades JM. **1984**. Soil organic matter and structural stability: mechanisms and implications for management. *Plant and Soil* **76**: 319–337.

Oburger E, Jones DL. **2018**. Sampling root exudates – Mission impossible? *Rhizosphere* **6**: 116–133.

Ola A, Dodd IC, Quinton JN. **2015**. Can we manipulate root system architecture to control soil erosion? *SOIL Discussions* **2**: 265–289.

Oldeman LR. **1994**. The global extent of soil degradation. *Soil resilience and sustainable land use* **9**.

Olson GW. **1981**. Archaeology: Lessons on future soil use. *Journal of Soil and Water Conservation* **36**: 261–264.

Osman N, Nordin Abdullah M, Abdullah C. **2011**. Pull-out and tensile strength properties of two selected tropical trees. *Sains Malaysiana* **40**: 577–585.

Pagès L, Pellerin S. **1994**. Evaluation of parameters describing the root system architecture of field grown maize plants (Zea mays L.). *Plant and Soil* **164**: 169–176.

Pagliai M, Vignozzi N, Pellegrini S. **2004**. Soil structure and the effect of management practices. *Soil and Tillage Research* **79**: 131–143.

Panagos P, Borrelli P, Meusburger K, *et al.* 2017. Global rainfall erosivity assessment based on high-temporal resolution rainfall records. *Scientific Reports* **7**: 4175.

Pang J, Ryan MH, Siddique KHM, Simpson RJ. **2017**. Unwrapping the rhizosheath. *Plant and Soil* **418**: 129–139.

Parker JS, Cavell AC, Dolan L, Roberts K, Grierson CS. **2000**. Genetic interactions during root hair morphogenesis in Arabidopsis. *The Plant Cell* **12**: 1961–1974.

Patrignani A, Ochsner TE. **2015**. Canopeo: A powerful new tool for measuring fractional green canopy cover. *Agronomy Journal* **107**: 2312–2320.

Pearce AJ. **1976**. Magnitude and frequency of erosion by hortonian overland flow. *The Journal of Geology* **84**: 65–80.

Pena MJ, Kong Y, York WS, O'Neill MA. **2012**. A galacturonic acid-containing xyloglucan is involved in arabidopsis root hair tip growth. *The Plant Cell* **24**: 4511–4524.

Peterson RL, Farquhar ML. **1996**. Root hairs: Specialized tubular cells extending root surfaces. *The Botanical Review* **62**: 1–40.

Petley D. **2012**. Global patterns of loss of life from landslides. *Geology* **40**: 927–930.

Piccolo A, Mbagwu JSC. **1999**. Role of hydrophobic components of soil organic matter in soil aggregate stability. *Soil Science Society of America Journal* **63**: 1801–1810.

Piccolo A, Pietramellara G, Mbagwu JSC. **1997**. Use of humic substances as soil conditioners to increase aggregate stability. *Geoderma* **75**: 267–277.

Pingali PL. **2012**. Green Revolution: Impacts, limits, and the path ahead. *Proceedings of the National Academy of Sciences* **109**: 12302–12308.

Pitts RJ, Cernac A, Estelle M. **1998**. Auxin and ethylene promote root hair elongation in Arabidopsis. *The Plant Journal* **16**: 553–560.

Poesen J, De Luna E, Franca A, Nachtergaele J, Govers G. **1999**. Concentrated flow erosion rates as affected by rock fragment cover and initial soil moisture content. *CATENA* **36**: 315–329.

Pollen N. **2007**. Temporal and spatial variability in root reinforcement of streambanks: Accounting for soil shear strength and moisture. *CATENA* **69**: 197–205.

Pollen N, Simon A. **2005**. Estimating the mechanical effects of riparian vegetation on stream bank stability using a fiber bundle model. *Water Resources Research* **41**.

Pollen N, Simon A, Collison A. **2013**. Advances in assessing the mechanical and hydrologic effects of riparian vegetation on streambank stability In: *Riparian Vegetation and Fluvial Geomorphology*. American Geophysical Union (AGU), 125–139.

Posthumus H, Deeks LK, Rickson RJ, Quinton JN. **2015**. Costs and benefits of erosion control measures in the UK. *Soil Use and Management* **31**: 16–33.

Pregitzer KS, DeForest JL, Burton AJ, Allen MF, Ruess RW, Hendrick RL. **2002**. Fine root architecture of nine North American trees. *Ecological Monographs* **72**: 293–309.

Price SR. **1911**. The roots of some North African desert-grasses. *New Phytologist* **10**: 328–340.

Prosser IP, Dietrich WE. **1995**. Field experiments on erosion by overland flow and their implication for a digital terrain model of channel initiation. *Water Resources Research* **31**: 2867–2876.

Prosser IP, Dietrich WE, Stevenson J. **1995**. Flow resistance and sediment transport by concentrated overland flow in a grassland valley. *Geomorphology* **13**: 71–86.

Quinton JN, Govers G, Van Oost K, Bardgett RD. **2010**. The impact of agricultural soil erosion on biogeochemical cycling. *Nature Geoscience; London* **3**: 311–314.

Rasse DP, Rumpel C, Dignac M-F. **2005**. Is soil carbon mostly root carbon? Mechanisms for a specific stabilisation. *Plant and Soil* **269**: 341–356.

Read DB, Bengough AG, Gregory PJ, *et al.* 2003. Plant roots release phospholipid surfactants that modify the physical and chemical properties of soil. *New Phytologist* **157**: 315–326.

Rengasamy P. **2006**. World salinization with emphasis on Australia. *Journal of Experimental Botany* **57**: 1017–1023.

Reubens B, Poesen J, Danjon F, Geudens G, Muys B. **2007**. The role of fine and coarse roots in shallow slope stability and soil erosion control with a focus on root system architecture: a review. *Trees* **21**: 385–402.

Rockström J, Lannerstad M, Falkenmark M. **2007**. Assessing the water challenge of a new green revolution in developing countries. *Proceedings of the National Academy of Sciences* **104**: 6253–6260.

Rodell M, Velicogna I, Famiglietti JS. **2009**. Satellite-based estimates of groundwater depletion in India. *Nature* **460**: nature08238.

Römkens MJM, Helming K, Prasad SN. **2002**. Soil erosion under different rainfall intensities, surface roughness, and soil water regimes. *CATENA* **46**: 103–123.

Ruiz-Vera VM, Wu L. **2006**. Influence of sodicity, clay mineralogy, prewetting rate, and their interaction on aggregate stability. *Soil Science Society of America Journal* **70**: 1825–1833.

Ruysschaert G, Poesen J, Verstraeten G, Govers G. **2004**. Soil loss due to crop harvesting: significance and determining factors. *Progress in Physical Geography: Earth and Environment* **28**: 467–501.

Schlesinger WH, Andrews JA. **2000**. Soil respiration and the global carbon cycle. *Biogeochemistry* **48**: 7–20.

Segal E, Kushnir T, Mualem Y, Shani U. **2008**. Water uptake and hydraulics of the root hair rhizosphere. *Vadose Zone Journal* **7**: 1027–1034.

Shane MW, McCully ME, Canny MJ, *et al.* 2010. Seasonal water relations of Lyginia barbata (Southern rush) in relation to root xylem development and summer dormancy of root apices. *New Phytologist* **185**: 1025–1037.

Shi ZH, Fang NF, Wu FZ, Wang L, Yue BJ, Wu GL. **2012**. Soil erosion processes and sediment sorting associated with transport mechanisms on steep slopes. *Journal of Hydrology* **454–455**: 123–130.

Shinohara Y, Otani S, Kubota T, Otsuki K, Nanko K. **2016**. Effects of plant roots on the soil erosion rate under simulated rainfall with high kinetic energy. *Hydrological Sciences Journal* **61**: 2435–2442.

Shit PK, Maiti R. **2012**. Effect of plant roots on soil anti-scouribility of topsoil during concentrated flow. *International Journal of Engineering Research* **1**: 8.

Simon A, Collison AJC. **2002**. Quantifying the mechanical and hydrologic effects of riparian vegetation on streambank stability. *Earth Surface Processes and Landforms* **27**: 527–546.

Singer M, Blackard J, Huntington G. **1980**. Plant cover helps control rangeland soil-erosion. *California Agriculture* **34**: 8–10.

Singh RB. **2000**. Environmental consequences of agricultural development: a case study from the Green Revolution state of Haryana, India. *Agriculture, Ecosystems & Environment* **82**: 97–103.

Singh HV, Thompson AM. **2016**. Effect of antecedent soil moisture content on soil critical shear stress in agricultural watersheds. *Geoderma* **262**: 165–173.

Six J, Bossuyt H, Degryze S, Denef K. **2004**. A history of research on the link between (micro)aggregates, soil biota, and soil organic matter dynamics. *Soil and Tillage Research* **79**: 7–31.

Smith RJ, Hopper SD, Shane MW. **2011**. Sand-binding roots in Haemodoraceae: global survey and morphology in a phylogenetic context. *Plant and Soil* **348**: 453.

Spaeth K, Pierson F, Weltz M, Blackburn W. **2003**. Evaluation of USLE and RUSLE estimated soil loss on rangeland. *Journal of Range Management* **56**: 234–246.

Sprent JI. **1975**. Adherence of sand particles to soybean roots under water stress. *New Phytologist* **74**: 461–463.

Stirzaker RJ, Passioura JB, Wilms Y. **1996**. Soil structure and plant growth: Impact of bulk density and biopores. *Plant and Soil* **185**: 151–162.

Stockmann U, Minasny B, McBratney AB. **2014**. How fast does soil grow? *Geoderma* **216**: 48–61.

Stokes A, Atger C, Bengough AG, Fourcaud T, Sidle RC. **2009**. Desirable plant root traits for protecting natural and engineered slopes against landslides. *Plant and Soil* **324**: 1–30.

Stokes A, Douglas GB, Fourcaud T, *et al.* 2014. Ecological mitigation of hillslope instability: ten key issues facing researchers and practitioners. *Plant and Soil* **377**: 1–23.

Stokes A, Fitter AH, Courts MP. **1995**. Responses of young trees to wind and shading: effects on root architecture. *Journal of Experimental Botany* **46**: 1139–1146.

Stokes A, Mattheck C. **1996**. Variation of wood strength in tree roots. *Journal of Experimental Botany* **47**: 693–699.

Stolzy LH, Barley KP. **1968**. Mechanical resistance encountered by roots entering compact soils. *Soil Science* **105**: 297–301.

Ström L. **1997**. Root exudation of organic acids: Importance to nutrient availability and the calcifuge and calcicole behaviour of plants. *Oikos* **80**: 459–466.

Strudley MW, Green TR, Ascough JC. **2008**. Tillage effects on soil hydraulic properties in space and time: State of the science. *Soil and Tillage Research* **99**: 4–48.

Sun Y, Schulze Lammers P, Lin J, *et al.* 2011. Determining root-soil anchorage strength with a modified penetrometer. *Transactions of the ASABE* **54**: 155–161.

Swaby RJ. **1949**. The relationship between micro-organisms and soil aggregation. *Journal of General Microbiology* **3**: 236–254.

Tengbeh GT. **1993**. The effect of grass roots on shear strength variations with moisture content. *Soil Technology* **6**: 287–295.

Tilman D, Balzer C, Hill J, Befort BL. **2011**. Global food demand and the sustainable intensification of agriculture. *Proceedings of the National Academy of Sciences* **108**: 20260–20264.

Tilman D, Wedin D, Knops J. **1996**. Productivity and sustainability influenced by biodiversity in grassland ecosystems. *Nature* **379**: 718.

Tisdall JM, Oades JM. **1982**. Organic matter and water-stable aggregates in soils. *Journal of Soil Science* **33**: 141–163.

Tomaz A, Patanita M, Guerreiro I, Boteta L, Palma JF. **2017**. Water use and productivity of maize-based cropping systems in the Alqueva region (Portugal). *Cereal Research Communications* **45**: 711–721.

Torri D, Sfalanga M, Del Sette M. **1987**. Splash detachment: Runoff depth and soil cohesion. *CATENA* **14**: 149–155.

Tosi M. **2007**. Root tensile strength relationships and their slope stability implications of three shrub species in the Northern Apennines (Italy). *Geomorphology* **87**: 268–283.

Totsche KU, Amelung W, Gerzabek MH, *et al.* 2018. Microaggregates in soils. *Journal of Plant Nutrition and Soil Science* **181**: 104–136.

Tscharntke T, Clough Y, Wanger TC, *et al.* 2012. Global food security, biodiversity conservation and the future of agricultural intensification. *Biological Conservation* **151**: 53–59.

Udoimuk, AB, Osang, J. E., Ettah, E. B., Ushie, P. O., Egor, A. O., Alozie, S. I. 2013. An empirical study of seasonal rainfall effect in Calabar, Cross River State, Nigeria. *IOSR Journal of Applied Physics* **5**: 07–15.

von Uexküll HR, Mutert E. **1995**. Global extent, development and economic impact of acid soils. *Plant and Soil* **171**: 1–15.

United Nations. **2015**. *World Population Prospects: The 2015 Revision, Key Findings and Advance Tables*. New York: United Nations, Department of Economic and Social Affairs, Population Division.

Unno Y, Okubo K, Wasaki J, Shinano T, Osaki M. **2005**. Plant growth promotion abilities and microscale bacterial dynamics in the rhizosphere of Lupin analysed by phytate utilization ability. *Environmental Microbiology* **7**: 396–404.

Valentin C. **1991**. Surface crusting in two alluvial soils of northern Niger. *Geoderma* **48**: 201–222.

Van Oost K, Govers G, De Alba S, Quine TA. **2006**. Tillage erosion: A review of controlling factors and implications for soil quality. *Progress in Physical Geography: Earth and Environment* **30**: 443–466.

Vanapalli SK, Fredlund DG, Pufahl DE, Clifton AW. **1996**. Model for the prediction of shear strength with respect to soil suction. *Canadian Geotechnical Journal* **33**: 379–392.

Vančura V, Hanzlíková A. **1972**. Root exudates of plants. *Plant and Soil* **36**: 271–282.

Vannoppen W, Vanmaercke M, De Baets S, Poesen J. **2015**. A review of the mechanical effects of plant roots on concentrated flow erosion rates. *Earth-Science Reviews* **150**: 666–678.

Varney GT, Canny MJ, Wang XL, McCully ME. **1991**. The branch roots of Zea. I. First order branches, their number, sizes and division into classes. *Annals of Botany* **67**: 357–364.

Veneklaas EJ, Stevens J, Cawthray GR, Turner S, Grigg AM, Lambers H. **2003**. Chickpea and white lupin rhizosphere carboxylates vary with soil properties and enhance phosphorus uptake. *Plant and Soil* **248**: 187–197.

Verheijen FGA, Jones RJA, Rickson RJ, Smith CJ. **2009**. Tolerable versus actual soil erosion rates in Europe. *Earth-Science Reviews* **94**: 23–38.

Volk LB da S, Cogo NP. **2008**. Interrelation of underground plant biomass with soil aggregate stability and rainfall erosion of a soil under different managements. *Revista Brasileira de Ciência do Solo* **32**: 1713–1722.

Volkens G. **1887**. *Die flora der aegyptisch-arabischen wtiste auf grundlage anatomisch-physiologischer forschungen: dargestelit von dr. Georg Volkens...* Berlindel: Gerbr" uder Boratraeger,(Ed. Eggers).

Waldron LJ, Dakessian S. **1981**. Soil reinforcement by roots: Calculation of increased soil shear resistance from root properties. *Soil Science* **132**: 427.

Wang ZH, Fang H, Chen M. **2017**. Effects of root exudates of woody species on the soil anti-erodibility in the rhizosphere in a karst region, China. *Peerj* **5**: e3029.

van Wart J, Kersebaum KC, Peng S, Milner M, Cassman KG. **2013**. Estimating crop yield potential at regional to national scales. *Field Crops Research* **143**: 34–43.

Wasson AP, Richards RA, Chatrath R, *et al.* 2012. Traits and selection strategies to improve root systems and water uptake in water-limited wheat crops. *Journal of Experimental Botany* **63**: 3485–3498.

Watt M, McCully ME, Canny MJ. **1994**. Formation and stabilization of rhizosheaths of Zea mays L.: Effect of soil water content. *Plant Physiology* **106**: 179–186.

Watt M, McCully ME, Jeffree CE. **1993**. Plant and bacterial mucilages of the maize rhizosphere: Comparison of their soil binding properties and histochemistry in a model system. *Plant and Soil* **151**: 151–165.

Wen T-J, Schnable PS. **1994**. Analyses of mutants of three genes that influence root hair development in Zea mays (Gramineae) suggest that root hairs are dispensable. *American Journal of Botany* **81**: 833–842.

White RG, Kirkegaard JA. **2010**. The distribution and abundance of wheat roots in a dense, structured subsoil – implications for water uptake. *Plant, Cell & Environment* **33**: 133–148.

Williams SM, Weil RR. **2004**. Crop cover root channels may alleviate soil compaction effects on soybean crop. *Soil Science Society of America Journal* **68**: 1403–1409.

World Bank. **2007**. *World development report 2008: Agriculture for development*. Washington, DC.: World Bank.

Wright G. **2015**. Antibiotics: An irresistible newcomer. *Nature* **517**: 442–444.

Wu W, Sidle R. **1995**. A distributed slope stability model for steep forested basins. *Water Resources Research* **31**: 2097–2110.

Wulfsohn D, Nyengaard JR. **1999**. Simple stereological procedure to estimate the number and dimensions of root hairs. *Plant and Soil* **209**: 129–136.

Wullstein LH, Pratt SA. **1981**. Scanning electron microscopy of rhizosheaths of Oryzopsis hymenoides. *American Journal of Botany* **68**: 408–419.

Xiao B, Wang Q, Wang H, Dai Q, Wu J. **2011**. The effects of narrow grass hedges on soil and water loss on sloping lands with alfalfa (Medicago sativa L.) in Northern China. *Geoderma* **167–168**: 91–102.

Yang Y, Chen L, Li N, Zhang Q. **2016**. Effect of root moisture content and diameter on root tensile properties. *PLoS ONE* **11**.

Young IM. **1995**. Variation in moisture contents between bulk soil and the rhizosheath of wheat (Triticum aestivum L. cv. Wembley). *New Phytologist* **130**: 135–139.

Záruba Q, Mencl V. **2014**. *Landslides and Their Control*. Elsevier.

Zhang G, Liu G, Wang G. **2012**. Effects of canopy and roots of patchy distributed Artemisia capillaris on runoff, sediment, and the spatial variability of soil erosion at the plot scale. *Soil Science* **177**: 409.

Zhang G, Tang K, Ren Z, Zhang X-C. **2013**. Impact of grass root mass density on soil detachment capacity by concentrated flow on steep slopes. *Transactions of the ASABE*: 927–934.

Zhang X, Yu GQ, Li ZB, Li P. **2014**. Experimental study on slope runoff, erosion and sediment under different vegetation types. *Water Resources Management* **28**: 2415–2433.

Zhao C, Gao J, Huang Y, Wang G, Xu Z. **2017**. The contribution of Astragalus adsurgens roots and canopy to water erosion control in the water–wind crisscrossed erosion region of the Loess Plateau, China. *Land Degradation & Development* **28**: 265–273.

Zhou Z-C, Shangguan Z-P. **2005**. Soil anti-scouribility enhanced by plant roots. *Journal of Integrative Plant Biology* **47**: 676–682.

Zhou ZC, Shangguan ZP. **2007**. The effects of ryegrass roots and shoots on loess erosion under simulated rainfall. *CATENA* **70**: 350–355.

Zhou Z-C, Shangguan Z-P. **2008**. Effect of ryegrasses on soil runoff and sediment control. *Pedosphere* **18**: 131–136.

Zhou Y, Watts D, Li Y, Cheng X. **1998**. A case study of effect of lateral roots of Pinus yunnanensis on shallow soil reinforcement. *Forest Ecology and Management* **103**: 107–120.

Zhu J, Kaeppler SM, Lynch JP. **2005**. Mapping of QTL controlling root hair length in maize (Zea mays L.) under phosphorus deficiency. *Plant and Soil* **270**: 299–310.

Zygalakis KC, Kirk GJD, Jones DL, Wissuwa M, Roose T. **2011**. A dual porosity model of nutrient uptake by root hairs. *New Phytologist* **192**: 676–688.